

THE EFFECT OF THE CATION TO ANION RESIN RATIO
ON MIXED-BED ION EXCHANGE PERFORMANCE
AT ULTRA-LOW CONCENTRATIONS

By

TAEKYUNG YOON
//

Bachelor of Engineering
Busan National University
Busan, Korea
1979

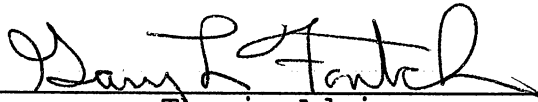
Master of Science
University of Nebraska-Lincoln
Lincoln, Nebraska
1986

Submitted to the Faculty of the
Graduate College of the
Oklahoma State University
in partial fulfillment of
the requirements for
the Degree of
DOCTOR OF PHILOSOPHY
May, 1990

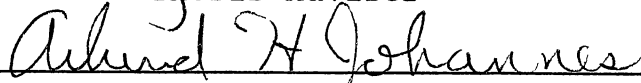
Thesis
1990B
Y59e
cop. 2

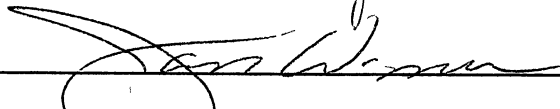
THE EFFECT OF THE CATION TO ANION RESIN RATIO
ON MIXED-BED ION EXCHANGE PERFORMANCE
AT ULTRA-LOW CONCENTRATIONS

Thesis Approved:

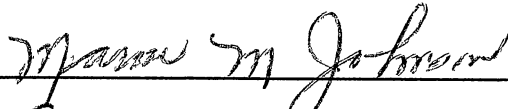


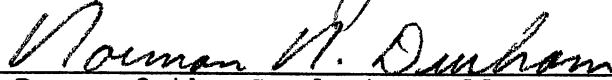
Thesis Adviser





Warren T. Ford





Dean of the Graduate College

TO THE MEMORY OF MY FATHER

PREFACE

The effect of the cation-to-anion resin ratio on mixed bed performance was studied at ultra-low solution concentrations. The effect was tested using the effluent concentration histories as a function of bed position and time for a laboratory scale continuous flow column until the cation and anion-exchange resins were exhausted.

Since the pressure drop due to the ion-exchange resin within the bed increased as time elapsed, an upward flow system was used. The breakthrough curves using the shallow-bed technique gave some detailed results: the shape of the breakthrough curves at different positions as a function of time; the movement of crossover points of sodium and chloride breakthrough curves as a function of resin ratio; effects of cation resin on the chloride breakthrough curve and anion resin on the sodium breakthrough curve; effect of bed homogeneity; and the effects on an unmixed bed.

The primary objective of this study is to test the existing mixed-bed model of Haub and Foutch (1986a) with experimental data. When the experimental data were compared with the model, the results showed that the model predicted mixed-bed ion-exchange behavior with

proper ionic-diffusion coefficients or mass-transfer coefficients. The mathematical model shows that the ionic-diffusion coefficients or mass-transfer coefficients influence the general shape of breakthrough curves. The ionic-diffusion coefficients of Robinson and Stokes (1959) or the mass-transfer coefficients of Kataoka, et al. (1972), are larger than the actual values observed during experimentation. Thus, to fit the actual data well, ionic-diffusion coefficients or mass-transfer coefficients are suggested for this mixed-bed ion-exchange system.

ACKNOWLEDGMENTS

I wish to express my deepest appreciation to my major adviser Dr. Gary L. Foutch for his guidance, encouragement, and invaluable assistance throughout my doctoral program. Further advice and criticism from the advisory committee members, Dr. Marvin M. Johnson, Dr. Jan Wagner, Dr. Arland H. Johannes, and Dr. Warren T. Ford, were also very helpful throughout the study.

Many thanks also go to my coworkers and officemates, Mr. Dariel W. King and Edward J. Zecchini for their suggestion and support throughout my stay at Oklahoma State University. I am also grateful to Mr. Charles L. Baker for his help on my experimentation.

Special gratitude and appreciation are expressed to my mother and wife. Their encouragement, sacrifice and financial support made this study possible.

Financial assistance from the School of Chemical Engineering at Oklahoma State University and the National Science Foundation for the completion of this study are gratefully appreciated.

TABLE OF CONTENTS

Chapter	Page
I. INTRODUCTION	1
II. LITERATURE REVIEW	5
Mixed-Bed Ion-Exchange Chemistry	6
Ion-Exchange Kinetics	7
Film Diffusion	12
Particle Diffusion	14
Mathematical Models	19
Mass Action Model	20
Fick's Law Model	20
Nernst-Planck Model	21
Mass-Transfer Coefficient Model	24
Mixed-Bed Ion Exchange	25
Column Design Methods	29
III. EXPERIMENTAL APPARATUS	34
Water Purification Column	34
Feed Solution Storage	36
Solution Distribution	36
Mixed-Bed Columns	37
Effluent Storage	38
Ion-Exchange Resins	38
Ion Exchange Chromatography	41
IV. EXPERIMENTAL PROCEDURE	44
Experimental Trials	44
Detailed Procedure	46
V. RESULTS	48
General Breakthrough Characteristics	50
Breakthrough Curve as a Function of Position	53
Effluent Concentration as a Function of Resin Ratio	69
Effect of Oppositely-Charged Resin on Breakthrough Curves	71

Chapter	Page
Effect of Bed Homogeneity	77
Unmixed Bed	78
VI. DISCUSSION	82
Experimental Technique	82
Accuracy and Reproducibility	83
Mathematical Model of Haub and Foutch	84
System Parameters	90
Diffusion Coefficients for the System	94
Mass-Transfer Coefficients for the System	102
VII. CONCLUSIONS AND RECOMMENDATIONS	129
Conclusions	129
Recommendations	131
REFERENCES	134
APPENDIXES	147
APPENDIX A - ERROR ANALYSIS FOR THE SYSTEM	148
Accuracy of Ion Chromatography Analysis	148
Experimental Error for the System	149
APPENDIX B - EXPERIMENTAL RESULTS	152

LIST OF TABLES

Table	Page
I. Physicochemical Properties of the Wet Resin and Bed Characteristics	40
II. Experimental Conditions for General Trends of Breakthrough Curves	55
III. Crossover Points of Sodium and Chloride Breakthrough Curves	70
IV. Experimental Conditions for the Effects of Oppositely-Charged Resin on Breakthrough Curves	72
V. Ionic-Diffusion Coefficients in Dilute Solutions (Values in 10^{-5} cm ² /sec)	93
VI. Ionic-Diffusion Coefficients in the System (Values in 10^{-5} cm ² /sec)	97
VII. Constants for Ionic-Diffusion Coefficients as a Function of Ionic Concentration	100
VIII. Constants for Mass-Transfer Coefficients in the System	123
IX. Accuracy of Ion Chromatography Analysis	149
X. Experimental Results	152

LIST OF FIGURES

Figure	Page
1. Equilibria in Mixed-Bed Exchangers	8
2. Crossed Equilibria in Mixed-Bed Columns	9
3. Flow Diagram for Mixed-Bed Columns	35
4. Calibration Plot of Sodium Concentration	51
5. Calibration Plot of Chloride Concentration	52
6. Solution Flow Rate in the Mixed-Bed Column	54
7. Sodium Breakthrough Curves for Cation/Anion Resin Ratio of 1/2	56
8. Sodium Breakthrough Curves for Cation/Anion Resin Ratio of 1/1.5	57
9. Sodium Breakthrough Curves for Cation/Anion Resin Ratio of 1/1	58
10. Sodium Breakthrough Curves for Cation/Anion Resin Ratio of 1.5/1	59
11. Sodium Breakthrough Curves for Cation/Anion Resin Ratio of 2/1	60
12. Chloride Breakthrough Curves for Cation/Anion Resin Ratio of 1/2	61
13. Chloride Breakthrough Curves for Cation/Anion Resin Ratio of 1/1.5	62
14. Chloride Breakthrough Curves for Cation/Anion Resin Ratio of 1/1	63
15. Chloride Breakthrough Curves for Cation/Anion Resin Ratio of 1.5/1	64
16. Chloride Breakthrough Curves for Cation/Anion Resin Ratio of 2/1	65

Figure	Page
17. Experimental Results and Model Prediction of the Effect of Anion Exchange Resin on Sodium Breakthrough Curve	73
18. Experimental Results and Model Prediction of the Effect of Cation Exchange Resin on Chloride Breakthrough Curve	74
19. Effect of Bed Homogeneity (Upper Anion Resin and Lower Cation Resin) . .	79
20. Sodium and Chloride Breakthrough Curves for an Unmixed Bed	80
21. Reproducibility of Experiments for Cation/Anion Resin Ratio of 3.0 g/3.0 g	85
22. Breakthrough Curves of Experimental and Theoretical Results for Cation/Anion Resin Ratio of 3.0 g/3.0 g	95
23. Deviations of Theoretical and Experimental Results for Cation/Anion Resin Ratio of 3.0 g/3.0 g (Using Constant Diffusivity) . . .	98
24. Deviations of Theoretical and Experimental Results for Cation/Anion Resin Ratio of 3.0 g/3.0 g (Using Variable Diffusivity) . . .	101
25. Deviations of Theoretical and Experimental Results for Cation/Anion Resin of 1.0 g/2.0 g with new constants in Table VIII	104
26. Deviations of Theoretical and Experimental Results for Cation/Anion Resin of 2.0 g/4.0 g with new constants in Table VIII	105
27. Deviations of Theoretical and Experimental Results for Cation/Anion Resin of 3.0 g/6.0 g with new constants in Table VIII	106
28. Deviations of Theoretical and Experimental Results for Cation/Anion Resin of 1.2 g/1.8 g with new constants in Table VIII	107
29. Deviations of Theoretical and Experimental Results for Cation/Anion Resin of 2.4 g/3.6 g with new constants in Table VIII	108

Figure	Page
30. Deviations of Theoretical and Experimental Results for Cation/Anion Resin of 3.6 g/5.4 g with new constants in Table VIII	109
31. Deviations of Theoretical and Experimental Results for Cation/Anion Resin of 1.5 g/1.5 g with new constants in Table VIII	110
32. Deviations of Theoretical and Experimental Results for Cation/Anion Resin of 3.0 g/3.0 g with new constants in Table VIII	111
33. Deviations of Theoretical and Experimental Results for Cation/Anion Resin of 4.5 g/4.5 g with new constants in Table VIII	112
34. Deviations of Theoretical and Experimental Results for Cation/Anion Resin of 1.8 g/1.2 g with new constants in Table VIII	113
35. Deviations of Theoretical and Experimental Results for Cation/Anion Resin of 3.6 g/2.4 g with new constants in Table VIII	114
36. Deviations of Theoretical and Experimental Results for Cation/Anion Resin of 5.4 g/3.6 g with new constants in Table VIII	115
37. Deviations of Theoretical and Experimental Results for Cation/Anion Resin of 2.0 g/1.0 g with new constants in Table VIII	116
38. Deviations of Theoretical and Experimental Results for Cation/Anion Resin of 4.0 g/2.0 g with new constants in Table VIII	117
39. Deviations of Theoretical and Experimental Results for Cation/Anion Resin of 6.0 g/3.0 g with new constants in Table VIII	118
40. Deviations of Theoretical and Experimental Results for Cation/Anion Resin of 3.0 g/5.0 g with new constants in Table VIII	119
41. Deviations of Theoretical and Experimental Results for Cation/Anion Resin of 3.0 g/1.0 g with new constants in Table VIII	120

Figure	Page
42. Deviations of Theoretical and Experimental Results for Cation/Anion Resin of 1.0 g/3.0 g with new constants in Table VIII	121
43. Deviations of Theoretical and Experimental Results for Cation/Anion Resin of 5.0 g/3.0 g with new constants in Table VIII	122
44. Curve Fit of Constant A and Cation-to-Anion Resin Ratio for Chloride Exchange	124
45. Curve Fit of Constant A and Cation-to-Anion Resin Ratio for Sodium Exchange	125
46. The Effect of Insufficient Contact Between Resin and Solution	127

NOMENCLATURE

A	Constant in Equation (3)
a_i	Constant for diffusivity of i in Equation (9), cm^2/sec
b_i	Constant for diffusivity of i in Equation (9), $\text{cm}^5/\text{sec}/\text{meq}$
C_i	Concentration of species i in liquid phase, meq/cm^3
c_i	Concentration of species i in solid phase, meq/cm^3
D_a	Axial diffusion or dispersion coefficient, cm^2/sec
D_e	Effective liquid phase diffusivity, cm^2/sec
D_i	Diffusion coefficient of species i , cm^2/sec
e	Bed void fraction
F	Faraday, 96,500 C/equiv
F_i	Feed solution concentration, meq/cm^3
B	
K_A	Selectivity coefficient for ion B in the solution replacing ion A in the resin phase
k_1	Liquid-phase mass-transfer coefficient, cm/sec
n	Constant in Equation (10)
n_+, n_-	Valencies of cation and anion, respectively
q	Limiting ionic conductances, $(\text{A}/\text{cm}^2) (\text{V}/\text{cm}) (\text{equiv}/\text{cm}^3)$
R	Gas constant, 8.314 J/(mol.K)
$R_{C/A}$	Cation-to-anion dry resin ratio
Re	Reynolds number

Sc Schmidt number
T Temperature, K
t Time, sec
u Superficial Solution Velocity, cm/sec
 y_i Equivalent fraction of species i in resin phase
z Distance from column inlet, cm

Greek Letters

β_1, β_2 Ratio of existing to entering ion diffusivities

Superscripts

* Interfacial equilibrium condition
o Bulk phase condition
r Reaction plane condition

Subscripts

Cl Chloride ion
H Hydrogen ion
Na Sodium ion
OH Hydroxide ion

CHAPTER I

INTRODUCTION

The mixed-bed ion-exchange process was discovered during World War II by the Permutit technologists of New York. However, only small-sized mixed-bed demineralizers were used with the resins discarded after use (Martin, 1952). The advent of spherical bead anion-exchange resins with different densities from cation-exchange resins (Chemical Engineering Progress, 1948) allowed separation and regeneration by the hydraulic method. Since then, the mixed-bed ion-exchange process has been used extensively in condensate-purification units for applications in the power, electronics, and chemical industries.

The mixed-bed ion-exchange process has been used predominantly in water treatment in several industries because this process provides an economical and convenient method to produce ultrapure water. This process is equivalent to operating an infinite number of two stage cation and anion exchanges in series. In removing salt from the solution, the selectivity coefficient for salt ions is infinite and therefore, the

efficiency of mixed beds is better than cation and anion beds in series. A single column, filled with an intimately mixed strong acid and strong base ion-exchange resins, produces water with conductivity as low as 0.04 micro-siemens per centimeter (Grimshaw and Harland, 1975), even lower than the conductivity of pure water, 0.055 micro-siemens per centimeter at 25°C reported by Grammont, et al. (1986), and Saunders (1988). Here, mixed beds use both cation-exchange resin in the hydrogen form and anion-exchange resin in the hydroxide form to produce ultrapure water.

Average sodium and chloride concentrations of less than 1 part per billion in the polisher effluent is required as boiler feedwater (Darji and McGilbra, 1980). Electric power-generation facilities need large volumes of pure water. Thus ion-exchange systems using deep-mixed beds of bead-form resin supply ultrapure water to industry (Harries, 1988).

Extensive use of mixed-bed ion exchange requires manufacturers to make high capacity resins for hundreds of applications. The theory of ion exchange accompanied by chemical reaction is far behind the corresponding existing technology. Thus, theoretical models and experimentation, that describe the actual industrial processes, are necessary to develop the basic understanding of this technology.

The overall objective of this research is to determine how key parameters influence mixed-bed ion exchange at ultra-low solution concentrations. To fulfill this objective, a rigorous theoretical model is derived, the actual system tested experimentally, and the data evaluated with the physical process model.

Haub and Foutch (1986a,b) derived a mathematical model for the mixed-bed ion-exchange process operating in the hydrogen cycle at ultra-low solution concentration. Thus, the primary objective of this study is to test experimentally the theoretical model which Haub and Foutch (1986a,b) derived. Experiments are performed to determine ion concentrations as a function of position and time in a mixed-bed column for concentration ranges below 10^{-4} M. Since ultrapure water is used, very precise data should be obtained. Experimental data should show accuracy and precision to show the adequacy of the experimentation.

Mixed-bed ion-exchange columns have been tested for cation and anion concentration ranges of 10^{-4} to 10^{-6} M, various cation and anion-resin ratios, regeneration effect of the resins, and different flow rates. Since ultra-low concentrations are treated, ion breakthrough can take a long time for relatively low flow rates. Thus, this study specifically concentrates on the effect of variations of cation and anion-exchange resin ratios

on the effluent concentrations as a function of column position and time. This includes the effects of bed homogeneity, unmixed bed, and oppositely-charged exchange resin on the breakthrough curve. Other parameters are recommended for future study.

The experimental results are compared with the model of Haub and Foutch (1986a,b). Using the different ionic-diffusion coefficients from investigators (Robinson and Stokes, 1959, Zecchini, 1989), and the different mass-transfer coefficients from Kataoka, et al. (1972), experimental data are discussed to describe the system. The deviations between these values are discussed to give better predictions for future study.

CHAPTER II

LITERATURE REVIEW

A comprehensive literature survey of ion exchange for the mixed-bed process has been completed by Haub (1984) and includes ion-exchange fundamentals, rate laws, column models, and mixed-bed modeling. Several references and classical books by Helfferich (1962, 1966), Kunin (1960), and Grimshaw and Harland (1975) review basic definitions and principles of ion exchange. The kinetic theories describing ion-exchange rates required in the column models are found in these references, as are discussions of the mixed-bed modeling with ion-exchange theory. This literature review updates Haub's thesis.

This chapter will review the properties of water and salt solutions. The equilibrium of mixed-bed ion exchange is described. Ion-exchange equilibria and kinetic approaches are reviewed. The mathematical models of the ion-exchange process are also reviewed. Finally, mixed-bed ion-exchange models and column design equations are described.

Mixed-Bed Ion-Exchange Chemistry

Hydrogen and oxygen atoms react to form water with a large energy release of 286 KJ/mole (liquid), so water is a stable molecule that has little tendency to dissociate to its elements. However, a water molecule is polar. This means that the water molecule tends to orient around an electrically charged ion to reduce the electric field of the ion. This property makes water a good solvent for ionized substances.

A crystal of mineral salt consists of positively charged cations and negatively charged anions held together in a crystal lattice. When this crystal is placed in water, the surrounding polar water molecules reduce the attractive force between cation and anion, break up the lattice, and dissolve the salt. Water dissolves all salts, acids, and bases to some extent (Saunders, 1988). Thus, water can contain salt ions, and these can be removed if necessary. One of the separation methods is the ion-exchange process which uses sites within polymeric structures or naturally occurring materials. Produced water from an ion-exchange process is purified, and the quality of the high-purity water is expressed by means of either conductivity, a quantitative measure of the ability to pass electric current with units of micro-siemens per centimeter, or resistivity,

the reciprocal of conductivity with units of megaohm centimeter.

The process in the mixed bed is a combination of salt splitting and neutralization, and expressed as "crossed equilibria," which is salt splitting by the strong acid cation exchanger followed by neutralization with the strong base anion exchanger, or the converse. These are written in the mass action expression and shown in Figures 1 and 2 (Hill and Lorch, 1988). As shown in these figures, four reactions occur simultaneously in the bed. Due to the simultaneous removal of both cations and anions, neutralization occurs which cannot be obtained from separate beds. The end product is water, and the quality can be increased by repeated stages. The mixed-bed column consists of counterless number of cation and anion-exchange units in series, and the ion concentration decreases analogous to the theoretical plate concept of distillation. The solution quality of a mixed bed is much higher than that of multiple bed systems, and the specific resistance of the effluent solution reaches theoretical maximum for water of 18.28 megaohm centimeter when hydrogen-form strong-acid resin and hydroxide-form strong-base resin are used.

Ion-Exchange Kinetics

Nachod and Wood (1944) tried to elucidate the rate-

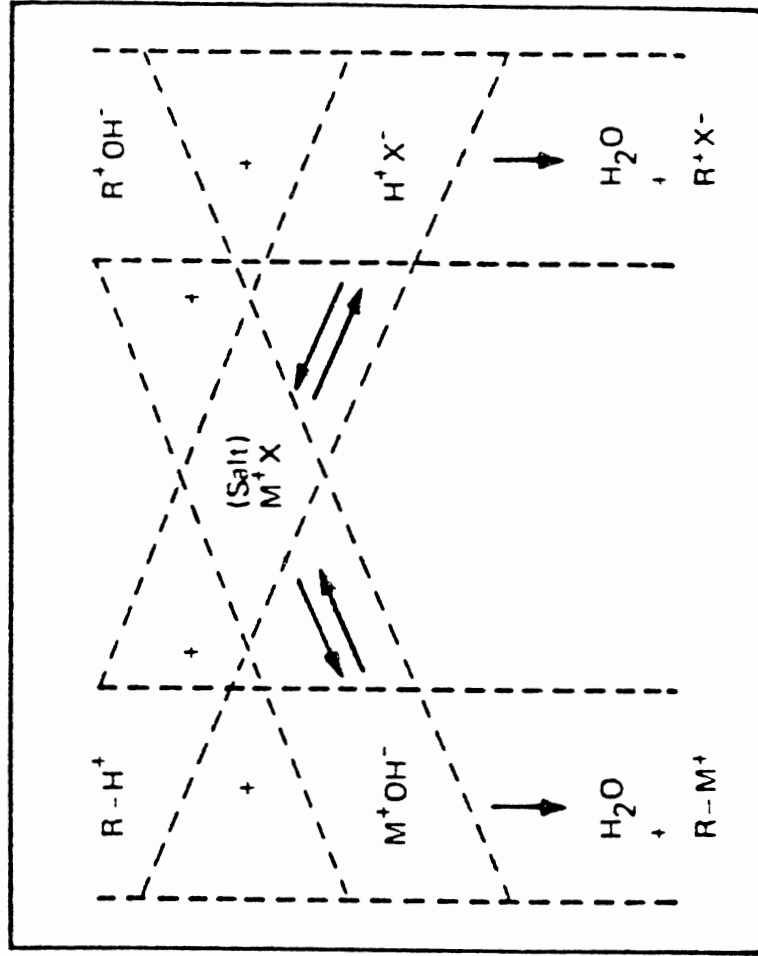


Figure 1. Equilibria in Mixed-Bed Exchangers
(Hill and Lorch, 1988)

Type of reaction	Reactions on cation exchanger (strongly acidic)	Reactions on anion exchanger (strongly basic)
Splitting of salts	$R^-H^+ + Na^+Cl^- \rightleftharpoons \boxed{H^+Cl^-} + R^-Na^+$	$R^+OH^- + Na^+Cl^- \rightleftharpoons \boxed{Na^+OH^-} + R^+Cl^-$
Neutralization	$R^-H^+ + \boxed{Na^+OH^-} \rightleftharpoons R^-Na^+ + H_2O$	$R + OH^- + \boxed{H^+Cl^-} \rightleftharpoons R + Cl^- + H_2O$

Figure 2. Crossed Equilibria in Mixed-Bed Columns
(Hill and Lorch, 1988)

controlling mechanism of the ion-exchange process. For various cation and anion exchangers at various temperatures, they found that the reaction mechanism was a group of second-order bimolecular reactions. To understand this heterogeneous process quantitatively, the mechanism of the rate-controlling process should be studied. Ion-exchange rates are believed to be determined by mass transfer steps; such as through a thin liquid film or through the particle; or by velocity of chemical exchange inside the particle. Boyd, et al. (1947), believed the ion-exchange rate is governed by a diffusion process. Bieber, et al. (1954), demonstrated, using the shallow bed technique, that the effect of chemical kinetics is negligible compared to the other steps. Although Streat (1984) claimed that the chemical reaction between the counterions and the fixed exchange sites is possible as a rate-controlling mechanism in certain cases, it is generally admitted that either particle or film diffusion or both control the ion-exchange rate-determining mechanism. Thus, ion-exchange kinetics has been usually described by a diffusional mass transfer mechanism between ion exchanger and solution. This is controlled by either interdiffusion of the two species of exchanging ions within the exchanger, or liquid concentration gradient (Nernst film) adherent to the exchanger surface, or in both regions simultaneously.

Since these controlling steps occur in series, the slower of these two will be the controlling resistance to ion exchange.

Boyd, et al. (1947), and Reichenberg (1953) concluded that solution concentrations determine the rate controlling step, and the step was elucidated as a function of inlet concentration by Boyd, et al. (1947), and Adamson and Grossman (1949). They found that film diffusion is rate controlling for very low solution concentration, while at higher concentrations particle diffusion is rate controlling. However, the rate-controlling step is not determined by only solution concentration. Helfferich (1962) derived the criterion theoretically to determine the controlling step by considering ion-exchange capacity, particle size, film thickness, diffusion coefficients, and separation factor as well as solution concentration.

It is mentioned by Haub (1984) that film diffusion is more complex than particle diffusion as the effects of mobile coions within the film must be considered. However, particle diffusion is more complex from a quantitative point of view, because only a small fraction of the particle interior is available as a diffusion medium and a large fraction occupied by the exchanger matrix leads to steric hindrance and tortuous diffusion paths (Streat, 1984).

Film Diffusion

Film diffusion rate controlling assumes that the exchange rate depends on the diffusion rate of ions through a very thin film of stagnant solution surrounding the particle, and that the concentrations both in the external solution and throughout the resin are uniform. Thus, the only concentration gradients exist across the film of the hydrostatic boundary layer. Parameters such as temperature or liquid velocity control the film thickness, and the film thickness affects this mechanism. Thinner film gives a higher mass-transfer rate.

Early cation-exchange kinetic studies (Boyd, et al., 1947, Gilliland and Baddour, 1953) concluded that the exchange process is controlled by liquid-film diffusion at solution concentrations less than 0.01 M. Later, other investigators (Frisch and Kunin, 1960; Kuo and David, 1963; Blickenstaff, et al., 1967a,b; Turner and Snowdon, 1968; Gomez-Vaillard, et al., 1981a,b) verified this by experiments.

Film diffusion can be represented by two kinds of models, ordinary and ionic film-diffusion (Glaski and Dranoff, 1963). The ordinary film-diffusion model uses Fick's law by assuming steady-state diffusion (Boyd, et al., 1947, Adamson and Grossman, 1949). However, this approach is good for isotopic exchange because of no diffusivity coefficient difference between counterions

(Huang and Tsai, 1977, Tsai, 1982a). The ionic film-diffusion model considers the electrostatic potential gradients as well as concentration gradients. This approach was suggested by Schloegl and Helfferich (1957), and used the Nernst-Planck equation. Smith and Dranoff (1964) measured the exchange rate of H^+ and Na^+ ions in a batch reactor and compared the experimental data with predictions based on the Nernst-Planck equations.

Helfferich (1965) was the first who considered the effects of accompanying reactions. Blickenstaff, et al. (1967a), and Graham and Dranoff (1972) made an experimental study of the neutralization of a strong-acid ion exchanger by strong base solutions and a strong-base ion exchanger by strong acid solutions, respectively, using a well-stirred batch reactor. Their experimental data showed a strong verification of the model suggested by Helfferich (1965) for ion exchange coupled with irreversible reaction in film-diffusion control.

Kataoka, et al. (1968), proposed an estimating equation for the liquid-phase effective diffusivity based on the film model, and then applied the hydraulic-radius model to compare the diffusivity (Kataoka, et al., 1973a) since the hydraulic-radius model looked preferable to the boundary-layer model for the hydraulic situation in packed bed. Later, Kataoka, et al. (1976c), extended this mechanism to ion exchange accompanied by

irreversible reaction. They derived the theoretical equations of liquid-phase effective diffusivity and the ratio of exchange rate with or without reaction, and verified the concept by experimental results. By considering the effects of the electric field and nonlinear isotherms, they studied the breakthrough curves in equal valence ion exchange (Kataoka, et al., 1976b) and ion exchange between divalent ions and monovalent ions (Kataoka, et al., 1977a). Recently, Kataoka, et al. (1987), analyzed a ternary system using the Nernst-Planck equation.

Van Brocklin and David (1972, 1975) claimed the two-dimensional boundary-layer model with ionic migration is appropriate in packed-bed ion exchange where flow rates are relatively low. They studied ionic migration effect by a ratio of electrolyte to nonelectrolyte mass-transfer coefficients using the Nernst-Planck equation and Fick's law, respectively. Haub and Foutch (1986a) extended liquid resistance-controlled reactive ion-exchange theory to very low solution concentrations, and used the ratio to explain bed parameters. They considered the effect of water dissociation as well as electric-potential gradient and concentration gradient on the ion-exchange rate.

Particle Diffusion

For particle-diffusion control, resistance to mass

transfer in the liquid phase is neglected. This step is mainly due to; high solution concentrations, large particle diameter, high degree of cross-linking of the beads, low concentration of fixed ionic groups, and vigorous solution agitation. Film-diffusion control is the opposite of these conditions (Helfferich and Plesset, 1958, Rao and Gupta, 1982b).

Early investigators proposed theoretically asymptotic solutions to describe equilibria with this controlling mechanism; favorable (Glueckauf and Coates, 1947), unfavorable (Hiester and Vermeulen, 1952), linear (Thomas, 1951), and irreversible (Vermeulen, 1953). Lapidus and Rosen (1954) conducted experimental investigations and found; for lower concentrations the band in the breakthrough curve diffuses as the front progresses down the column because of linearity of the isotherm, while for higher concentrations the breakthrough curve showed only slight variation in shape due to the favorable isotherm.

Ion-exchange kinetics are usually represented by Fick's law for this mechanism with a constant effective diffusion coefficient for the binary systems, or by theoretically correct and experimentally confirmed Nernst-Planck equations (Helfferich and Plesset, 1958; Plesset, et al., 1958; Helfferich, 1962; Rao and Gupta, 1982a). Hering and Bliss (1963) measured ion-exchange

rates for six ion pairs and interpreted data with a Fick's law model and a Nernst-Planck model. They found both models represented the results well. The Nernst-Planck model described the diffusion phenomenon, while the Fick's law model was suitable for the design of a commercial unit because of ease in fixed-bed design calculations. Later, Morig and Rao (1965) modified the Nernst-Planck model by adding self-diffusion curves for the ions. Cooper (1965) derived a general solution for the ion-exchange column with irreversible equilibrium. He solved the time dependent equation for several diffusion models. In addition to the exact solution, several approximations were examined because of mathematical simplicity. Petruzzelli, et al. (1987a), reviewed the state-of-the-art mathematical models with intraparticle rate control. By the kinetics of chloride-sulfate reverse exchange and sulfate self-exchange at high salinity, Petruzzelli, et al. (1987b), showed that intraparticle diffusion controls the mechanism. The transient concentration profiles of these exchanges in the solid phase were directly visualized by autoradiography and light microscopy (Petruzzelli, et al., 1988).

To describe ion exchange with particle diffusion or film diffusion control accurate diffusion coefficients are needed. The effective diffusivity for an ion is a

function of the other ion (coion) present in the resin. Even the self-diffusion coefficient, which is normally used in the Nernst-Planck equation, varies with composition and type of coions (Graham and Dranoff, 1982a). Kataoka, et al. (1974), developed an equation to estimate resin phase diffusivities in isotopic ion exchange. They applied this equation to estimate diffusivities between different ions which accompanied by resin volume change (1975), and resin phase self-diffusivity (1976a). Goto, et al. (1981a,b), proposed a method to evaluate both the interphase mass transfer coefficient and the intraparticle diffusivity simultaneously in batchwise stirred tanks using linear and nonlinear isotherms. Smith (1985) developed a moment analysis scheme for the straightforward calculation of self-diffusivity coefficients of counterions.

Besides film-diffusion control, Blickenstaff, et al. (1967b), and Graham and Dranoff (1972) collected consistent experimental data for particle-diffusion control with Helfferich (1965) of the neutralization of a strong-acid ion exchanger by strong base solutions and a strong-base ion exchanger by strong acid solutions, respectively. They used a well-stirred batch reactor, except explaining the effects of different coions. Kataoka, et al. (1977c), proposed a model for intraparticle mass transfer coupled with irreversible

reaction. The numerical solutions of this model were compared with the Nernst-Planck equation, and verified by the experimental results. Kataoka, et al. (1977b, 1978), suggested theoretical breakthrough curves where equilibrium constant is infinite. They evaluated the effect of electric field by the diffusivity difference on breakthrough curves by applying the Nernst-Planck equation. They verified their theoretical values with experimental results.

Bajpai, et al. (1974), and Yoshida and Kataoka (1987) extended this controlling mechanism to a ternary system. They showed by experiments that the Nernst-Planck equation can be used to this system. Hwang and Helfferich (1987) developed a generalized model for multispecies systems with fast and reversible reactions. They set up a computer program of the model based on the Nernst-Planck equations and a reaction matrix composed of stoichiometric coefficients and reaction-coupling factors. Shallcross, et al. (1988), proposed a semi-theoretical model with a thermodynamic basis to describe multicomponent ion exchange equilibria. They applied the Pitzer approach to the solution nonidealities, and the Wilson approach to the resin. They showed that the model agrees well with experimental data and more accurate than the existing models. Allen, et al. (1989), characterized binary and ternary ion-exchange equilibria using the

Debye-Hueckel relationship for solution phase activity coefficients and the Wilson equation for the resin phase. They observed a reciprocal relationship between the two Wilson parameters for each pair interaction for binary systems. With the Hala constraints, the number of parameters required to characterize the system was reduced significantly.

Huang and Li (1973) and Tsai (1982b, 1985) proposed mathematical models containing both film and particle diffusion with linear and nonlinear concentration profiles in the liquid film. They observed the overall exchange rate by various parameters, and suggested criterion for film and particle-diffusion control. Petruzzelli, et al. (1987b), developed a computer program which can be applied to rate control by a combination of film and particle diffusion. This program calculates the rates and concentration profiles of the binary exchange of ions of arbitrary valences, diffusivities, and selectivity coefficients.

Mathematical Models

The reaction mechanism for ion exchange has been described mathematically. These models include mass action, Fick's first law of diffusion, Nernst-Planck equation, and a mass-transfer coefficient of a reversible rate constant type. Since the ion-exchange rate in

mixed-bed processes usually deals with dilute solutions and is believed to be controlled by a liquid-phase mass-transfer resistance, this section concentrates on the liquid-phase mass-transfer mechanism.

Mass Action Model

The exchange rate is usually written as a reversible second-order reaction. The mass action relationships are based on the stoichiometric interchange of equivalent amounts of cation or anion in the ion-exchange reaction. Early studies of ion-exchange reactions for various cation and anion exchangers in dilute solutions by Nachod and Wood (1944) showed that the reactions were second-order, bimolecular reactions. Other investigators (Dranoff and Lapidus, 1961; Adamson and Grossman, 1949; Gilliland and Baddour, 1953; Hiester and Vermeulen, 1952) found that this type of rate equation represents data in a satisfactory manner over their system variables. This model was especially useful in the multicomponent systems of Dranoff and Lapidus (1958, 1961) to calculate the kinetic behavior of an ion exchange column.

Fick's Law Model

Boyd, et al. (1947), and Adamson and Grossman (1949) used Fick's first law for diffusion in the solid and liquid phases. This kinetic model, based on a simple

diffusion process, has received attention because of the simplicity and ease for the design of commercial ion exchange columns (Hering and Bliss, 1963). This molecular diffusion model is more useful for isotopic exchange where precise boundary conditions are described, and usually needs the assumptions of spherical and uniform particle size. Since this model does not consider the electrical potential which is normally encountered in ion exchange processes, the Nernst-Planck model is sometimes recommended.

Nernst-Planck Model

When a salt solution is treated, the solutes which diffuse in the solution are not molecules but ions. Thus, the gradient of electrical potential of the species as well as the concentration gradient should be considered together to describe the ionic-flux equation.

The diffusion rate of the exchanging ions varies with progression of exchange, and the diffusivities of the ions are not equal due to different mobilities of the ions. Thus, an electric potential arises within the film. The electric field by the counter diffusion of ions of different mobilities slows down the faster ion and speeds up the slower ion in order to preserve electroneutrality. Helfferich and co-workers (Helfferich and Plesset, 1958; Plesset, et al., 1958; Schloegl and

Helfferich, 1957) considered the electric field due to ion charges. They introduced the Nernst-Planck theory which includes the ionic effect on the exchange rate. Thus, this model is an ionic film-diffusion model as compared to the Fick's law model. Many investigators (Glaski and Dranoff, 1963; Hering and Bliss, 1963; Helfferich, 1963; Smith and Dranoff, 1964; Morig and Rao, 1965; Turner and Snowdon, 1968; Bajpai, et al., 1974) have used this model to describe binary ion exchange. This theory has also been applied to a liquid anion exchanger (Kataoka, et al., 1973b) and multicomponent systems (Bajpai, et al., 1974; Evangelista and Berardino, 1986; Hwang and Helfferich, 1987). The original Nernst-Planck theory was extended to include chemical reaction and transport of coions by Helfferich (1965), and confirmed experimentally by Rao and Gupta (1982b).

Since the ion-exchange rate is influenced by the diffusivity ratio of the counterions, the equilibrium constant, and the valence of counterions and non-counterions, Kataoka, et al. (1968), derived an estimating equation for the liquid phase effective diffusivity based on the film model by applying the Nernst-Planck equation. Their equation showed good agreement with the data from other investigators (Gilliland, et al., 1957; Kuo and David, 1963; Moison and O'Hern, 1959; Rao and David, 1964).

Haub and Foutch (1986a) derived the flux equations which consider the neutralization reaction front and water dissociation. These flux equations are based on the Nernst-Planck theory with the static-film hydrodynamic model and nonionic mass-transfer coefficient correlations for packed beds.

Kataoka, et al. (1988), recently developed a theory for the case when combined intraparticle and liquid phase diffusion resistances exist by applying the Nernst-Planck equation. They showed the effect of neutralization when the bulk solution contains a neutral salt and an acid or a base.

With the Stefan-Maxwell equations, which described diffusion in mixture of ideal gases, Graham and Dranoff (1982a,b) developed general expressions for the ionic flow rates for a binary system of concentrated electrolyte solutions in the interior of ion-exchange resins. They believed that the resin is composed of a matrix, however a quasi-homogeneous state in the resin phase is assumed, so some sort of ionic interactions are possible especially for high concentration (Graham and Dranoff, 1982a, Buck, 1985). Using the limiting tracer coefficient instead of self-diffusion coefficient, Graham and Dranoff (1982a) and Graham (1985) predicted ion exchange better than the Nernst-Planck equation. Later, Graham (1985) and Pinto and Graham (1987) extended this

to multicomponent exchange by considering a significant activity coefficient which is normally neglected in dilute solutions. Although other theories were suggested, the Nernst-Planck theory gives a sensible model with simplicity, is believed to be correct, especially for dilute electrochemical solutions, and provides the best tool for the ion exchange process at this time (Turner, 1985, Petruzzelli, et al., 1987a).

Mass-Transfer Coefficient Model

The classical method to describe the driving potential between interphases or intraphases is the mass-transfer coefficient. For packed bed operations, Wilke and Hougen (1945) evaluated the mass-transfer coefficient for design purposes. Bieber, et al. (1954), used this model to study rate mechanisms for cation exchange using variables of flow rate, particle size, feed concentration, and pH of the feed. Frisch and Kunin (1960), who used both mass transfer and diffusivity coefficients in a liquid-film mechanism, obtained a similar correlation from their experiments of mixed-bed ion exchange.

Carberry (1960) obtained the average mass-transfer coefficient in a packed bed of spherical particle using a boundary-layer model. He assumed that the boundary layer is developed and collapsed over a distance approximately

equal to one particle diameter. His mass-transfer coefficient was good at moderate Reynolds numbers larger than 10, but deviated for lower Reynolds numbers. Thus, Kataoka, et al. (1972), applied the hydraulic radius model to laminar flow in a packed bed, and proposed a reasonable approximation solution to fit the liquid-phase mass-transfer coefficients at low Reynolds numbers ($Re < 100$). Recently, Haub and Foutch (1986a) used Carberry's and Kataoka's correlations for Reynolds numbers less than and larger than 20, respectively, to calculate nonionic mass transfer coefficients.

Mixed-Bed Ion Exchange

For efficient equipment design, Caddell and Moison (1954) showed the effect of flow rate in the mixed bed. They found that influent concentration, not flow rate, affected the capacity of bed to produce high-purity water. Frisch and Kunin (1960) performed comprehensive experiments for the mixed-bed deionization of 0.0002 to 0.01 N NaCl solutions at wide ranges of flow rate, bed depth, and temperature, and found that the ion-exchange rate is limited by a liquid-film control. Kinetic studies indicated that the rate of the exchange process was controlled by diffusion of the stationary liquid film at low electrolyte concentrations normally encountered in mixed-bed operation. Tittle, et al. (1980), and Tittle

(1981) investigated the effects of regeneration and different performance of cation and anion resins. They studied actual reactions of mixed bed in a condensate-polishing plant of industrial scale by placing seven point sampling probes in the bed. Tittle (1981) proposed correlations of cation and anion concentrations against bed depth using a boundary-layer diffusion model. For anion exchangers in mixed beds, Harries and Ray (1984) claimed, from laboratory column data, that the rate-controlling step is simple liquid boundary-layer diffusion.

Helfferich (1965, 1966) was the first who presented a theoretical analysis of ion-exchange processes accompanied by ionic reactions with both neutralization and complex formation. He presented eleven characteristic examples for the four different types. This analysis was continued by Kataoka, et al (1976b). They derived equations of liquid-phase effective diffusivity and the exchange ratio with chemical reaction to that without reaction. They confirmed these equations by experimental data. An experimental study was done by Rao and Gupta (1982b), and concluded that the neutralization rate of weak-base resins is controlled by pore diffusion even in dilute solutions, while that of strong-acid resins is controlled by film diffusion in dilute solutions.

Harries (1988) showed that the mass-transfer coefficient for sodium is large in alkaline solutions while that for chloride is large in acidic solutions. From an elemental analysis technique of X-ray photoelectron spectroscopy, he pointed out that the crushed bead of new and used strongly basic resins has only strongly basic groups in the bulk, but the surface of the resins has both strongly and weakly basic groups. The strongly basic groups are active over a wide range of pHs, but the weakly basic groups are active only in acidic solution. Thus, acidic solution can give anion-exchange resin more active sites than neutral or alkaline solution. Therefore, pH affects the mass-transfer coefficient for sodium, and this can also be applied to the cation exchange resins. Alkaline solution gives cation-exchange resins more active sites than neutral or acidic solution. For the change of pH from neutral to acidic, the mass-transfer coefficient for chloride increased sharper than the mass-transfer coefficient for sodium as pH changes from neutral to alkaline (Harries, 1988). Harries (1987) reported that the mass-transfer coefficient for chloride decreased as the relative amount of anion resin is increased because solution became more alkaline. However, the net rate of anion exchange is faster than that of cation exchange.

Since small-bead size exchangers have larger surface area, small ones give faster exchange than large ones. Thus small-bead size resins can reduce the depth of exchange zones. Harries (1988) studied the effect of cation-exchange resin size on anion-exchange kinetics using two sizes of cation exchanger, mean bead diameters of 0.71 and 0.82 mm. He pointed out that a relatively small increase of bead size caused a significant reduction in anion exchange kinetics due to the pH changes within the bed.

Harries (1988) claimed that the simple boundary layer diffusion model based on experimental data is more amendable. However, he showed that the mass-transfer coefficient was dependent on influent concentration or solution pH, which should be constant in the model. The theoretical model which included electrostatic and diffusion functions (Haub and Foutch, 1986a) can also predict the behavior of the column performance. Some assumptions are usually made to simplify theoretical models. By the assumptions which will be mentioned later, Haub and Foutch (1986a) derived rate expressions for reactive ion exchange at low solution concentrations and applied these to mixed-bed ion exchange. Since neutralization can occur in the bulk phase and the liquid film, these two cases were considered simultaneously.

Column Design Methods

As any other continuous column unit operation processes, ion exchange uses the principle of material balance. Processes such as a moving fixed bed, or a countercurrent ion exchange, or fluidized stages of resin particles with periodic transfer of resin, allows a continuous steady state process (Wildhagen, et al., 1985; Streat, 1986; Wesselingh, et al., 1986). However, ion exchange operations are traditionally conducted in fixed beds. The unsteady state nature of fixed beds needs interpretation of more complex mass-transfer mechanism (Moison and O'Hern, 1959). Other principles for ion exchange processes are rate equation, equilibrium relationship at the fluid-solid interface, and hydrodynamics. These principles are needed to model and design ion exchange columns.

To design the process, model parameters, such as equilibrium isotherm, intraparticle diffusivity, and film mass-transfer coefficient, are obtained from experiments and applied to the model equation. Then, the experimental breakthrough curve, i.e., the shape and position of an effluent concentration history, obtained at the laboratory scale, is compared with computer simulations to test the validity of the theoretical model. Good models enable us to predict column performance over a wide range of conditions using data,

and can then be applied to the bench or industrial scale. The actual system can then be built by scale-up methods, which is influenced by hydrodynamic parameters.

A simple design method for deep fixed-bed ion-exchange columns was described by Michaels (1952) using the exchange-zone concept. He assumed the exchange takes place within a constant depth and this depth descends through the bed. Later, Moison and O'Hern (1959) obtained correlations for favorable equilibrium from experiments to design both batch and continuous countercurrent packed beds using this concept.

Ion-exchange equilibrium represents the behavior of exchange resin with bulk solution. Different equilibrium affinities for the different components of the exchanger can separate the mixtures. Equilibrium theory is widely used to design ion-exchange processes (Tondeur and Bailly, 1986; Rodrigues and Costa, 1986; Wilson, 1986). Local equilibrium theory is described in detail by Klein (1986). This theory was extended to systems accompanied by reactions (Hwang, et al., 1988). Equilibrium in the multicomponent system was studied experimentally (Dranoff and Lapidus, 1957; Pieroni and Dranoff, 1963; Klein, et al., 1967; Kataoka and Yoshida, 1980; Myers and Byington, 1986) and theoretically (Helfferich, 1967, 1984) to calculate the kinetic behavior of an ion-exchange column.

In equilibrium theory, local equilibrium between the two phases is assumed to occur at all points. The unsteady-state material balance on a differential slice of column is given as

$$e \frac{\partial C}{\partial t} + (1 - e) \frac{\partial c}{\partial t} + u \frac{\partial C}{\partial z} = \frac{\partial}{\partial z} \left[D_a \frac{\partial C}{\partial z} \right] \quad (1)$$

The equilibrium model neglects the axial diffusion term, i.e., right hand side (Tondeur and Bailly, 1986). Since there are no mass-transfer resistances for the ionic species from bulk solution to exchange site, concentrations of these two phases are assumed to be equal. Thus, equations of material balance, equilibrium isotherm, initial and boundary conditions are needed to model the equilibrium theory.

When kinetically controlled phenomena are dealt with, kinetic laws of transport, described in previous sections, are added to the equilibrium model. The so-called rate theory uses material balance, equilibrium isotherm, kinetic law, and initial and boundary conditions. This theory includes film-diffusion and particle-diffusion controls, and produces solution concentration as a function of time and column position.

Beyer and James (1966) investigated the effect of column shape on the performance of fixed-bed ion-exchange columns, and showed the breakthrough time was independent

of the column geometry if the fluid flow rate, volume, and criteria for breakthrough are fixed when the rate law depends on concentration. Later, Cooney (1967) extended this to the system when rate laws depend on fluid velocity.

When complex rate equations or equilibrium relations, irregular boundary conditions, or tedious calculations are met, numerical methods can be used. Also, computer aided design for modeling and simulation of ion-exchange processes will be used by chemical engineers. Acrivos (1956) applied an explicit method, "the method of characteristics technique," which reduces first-order hyperbolic partial differential equations to an equal sized system of ordinary differential equations (Costa, et al., 1986), to adsorption packed columns. Then, many investigators (Helfferich, 1962, Omatete, et al., 1980) used this method to solve material balance equations in binary and multicomponent ion-exchange columns (Dranoff and Lapidus, 1958, 1961). Later, Haub and Foutch (1986a) applied this method to the material balances for cation and anion resins in mixed bed. Implicit methods are also an alternative way to solve material balance equation. Liapis and Rippin (1979) applied orthogonal collocation to the adsorption column. Later, using the method of lines with a finite element collocation method, Loureiro, et al. (1985), solved

nonlinear parabolic partial differential equations which arise in equilibrium models and film and homogeneous particle diffusion models. General numerical methods which solve ion-exchange models and equations were reviewed and referenced by Costa, et al (1986).

CHAPTER III

EXPERIMENTAL APPARATUS

To study the effect of the cation-to-anion resin ratios of a mixed-bed ion-exchange process at ultra-low solution concentrations, a glass-column experiment was carried out to measure the concentration of the solution as a function of time and position within the bed. This study does not include temperature effects; all experiments were made at room temperature. The average temperature was 23°C and the variation was $\pm 2^\circ\text{C}$.

Figure 3 shows the schematic diagram of the whole system of the laboratory mixed-bed ion-exchange test column. It is composed of a large water purification column, a feed solution storage carboy, a solution distribution peristaltic pump, mixed-bed columns and effluent solution storage carboys. Also included is off-line ion-exchange chromatography, and output recorder.

Water Purification Column

Glass distilled column (mega-pure system of Corning Science Products) was used to make double distilled water, but because of low capacity of the column it could

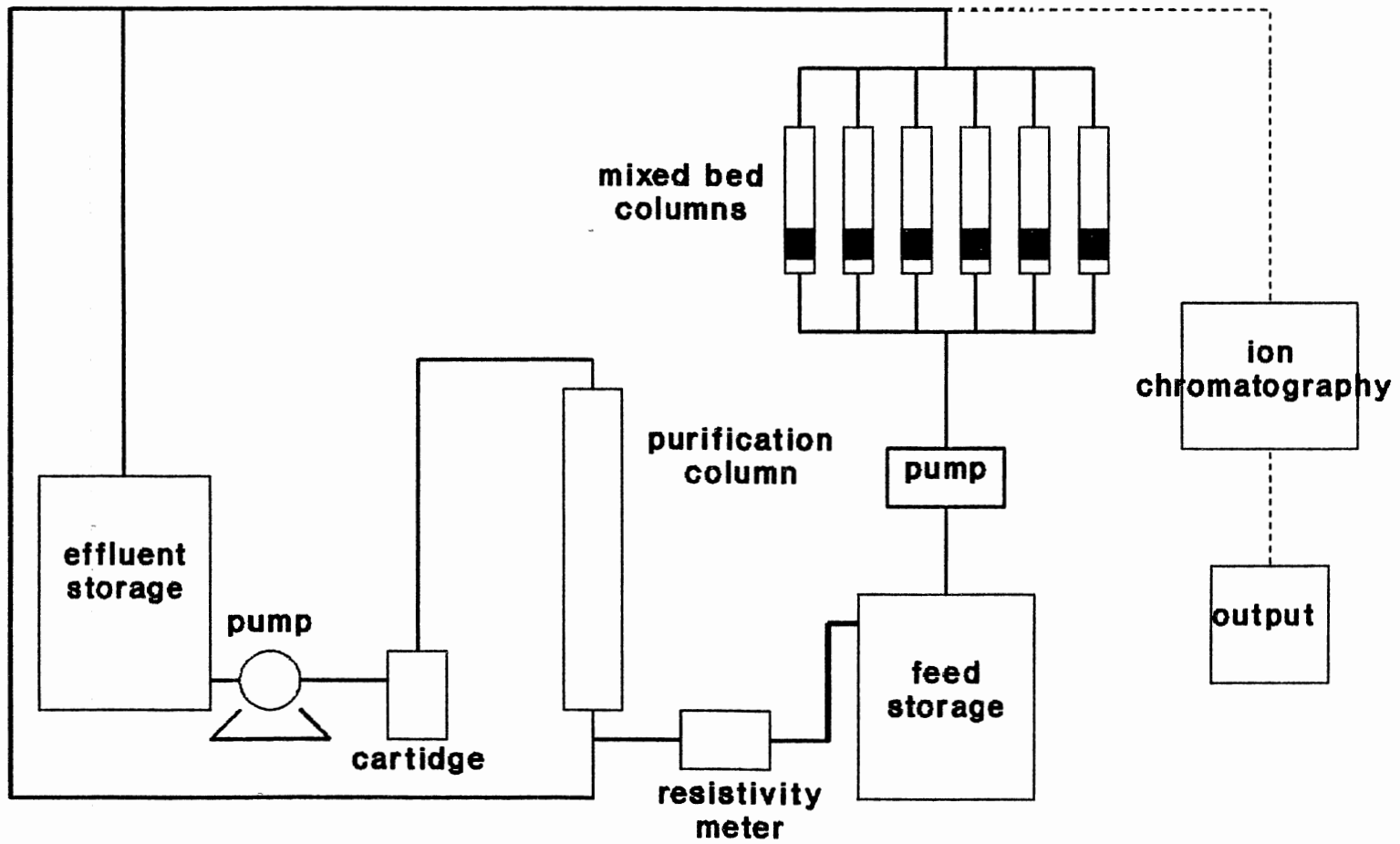


Figure 3. Flow Diagram for Mixed-Bed Columns

not supply the necessary amount of pure water. Thus, a large mixed-bed ion-exchange column was used to supply ultrapure water to make feed solutions. The water was fed into the column after treated by distillation and a filter housing cartridge (Corning mega-pure system, 3508-FH). The produced water was good quality with a resistivity reading (Signet Scientific) of 18.3 megaohm-cm, the standard of ultrapure water.

Feed Solution Storage

The feed solution storage carboy was low-density polyethylene with a spigot of Nalgene Labware by Nalge Company and has a 50 liter capacity. The carboy was charged by filling with purified column effluent water after the addition of the calculated quantity of analytical reagent grade sodium chloride (J. T. Baker Chemical Company) to the carboy. Before filling the carboy with a feed solution, sodium chloride solution of 10^{-4} M was made in a 10 liter carboy. Vigorous agitation was made in the 10 liter carboy and complete mixing was checked by conductivity measurement. Since one feed solution concentration was used, only one 50 liter carboy was used as a feed reservoir.

Solution Distribution

Feed solution was distributed using a peristaltic

pump. The pump was a Masterflex ten-channel drive from Cole-Parmer Instrument Company of Chicago, Illinois with a maximum flow range per channel of 380 ml/min. In order to maintain constant flow rate over long periods of time, up to 2 months, it was necessary to use silicone tubing for the pump. The strength and thickness of silicone tubing (Masterflex J-6411-24, Cole-Parmer Instrument Company) made this experiment possible. Flow rate was measured between the effluent samplings by checking the effluent volume collected in a given time period. The flow rate was almost constant and accurate so that the effluent volume could be calculated on the basis of elapsed time and measured flow rate. The volumetric flow rate ranged from 0.41 to 0.45 liter/hour.

Mixed-Bed Columns

To make sure that the bed is homogeneously mixed with cation and anion-exchange resins, the column should be directly visualized. The experimental columns were prepared by Pyrex glass from the glass shop in the Chemistry Department. Attention was also given to the uniform external voids between resin and solution. The inside diameter of the columns were 1 inch (2.54 cm.), and the height of the columns were about 50 cm above the fritted glass disk of extra-coarse porosity, which was sealed into the bottom of the column, ensuring uniform

flow distribution, and served as a support for the mixed-bed resins. Feed lines to the column from the pump were used of 1/4 inch Tygon tubing. For time efficiency and productivity, up to six columns were used simultaneously. The pump limits to ten columns.

Effluent Storage

Effluent solution was discharged from the experimental columns to the 25 liter carboys and recycled through large water-purification column. Effluent solution was treated in the water-purification column and filter-housing cartridge at least twice to ensure water quality before making the influent feed solution.

Ion-Exchange Resins

To produce completely deionized water, which has the conductivity of water dissociation, the mixed bed should consist of an intimate mixture of a strongly acidic cation-exchange resin and a strongly basic anion-exchange resins (Kunin and McGarvey, 1951). Since gel-type exchangers fouled irreversibly when used with water containing acids, cross-linked resins are usually used in industry. Lower cross-linked resins are physically unstable in the column, so the so-called macroporous or macroreticular resins are used.

In this study, Ambersep 200 H, for cation exchange, and Ambersep 900 OH, for anion exchange, from Rohm and Haas Company, were used. Both cation and anion resins are the macroreticular type. The Ambersep system has the following advantages compared with conventional mixed-beds: perfect physical and visible separation, very low ionic leakage, and very short rinse requirements (Hill and Lorch, 1988). Since this study does not concern the regeneration step, inert resin, which has an intermediate density between the top strong basic anion resin and the bottom strong acidic cation resin, was not used. Only cation and anion-exchange resins were mixed. Resin particles are small enough with respect to the inside diameter of the glass column, so wall effects were minimized. The physicochemical properties of these resins and bed characteristics are shown in Table I. Resins were weighed when fully dried at atmosphere to keep a consistent measurement. Air dry weight resins were charged to the ion-exchange column after fully swollen overnight with pure water. The weight of air dry resin will vary day to day due to the moisture content of air. However, almost a consistent air condition was maintained in the laboratory, so a serious effect was not expected. The moisture content of air dry resin of Ambersep 200 H and Ambersep 900 OH was measured by drying in an oven at 110°C overnight, and found to be 4.9 % and

5.9 %, respectively. The probable error was estimated in Appendix A. The effect of regeneration was not included in this study, so all experimental runs were made with fresh resin.

TABLE I
PHYSICOCHEMICAL PROPERTIES OF THE WET RESIN
AND BED CHARACTERISTICS

Bed Diameter	2.54 cm
Bed Height	up to 10 cm
Internal Porosity	0.25-0.30
Void Fraction	0.34-0.38 (0.35)
Resin Bead Radius (Harmonic Mean Particle Size)	
Ambersep 200 H	0.80-0.85 mm
Ambersep 900 OH	0.58-0.62 mm
Bulk Density	
Ambersep 200 H	46-50 lb/ft ³
Ambersep 900 OH	39-44 lb/ft ³
Exchange Capacity	
Ambersep 200 H	1.6-1.7 eq/liter
Ambersep 900 OH	0.8-0.9 eq/liter
Specific Gravity	
Ambersep 200 H	1.18
Ambersep 900 OH	1.06
Selectivity Coefficient	
Ambersep 200 H Na/H	2.0-2.5
Ambersep 900 OH Cl/OH	15-18

Ion Exchange Chromatography

The effluent ionic concentrations of solution from the experimental columns were analyzed by ion chromatography (2000i/SP, Dionex Corporation). Ion chromatography enables us to analyze water with an impurity range low to 10 part per billion.

This liquid chromatographic technique uses ion exchange mechanisms and suppressed conductivity detection for the separation and determination of anions and cations using a conductivity cell as a detector (Small, et al., 1975). Conductivity is a universal property of ionic species in solution, and shows a simple dependence on species concentration. The output from the conductivity meter, which was proportional to the conductivity of the sample in the cell, was expressed on a strip chart recorder. Since the peak height or peak area is proportional to feed concentration, peak height was measured to obtain quantitative results in this study. Peak height is recommended by Dionex Corporation (Dionex, 1983) since peak height measurements yield excellent precision and are straightforward. The output record used was a 5890 A Series GC Terminal from the Hewlett Packard Company.

Since columns in the system such as separator columns, guard columns, packed-bed suppressor columns, should be kept clean when not used, the columns were

rinsed with deionized water before and after the eluant and regenerant flow. High quality water of less than background resistivity of 16.67 megaohm-cm for preparation of aqueous eluants and regenerants and for rinsing reduces background interference. To make sure of the steady flow of eluant and regenerant, 3 to 4 hours were used to stabilize the base-conductivity. Samples were injected into the column by Becton-Dickinson 3cc Syringes. When this syringe was once used, it was disposed of to reduce contamination from previous samples. To reduce leaching of the syringe itself or from the atmosphere, samples were injected as soon as possible and no time effects were observed.

Eluant solutions for the chromatography were prepared from fully deionized water and reagent grade chemicals. The cation eluant was the mixture of 27.5 mM Hydrochloric Acid (Fisher Scientific Company), 2.25 mM DL-2,3-Diaminopropionic acid monohydrochloride (Fluka Chemical Corporation), and L-Histidine-monohydrochloride Monohydrate (Fluka Chemical Corporation). For anion analysis, eluant of a mixture of 1.8 mM Sodium Carbonate (Fisher Scientific Company) and 1.7 mM Sodium Bicarbonate (Fisher Scientific Company) was used. The flow rates used were 1.0 ml/min for cation and 2.0 ml/min for anion, respectively. Used cation and anion regenerants were 70 mM Tetrabutylammonium Hydroxide (55% Aqueous Solution,

Southwestern Analytical Chemicals Incorporated of Austin, Texas) and 0.025 Sulfuric Acid (Fisher Scientific Company), respectively. The regenerant flow rates were 5.0 ml/min for cation and 2.5 ml/min for anion, respectively.

CHAPTER IV

EXPERIMENTAL PROCEDURE

Some preliminary experiments were used to determine the proper flow configuration. The preliminary experiments were mainly to get over increasing pressure drop problems due to the tightened resins as time elapsed. A series of glass columns were tried and finally upflow columns were chosen. A detailed description of the experimental trials is given here to avoid experimental failures in future studies.

Experimental Trials

First, the column experiments were performed using the flow from top to bottom. Since the pressure drop due to the exchanger bed increased as time elapsed, the flow rate was reduced significantly. The 1/4 inch Tygon tubing expanded 2 to 3 times in diameter because of resin blocking. Thus, experiments could not continue until the effluent concentration reached breakthrough.

Second, a column with sparse mixture of resins was tried. Although the pressure drop problem was solved, insufficient contact between resin and solution gave

higher effluent ion concentration than expected. Thus, the inlet flow was changed upward the third trial.

Third, the column with two extra-coarse frits at the upper and lower ends were used. However, serious pressure drop to the upper direction happened again. Thus, this change did not help the pressure drop problem.

Fourth, upflow with a frit on the bottom side only was tried. Mixed bed uses infinite pairs of cation and anion resins. However, the column looked like a fluidized bed with moderate flow rates. Since anion-exchange resin has much lower density than cation-exchange resin, anion resin was much richer in the upper part of the mixed bed. Thus, separation of the resins should be avoided to get a real mixed bed.

Fifth, the experimental conditions with slow flow rates were used, so that the mixed bed was kept stable and homogeneous with cation and anion-exchange resins. However, keeping a homogeneous bed to measure solution concentration as a function of position in a long column was practically difficult because of the significant density difference of cation and anion-exchange resins.

Finally, many columns instead of one column were used to measure the concentration as a function of position in the column, because the purpose of this experiment is to get accurate and precise data. At least, this method guaranteed the total amount of mixed

resin of the desired position although not completely mixed. This method needed a long experimentation period. Thus, not a deep bed but a multi-stage shallow beds of bed depth up to 10 cm was used. The flow rate was about 0.41 - 0.45 liter/hour. Runs were continued in all cases until effluent was sure to reach breakthrough.

Detailed Procedure

A detailed description of the glass column experiment of the mixed-bed ion exchange with continuous upflow system is given below. Although somewhat duplicated with the equipment description, this describes the step-by-step procedure for the system.

1. Very pure water was made from recycled solution from the system or new water from the distillation column. Resistivity of 18.28 megaohm-cm was checked to make sure the quality of water.

2. Water produced from step 1 was collected in a 10 liter carboy. After 10 liters were collected, 0.0584 g of sodium chloride crystals was added and vigorously agitated. Then, 10^{-4} M sodium chloride solution was stored in the 50 liter feed storage carboy.

3. Sodium chloride solution from step 2 was distributed to the mixed-bed columns. The flow rate for each column was regularly checked and also samples were collected in syringes on a regular time basis.

4. Discharged solution from the glass columns was collected in the effluent storage carboy.

5. Collected samples were analyzed by ion chromatography. These results were plotted as figures in the next chapter and listed in Appendix B.

CHAPTER V

RESULTS

The purpose of this study is to test experimentally our existing theoretical model of liquid resistance controlled reactive ion-exchange theory at ultra-low solution concentrations in mixed-bed ion exchange. For solution concentrations above 10^{-4} M the model agrees with early development (Haub and Foutch, 1986a), but for below 10^{-4} M experimental data are not available in the literature. Thus, influent concentration of 10^{-4} M NaCl solution is chosen in this study. This also meets maximum electrolyte concentration which is produced in condensate polishing plants (Tittle, 1981).

As shown in Figure 3, NaCl solution is continuously fed to the column, and the treated solution is continuously removed. However, the mixture of cation and anion-exchange resin in the column is exhausted gradually, so this is an unsteady-state process. The solution concentration will vary with both the bed position and elapsed time before cation and anion-exchange resins are exhausted.

Many system parameters influence the shape of breakthrough curves in mixed-bed ion exchange. The system parameters are; initial equivalent fractions of sodium in the cation resin and chloride in the anion resin, cation and anion resin particle diameters, bed void fraction, feed solution concentration, volumetric flow rate, system temperature, column diameter, height of packed resin, cation and anion resin capacities, types and ionic form of resins, selectivity coefficients for the sodium-hydrogen and chloride-hydroxide exchange, solution viscosity, solution density, cation-to-anion resin ratio, and diffusivities of the involved ions. Among these parameters, the cation-to-anion resin ratio is the only parameter considered in this study.

Fifteen runs were made to characterize general trends of breakthrough curves with the system described in Chapters III and IV. Duplicated runs were made to determine the reproducibility of the experimental data. Other experimental conditions were chosen to study; the effects of oppositely-charged resin on breakthrough curve, homogeneity of the mixed bed, and trends for unmixed beds. All the laboratory scale data are plotted in the following sections to explain the effects mentioned above, and the raw data are listed in the Appendix B.

General Breakthrough Characteristics

The experimental effluent concentration histories are given in dimensionless form of C/C_0 , i.e., effluent ion concentration divided by influent ion concentration, to interpret the results on a comparable basis. The breakthrough curves of the separate cation and anion exchange from a single mixed bed will be given to study the effects of cation-to-anion resin ratio. When plotted, the data show some scattering which varies from one run to another, but in most cases the data are consistent enough to allow a smoothed breakthrough curve to be drawn.

Calibration plots of sodium and chloride concentrations are made from standard solutions to interpolate the chromatogram peak height from the ion chromatograph. These plots are shown in Figures 4 and 5 for sodium and chloride concentrations, respectively. The close linear dependence between peak height and ion concentration is indicated in Figures 4 and 5 for the various attenuations of the recorder. Thus, the effluent ion concentrations are linearly interpolated from the chromatogram peak heights.

Kataoka and Yoshida (1976c) pointed out that hydroxide-form resin beads presented a lot of congregated clusters that resulted in nonuniform distribution of void fraction in the bed and irregular flow patterns. In

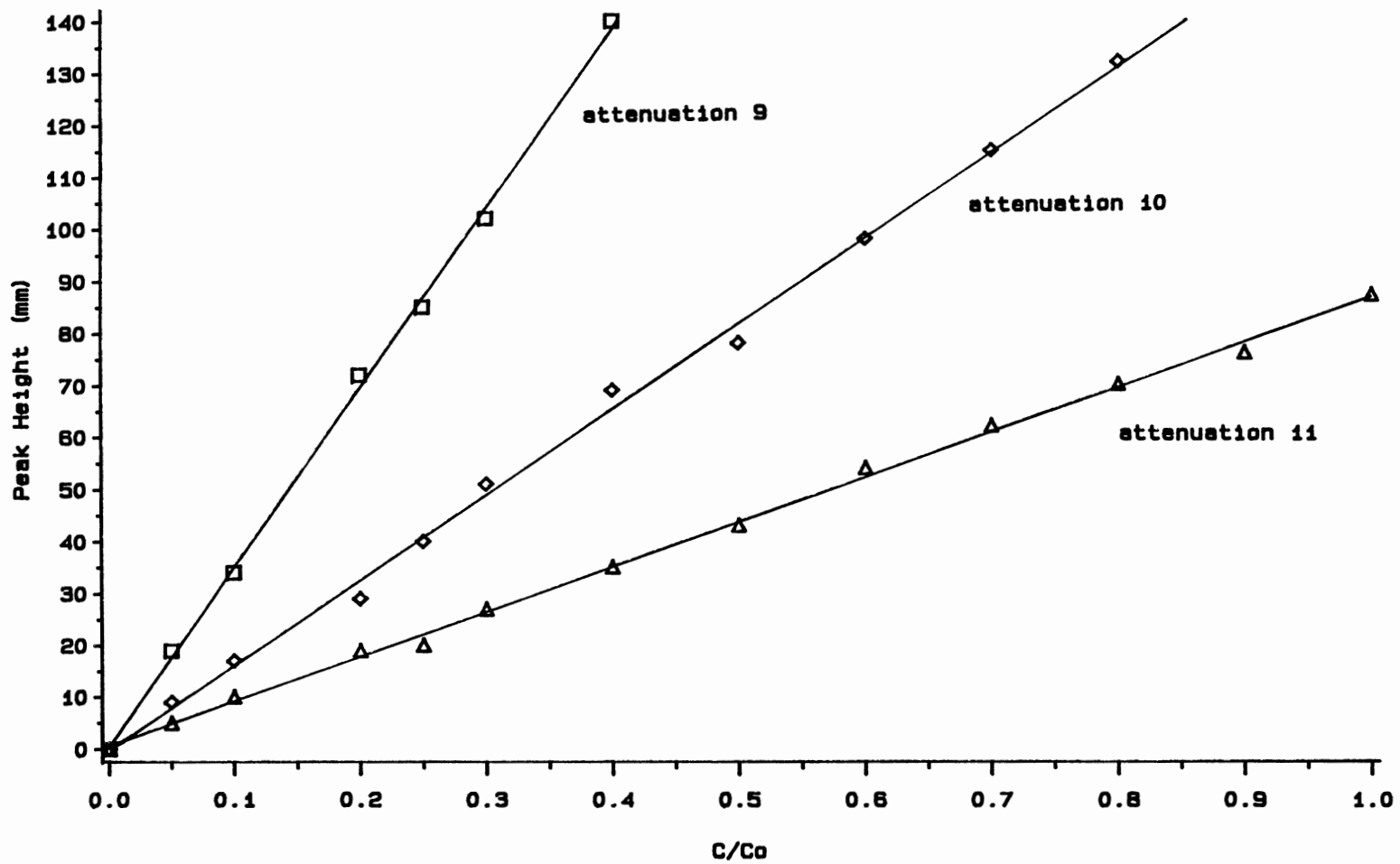


Figure 4. Calibration Plot of Sodium Concentration

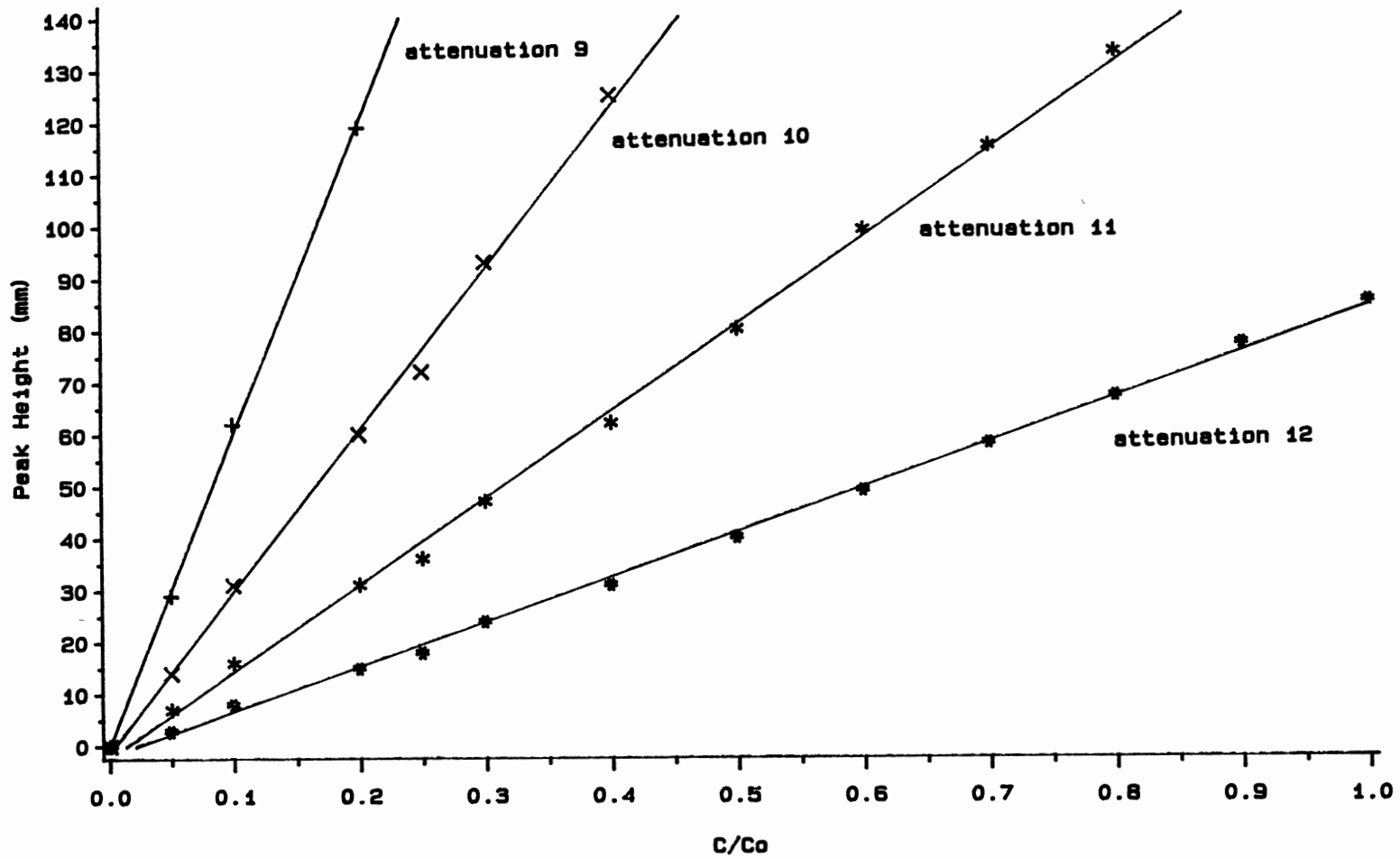


Figure 5. Calibration Plot of Chloride Concentration

these experiments, clusters were removed by the rigorous agitation in water, and the wet mixed resins were kept in a beaker for more than a week. The flow rates through the frit and the mixed bed contained in a glass column were regularly checked and found to be almost constant. A sample case for a cation/anion resin ratio of 3.0 g/3.0 g (dry weight), and an average volumetric flow rate of 0.42 liter/hour is shown in Figure 6.

Breakthrough Curve as a Function of Position

Fifteen experimental conditions for the general trends of breakthrough curves are shown in Table II. The cation-to-anion resin ratio of 1/2, 1/1.5, 1/1, 1.5/1, and 2/1 are used for the total dry resin weight of 3.0, 6.0, and 9.0 g.

Figures 7 through 11 for cation exchange and 12 through 16 for anion exchange, respectively, show the breakthrough curves of different total amount of mixed resin for each of the same cation-to-anion resin ratios. The experimental conditions for Figures 7 through 16 are described in Table II. The abscissa of these Figures is the amount of effluent volume treated, and the ordinate is C/C_0 . The bed depth is proportional to the resin amount, so Figures 7 to 16 show either sodium or chloride breakthrough curves as a function of the bed depth.

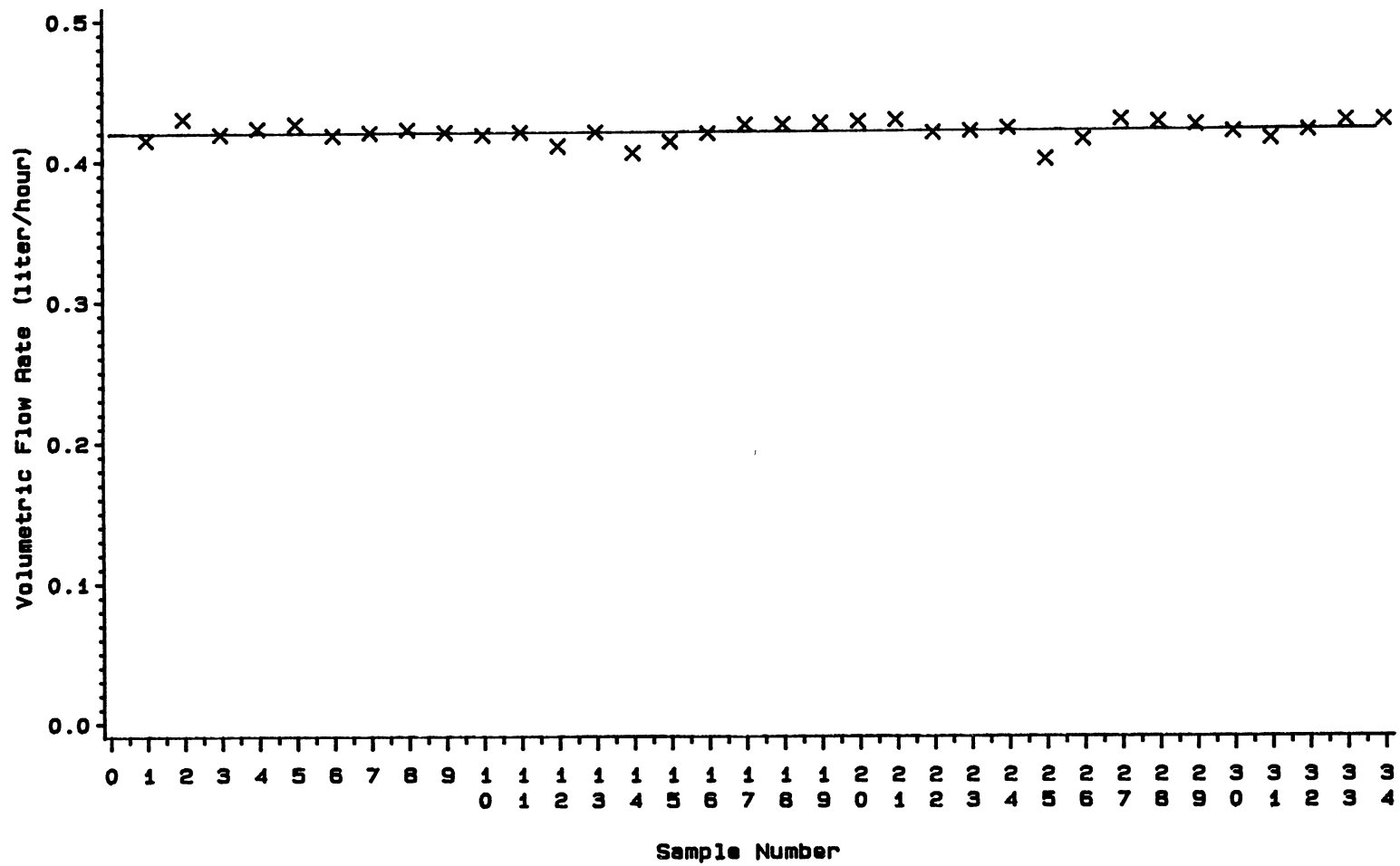


Figure 6. Solution Flow Rate in the Mixed-Bed Column

TABLE II
EXPERIMENTAL CONDITIONS FOR GENERAL TRENDS
OF BREAKTHROUGH CURVES

Cation/Anion (dry weight)	Resin Amount (g/g)		
	3.0 g	6.0 g	9.0 g
1/2	1.0/2.0	2.0/4.0	3.0/6.0
1/1.5	1.2/1.8	2.4/3.6	3.6/5.4
1/1	1.5/1.5	3.0/3.0	4.5/4.5
1.5/1	1.8/1.2	3.6/2.4	5.4/3.6
2/1	2.0/1.0	4.0/2.0	6.0/3.0

Figures 7 through 16 show that different levels at initial leakage appear in the effluent of the cation and anion-exchange process. The initial leakage is not observed for anion exchange of mixed resin of 6.0 g or 9.0 g. For the mixed resin of 3.0 g, the initial leakage for anion exchange varies from 0.02 to 0.07, depending on anion resin amount in the bed. The initial leakage up to 0.24 is observed for cation exchange with cation resin of 1.0 g in Figure 7. Cation exchange, except for the mixed resin of 9.0 g, shows the initial leakage depending on the bed depth. Under comparable conditions, the cation effluent concentration gives a higher level of leakage

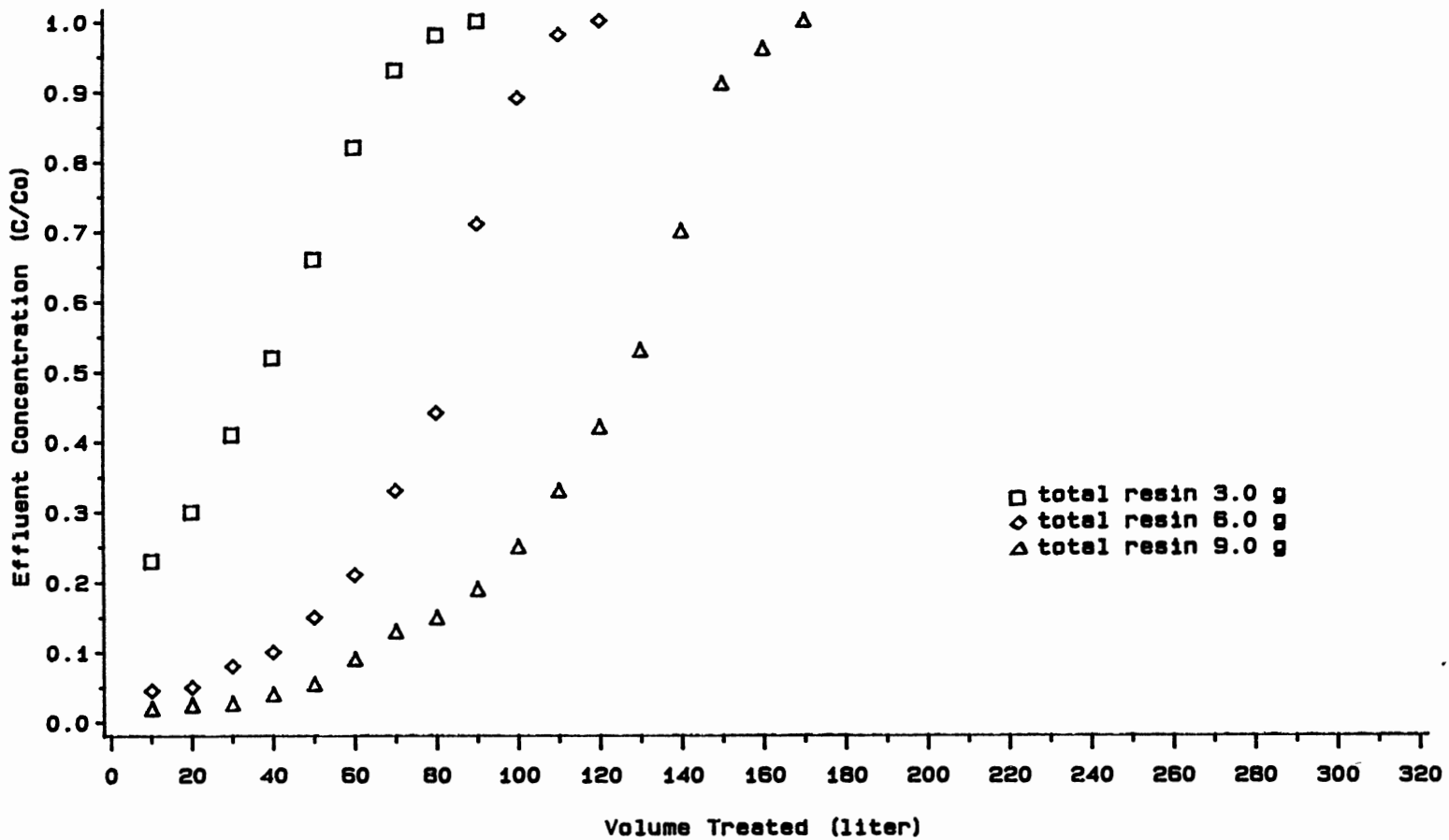


Figure 7. Sodium Breakthrough Curves for Cation/Anion Resin Ratio of 1/2

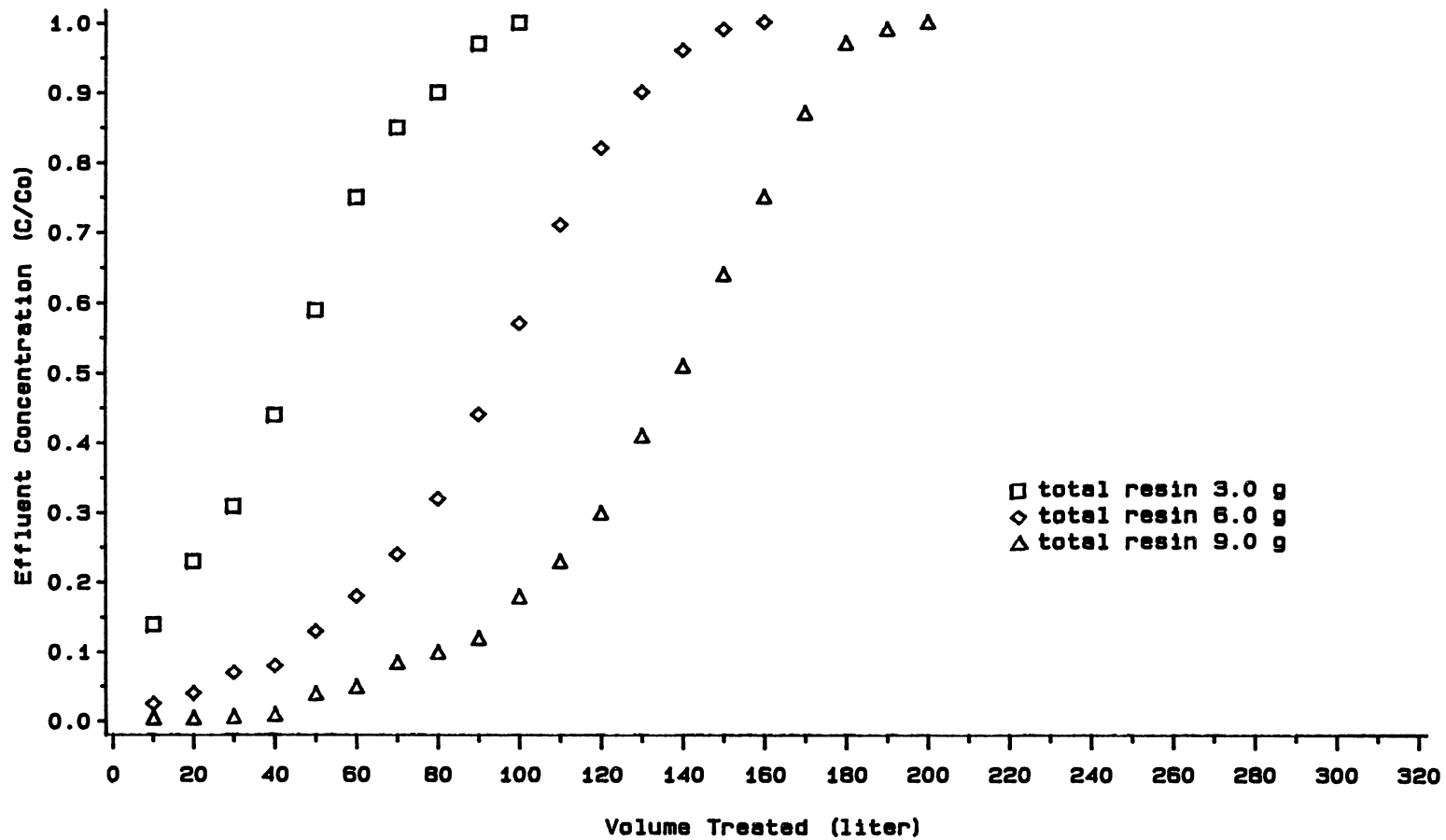


Figure 8. Sodium Breakthrough Curves for Cation/Anion Resin Ratio of 1/1.5

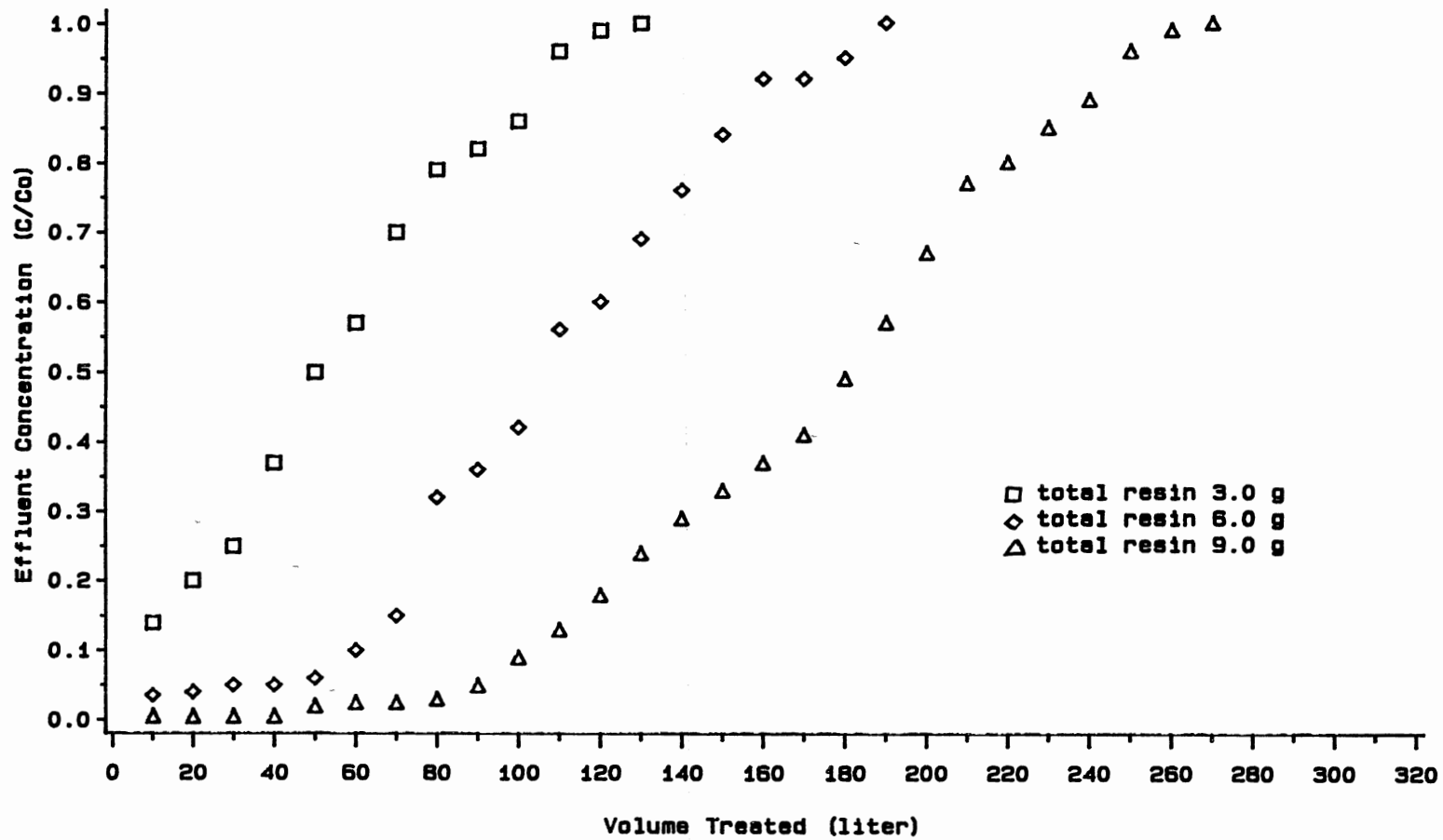


Figure 9. Sodium Breakthrough Curves for Cation/Anion Resin Ratio of 1/1

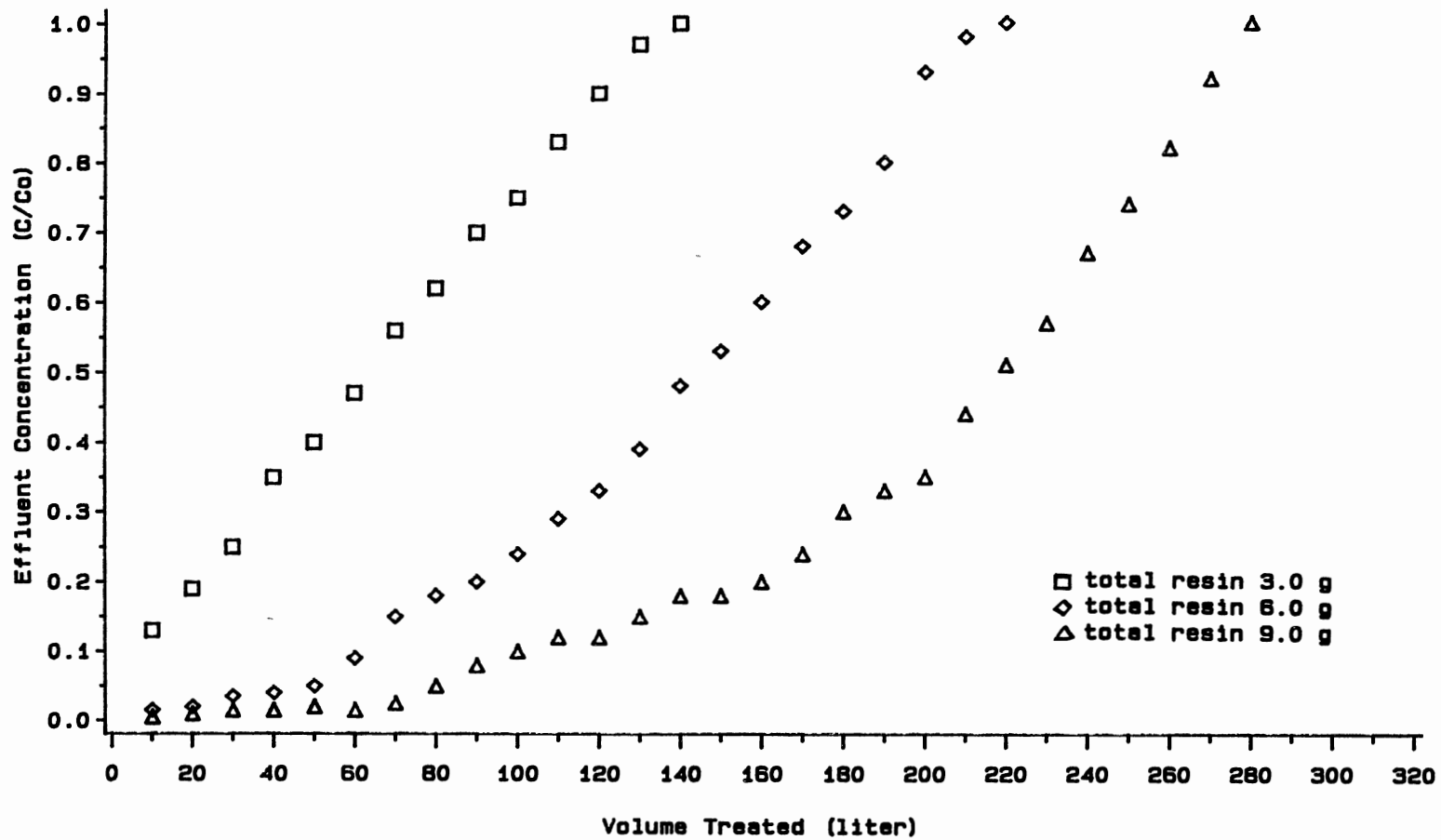


Figure 10. Sodium Breakthrough Curves for Cation/Anion Resin Ratio of 1.5/1

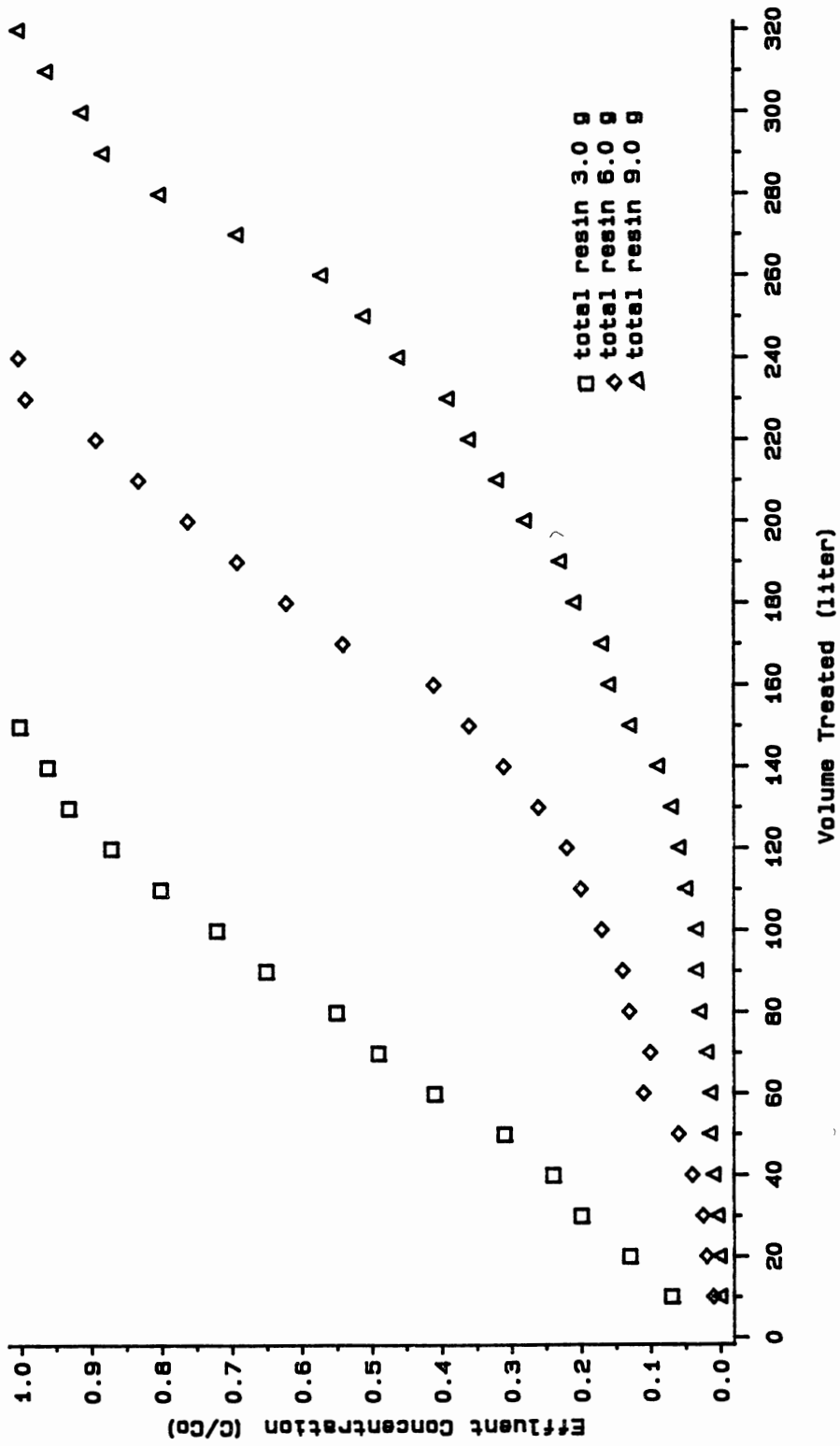


Figure 11. Sodium Breakthrough Curves for Cation/Anion Resin Ratio of 2/1

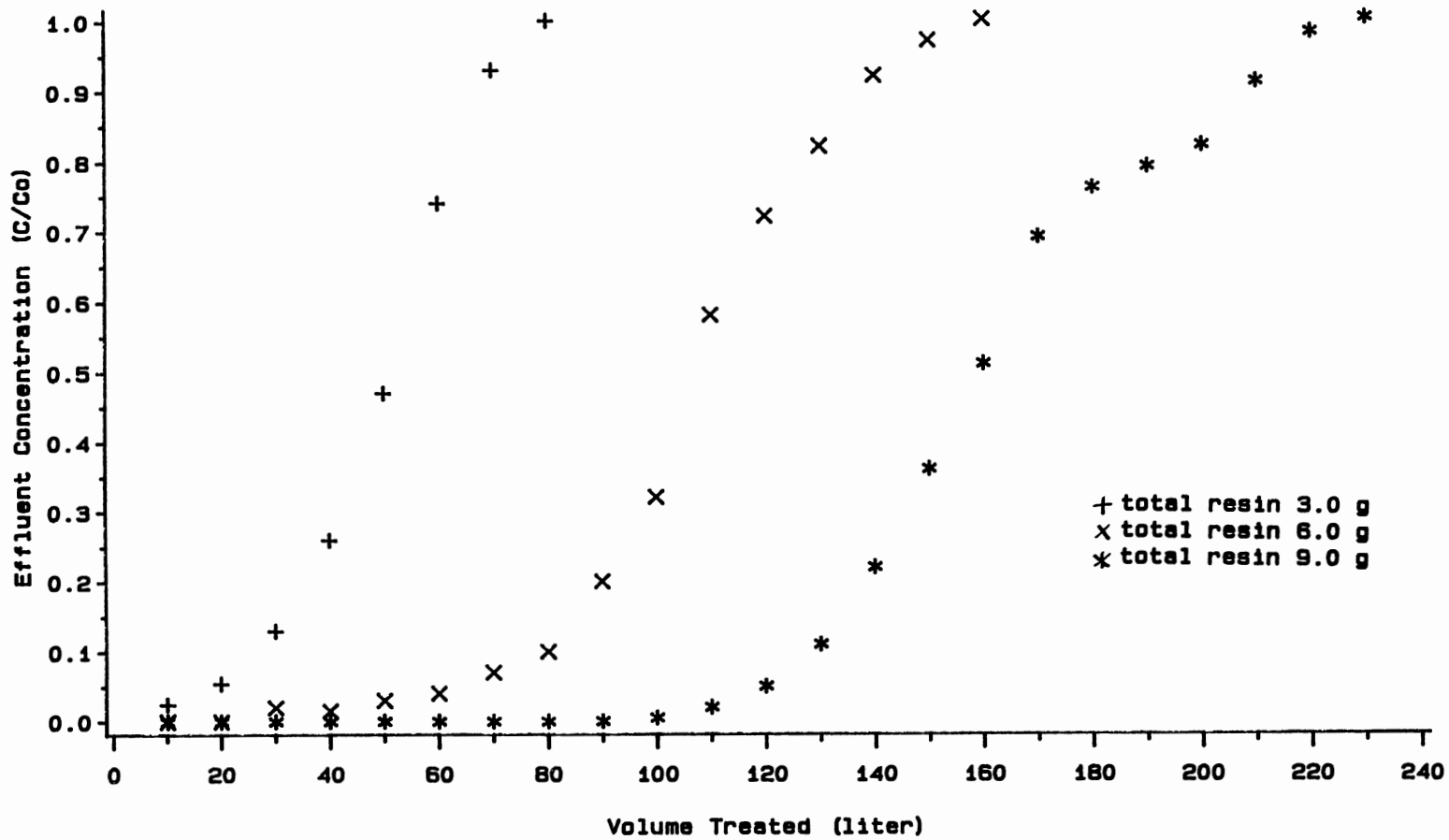


Figure 12. Chloride Breakthrough Curves for Cation/Anion Resin Ratio of 1/2

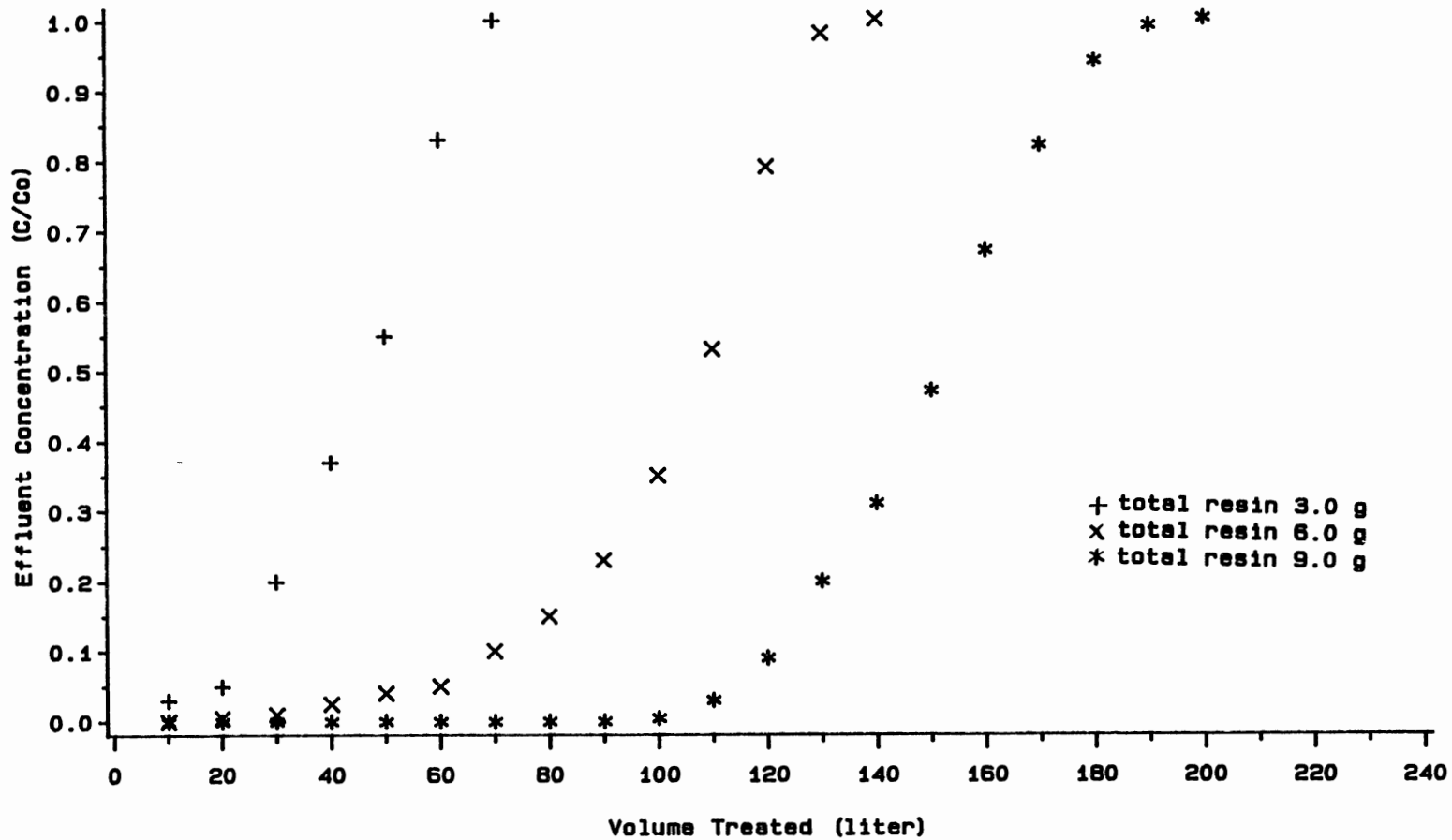


Figure 13. Chloride Breakthrough Curves for Cation/Anion Resin Ratio of 1/1.5

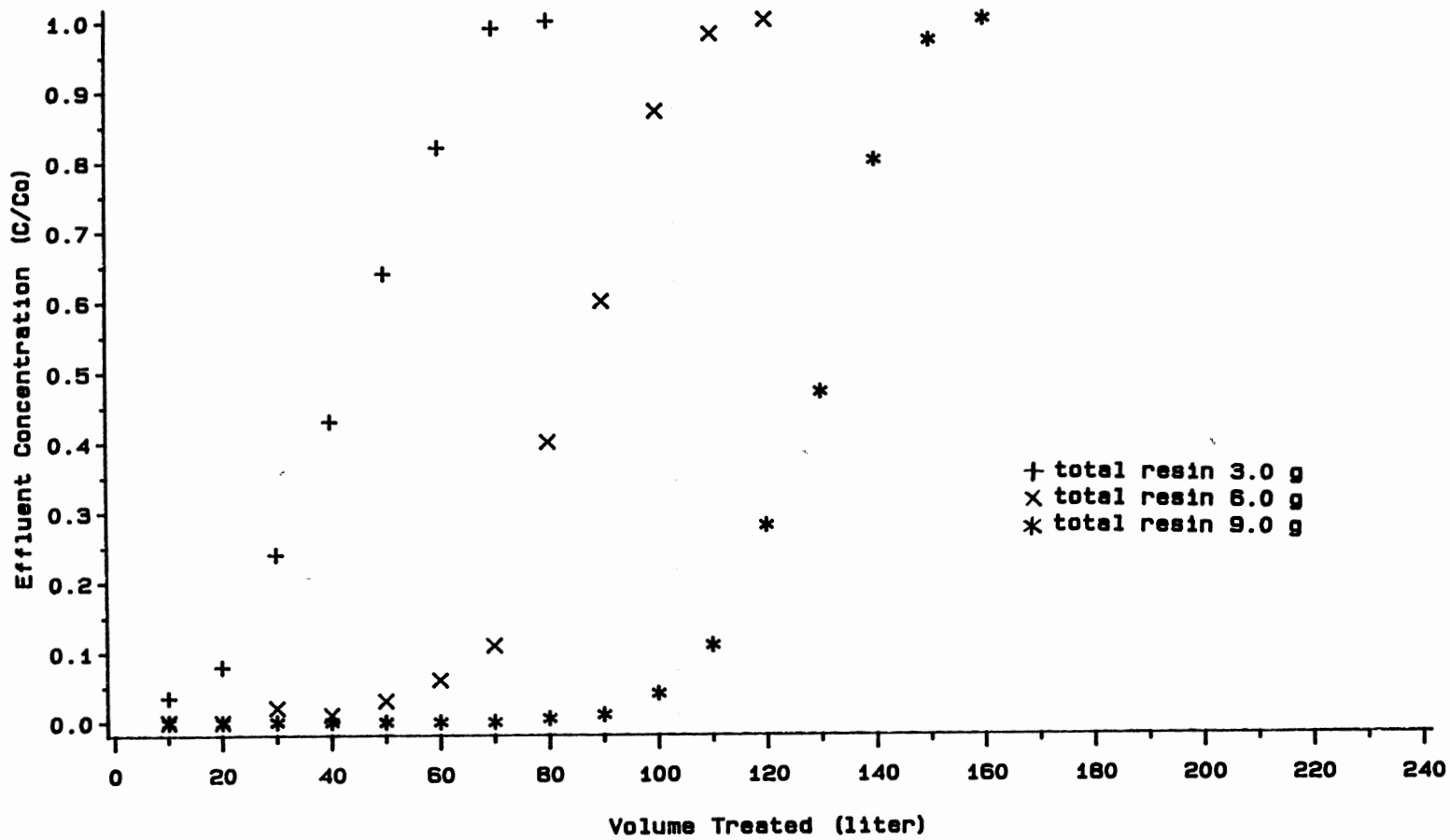


Figure 14. Chloride Breakthrough Curves for Cation/Anion Resin Ratio of 1/1

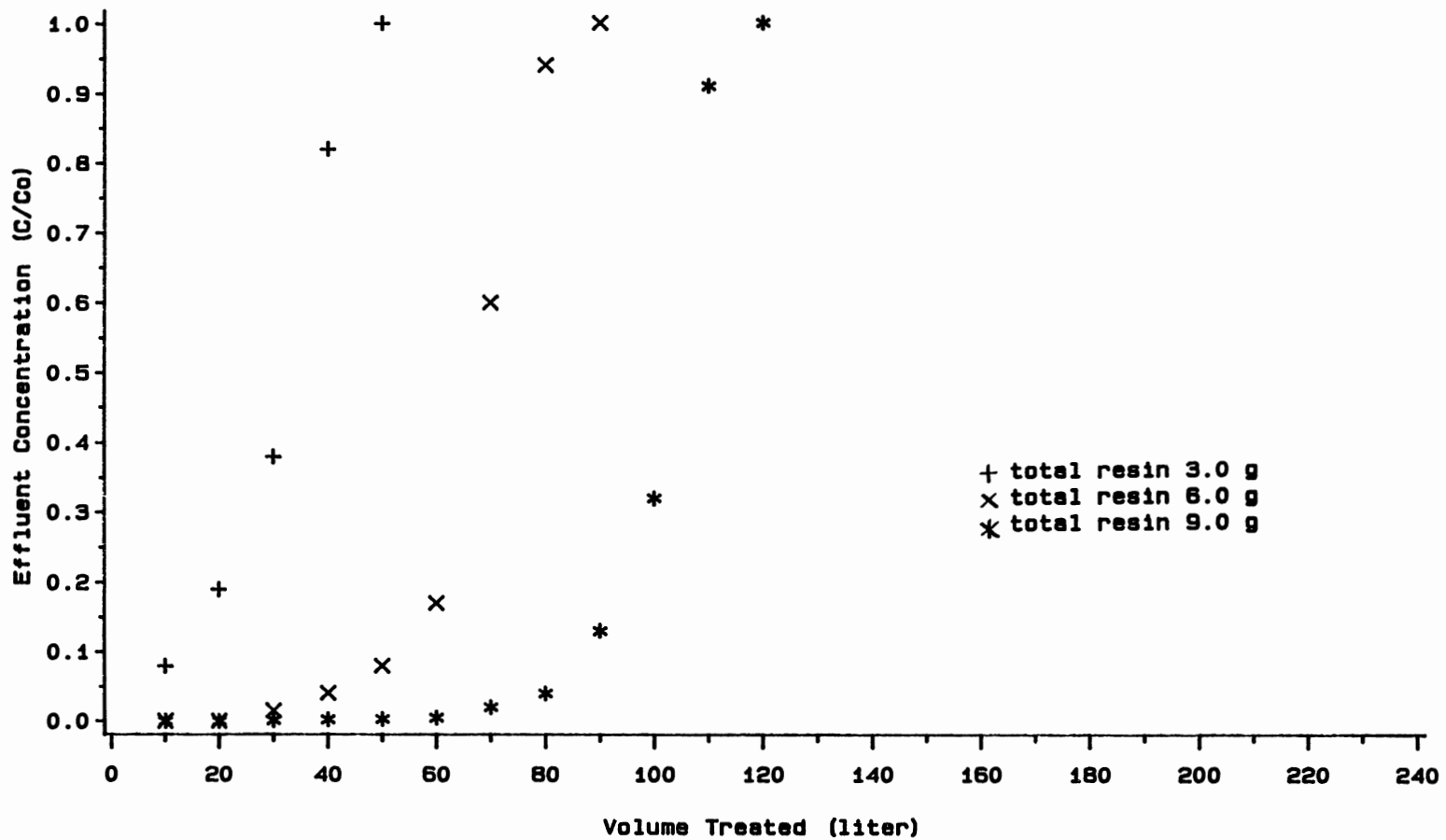


Figure 15. Chloride Breakthrough Curves for Cation/Anion Resin Ratio of 1.5/1

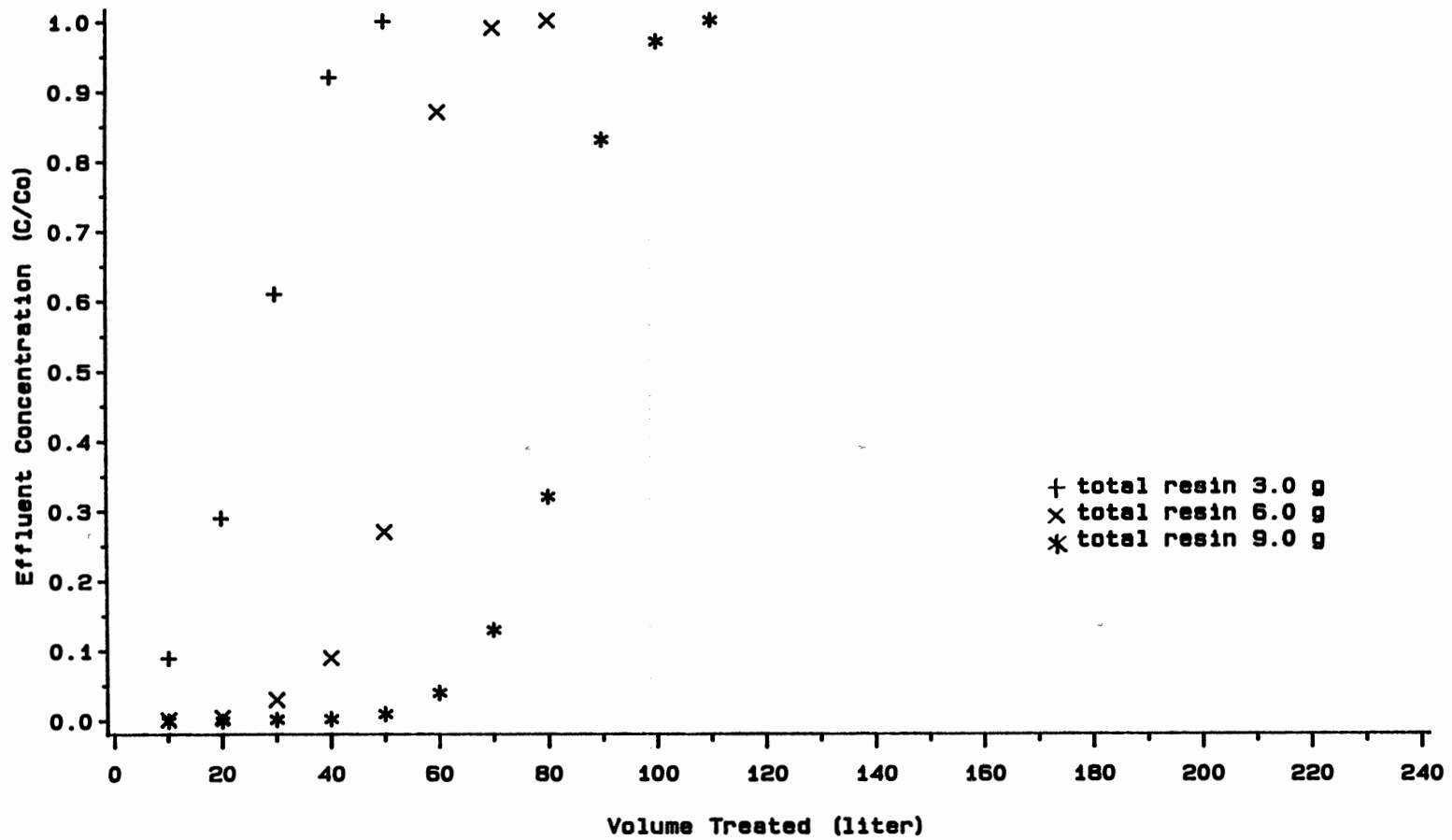


Figure 16. Chloride Breakthrough Curves for Cation/Anion Resin Ratio of 2/1

than anion effluent concentration. This will be due to the larger selectivity coefficient of anion-exchange resin than cation-exchange resin. The levels of leakage for anion exchange are almost constant, with a very low level for a lengthy period of time before the breakthrough curves started to rise. This is true except for very short beds because of insufficient contact between solution and resin. The levels of leakage for cation exchange are also almost constant for a long bed depth (total resin amount of 6.0 g or 9.0 g), but relatively broad compared to leakage levels for anion exchange.

Vermeulen and Hiester (1959) pointed out that the shape and position of a breakthrough curve depend upon equilibrium, rate, and stoichiometry. The equilibrium isotherms for the system influence the breakthrough curves especially when the equilibrium is very favorable or very unfavorable (Vermeulen, et al., 1984). Thus, the selectivity coefficient for the exchange influences the breakthrough curve, i.e., the relative steepness or sharpness of breakthrough curves (Vermeulen and Hiester, 1959, Helfferich, 1962). The more favorable the equilibrium is, the steeper the breakthrough curve. The limiting slope of the breakthrough curve is reached in a shorter height of bed for a favorable equilibrium, while an unfavorable equilibrium gives a more gradual and

nonsharpening breakthrough curve for a given set of diffusion coefficients. For a favorable equilibrium, breakthrough curves appear identical in pattern, while for an unfavorable equilibrium, breakthrough curves show a pattern of behavior proportionate to the bed volume or time through which it passes. The exchange wave continues to spread with distance through the column. Since the liquid-film diffusion rate control is assumed in this study, liquid-phase diffusion coefficients of ions, and selectivity coefficients for the sodium-hydrogen and chloride-hydroxide exchange will influence the breakthrough curve. Diffusion coefficients of the involved ions and selectivity coefficients for the exchange are properties of their own system. Thus, an accurate model which includes the rate expression with the appropriate system parameters predicts the behavior of the breakthrough curve.

Sodium breakthrough curves show that the leading band becomes diffuse as it progresses through the column, especially in Figures 9 through 11 with relatively large cation resin amount. This is partly because of relatively unfavorable equilibrium of cation-resin selectivity coefficient for sodium-hydrogen exchange of 2.0-2.5. This trend coincides with the results of Lapidus and Rosen (1954) who used hydrogen-form Dowex 50 for NaCl solution. Chloride breakthrough curves in

Figures 12 through 16 show a consistent pattern of behavior. However, the response is not as consistent as expected, considering the very favorable equilibrium as indicated by a selectivity coefficient for chloride-hydroxide of 15-18. This can be explained by the claims of Coppola and Levan (1983) who studied adsorption with a constant pattern behavior in shallow beds. They claimed that the exchange wave approaches the constant pattern shape in deep beds with a favorable equilibrium, which corresponds to the maximum possible breadth of the mass-transfer zone. However, the mass-transfer zone can occupy a substantial fraction of the total bed length in shallow beds, so the constant pattern shape is not approached in shallow beds and the shape of breakthrough depends on the bed depth. The bed depths of our experimental columns are higher than typical shallow beds. For the total resin amount of 6.0 g or 9.0 g, the constant pattern is observed, but a slightly inconsistent pattern is observed for 3.0 g in Figures 12 through 16. Inconsistent pattern in Figures 15 and 16 is more serious than in Figures 12, 13, and 14. This effect is due to the bed depth, and our configuration is between shallow bed and deep bed. This trend is also observed in sodium breakthrough curves. Thus, generally speaking, the parameter of bed depth affects the pattern of the sodium breakthrough curve but not the chloride breakthrough

curve in sufficiently deep beds because of the selectivity difference.

Effluent Concentration as a Function of Resin Ratio

Using Figures 7 through 16 from the experimental conditions in Table II, the effects of the cation-to-anion resin ratio on the effluent concentration can be observed. Five resin ratios for the total dry resin weights of 3.0, 6.0, and 9.0 g give each five crossover points of cation and anion breakthrough curves. These are not plotted in the figures since ten breakthrough curves are hard to distinguish in a figure, however Table III presents the numerical values of crossover points of sodium and chloride breakthrough curves.

The capacities of used cation-exchange resin (Ambersep 200 H; 1.6-1.7 eq/liter) and anion-exchange resin (Ambersep 900 OH; 0.8-0.9 eq/liter) are different in this study. The conditions of the cation-to-anion resin ratios of 1/1.5, 1/1, 1.5/1, and 2/1 are expected to have higher cation-exchange rates than anion-exchange rates, while resin ratio of 1/2 is expected to have almost even cation and anion-exchange rates. However, because of some other parameters which influence the ion-exchange phenomena, the behavior of breakthrough curves are not simply dependent only on resin capacity. As mentioned in previous sections, selectivity coefficients

of resins, mass-transfer coefficients for packed beds, and diffusion coefficients of ions are expected to affect the shape of the breakthrough curve. The selectivity of the resin towards the exchanging ions determines the sharpness of the exchange wave.

TABLE III
CROSSOVER POINTS OF SODIUM AND CHLORIDE
BREAKTHROUGH CURVES

Cation/Anion (dry weight)	Volume Treated (L), C/Co		
	3.0 g	6.0 g	9.0 g
1/2	74, 0.95	-----	-----
1/1.5	40, 0.42	120, 0.82	185, 0.98
1/1	24, 0.22	70, 0.15	110, 0.15
1.5/1	11, 0.12	30, 0.03	70, 0.02
2/1	-----	10, 0.02	40, 0.01

Some sodium and chloride breakthrough curves cross at a point regardless of the different total amounts of mixed resin in the column, and some do not cross. Since anion-exchange resin has a higher selectivity coefficient than cation-exchange resin, the chloride breakthrough curve is much steeper than the sodium breakthrough curve

as shown in Figures 7 through 16. This is why sodium and chloride breakthrough curves meet at a point if the amount of one resin is not much larger or smaller than the other resin in the mixed bed. The crossover points of sodium and chloride breakthrough curves have the trends that the lower cation-to-anion resin ratio shows the higher effluent concentration or treated volume of the crossover point regardless of the total resin amount. The numerical values of effluent concentrations and treated effluent volume at crossover points as a function of resin ratio are listed in Table III.

Effect of Oppositely-Charged Resin on Breakthrough Curves

To investigate the effects of anion-exchange resin on sodium breakthrough curves and cation-exchange resin on chloride breakthrough curves in the mixed bed, experiments were performed by adding 1.0, 3.0, and 5.0 g of the oppositely-charged resin to 3.0 g of each cation or anion exchange resin. These conditions are given in Table IV.

The effects of anion-exchange resin on sodium breakthrough curve and cation-exchange resin on chloride breakthrough curve are plotted in Figures 17 and 18, respectively. As shown in Figure 17, the slope of the sodium breakthrough curve with higher anion-resin ratio (5.0 g of anion resin) is steeper than with the lower

anion-resin ratio (1.0 g of anion resin). Similarly, the slope of the chloride breakthrough curve with the higher cation-resin ratio (5.0 g of cation resin) is steeper than with lower ratio (1.0 g of cation resin) as shown in Figure 18. When Figures 17 and 18 are compared, the slope changes of both sodium and chloride breakthrough curves show similar trends except chloride breakthrough curve is steeper than sodium breakthrough curve.

TABLE IV
EXPERIMENTAL CONDITIONS FOR THE EFFECTS OF
OPPOSITELY-CHARGED RESIN ON
BREAKTHROUGH CURVES

Effect	Cation/Anion Resin (g/g)		
Cation Resin	1.0/3.0	3.0/3.0	5.0/3.0
Anion Resin	3.0/1.0	3.0/3.0	3.0/5.0

In these experiments, a neutral salt (NaCl) solution is used as a feed solution. Exchange resins are ionic forms of hydrogen and hydroxide for cation and anion exchange, respectively. The same amount of cation-exchange resin with smaller amounts of anion-exchange resin produces a faster rate of hydrogen exchange than with greater amounts of anion-exchange resin. This

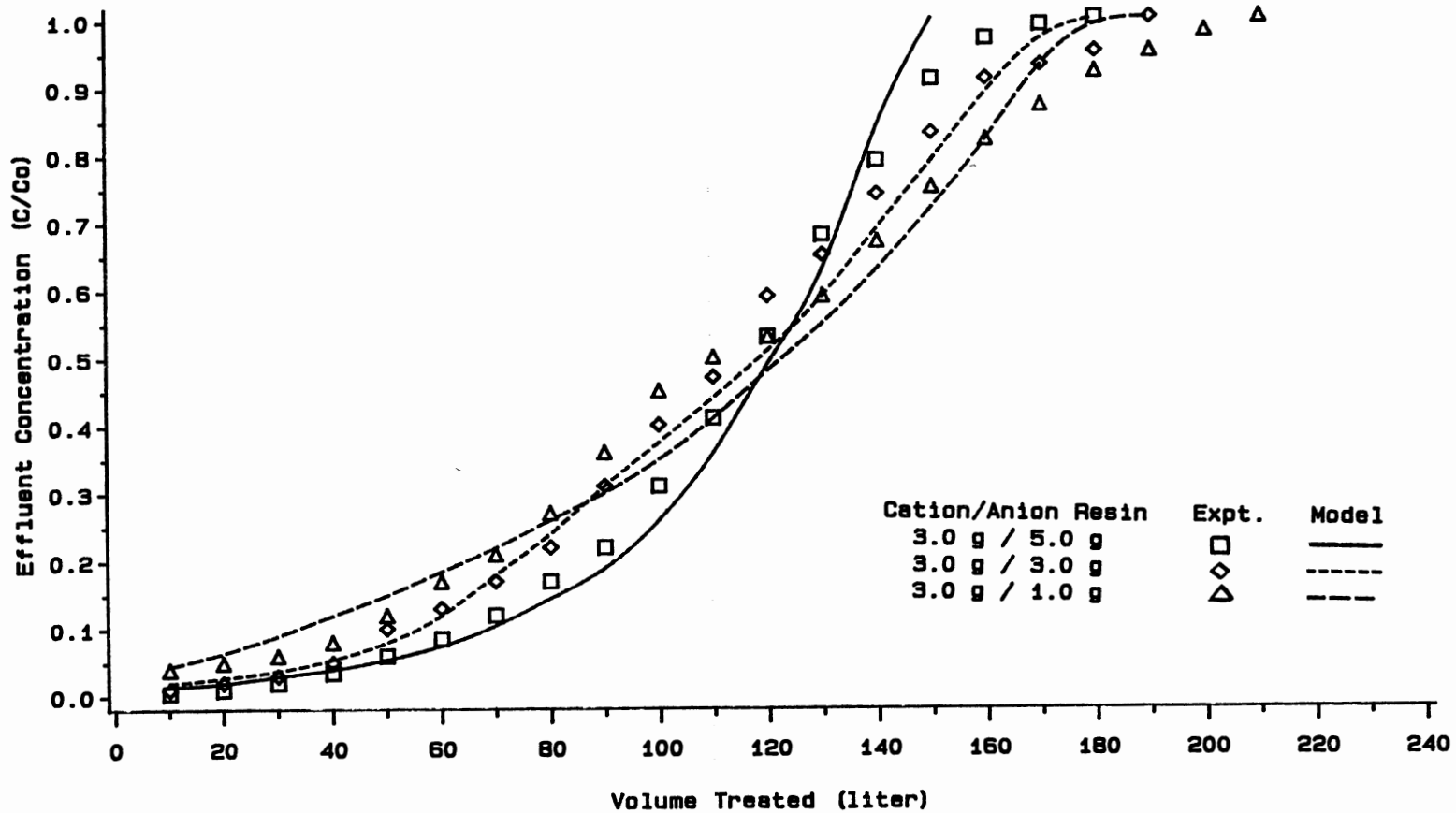


Figure 17. Experimental Results and Model Prediction of the Effect of Anion Exchange Resin on Sodium Breakthrough Curve

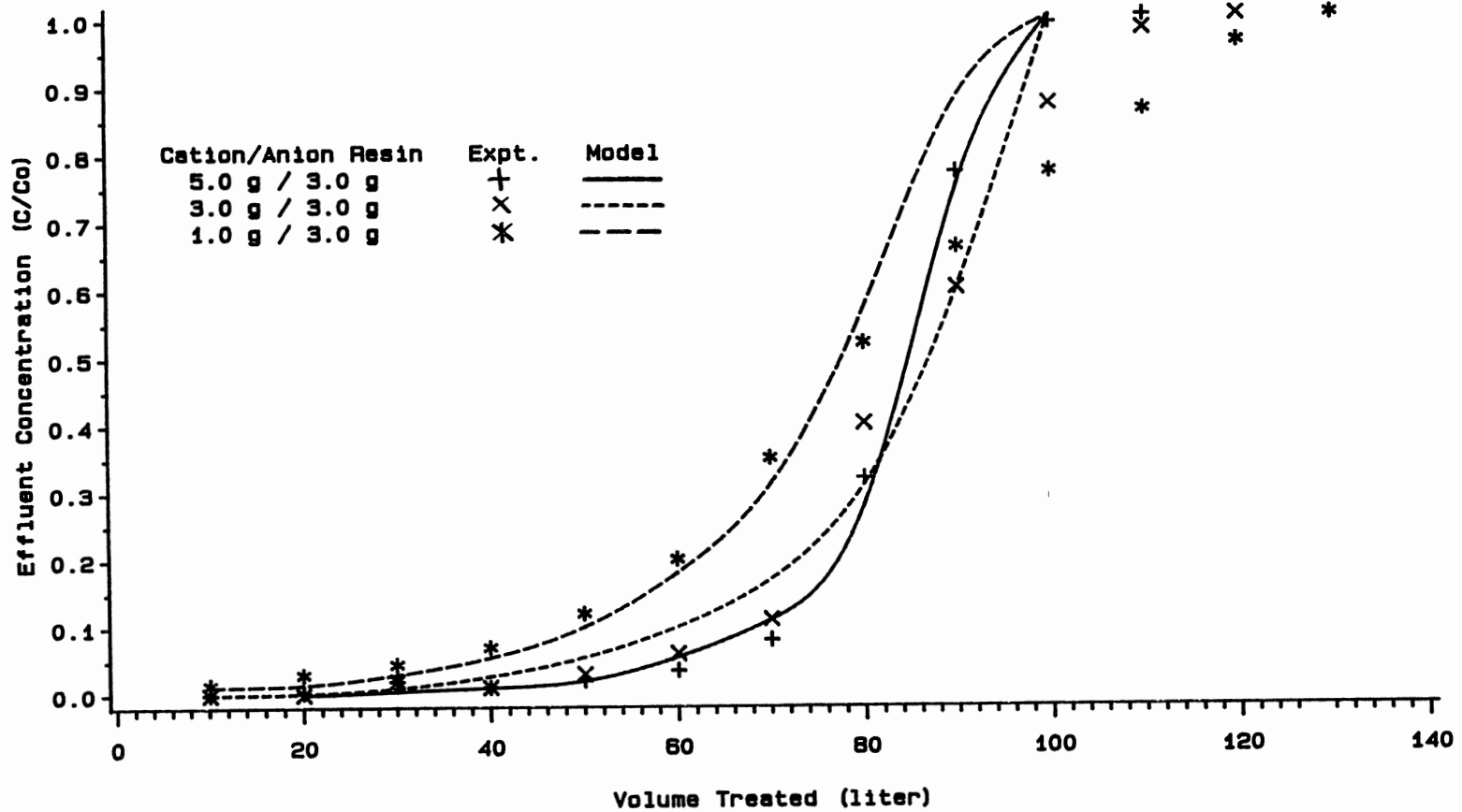


Figure 18. Experimental Results and Model Prediction of the Effect of Cation Exchange Resin on Chloride Breakthrough Curve

produces an aqueous phase with an acidic pH. On the contrary, cation-exchange resin with more anion-exchange resin produces a lower rate of hydrogen exchange, so the aqueous phase has an alkaline pH. The same effects can also be applied to the anion-exchange resin.

Harries (1988) showed the effect of pH of the aqueous phase in both cation and anion-exchange rates. He showed that the cation exchange is faster in an alkaline medium than a neutral or acidic medium since the mass-transfer coefficient of sodium is higher at high pH, while the anion exchange is more rapid in an acidic medium than a neutral or alkaline medium since the mass-transfer coefficient of chloride is higher at low pH. Thus, the cation exchange with a higher anion-exchange resin ratio produces a steeper sodium breakthrough curve, and anion exchange with a higher cation-exchange resin ratio produces a steeper chloride breakthrough curve. Cation or anion exchange with a lower oppositely-charged resin ratio produces a broad breakthrough curve. The experimental results in Figures 17 and 18 show the same trends as Harries (1988) claimed. The change of the cation-to-anion exchange resin ratio will thus change the pH of the aqueous phase within the bed, resulting in the change of the shape of the breakthrough curve. This is also compared with the model of Haub and Foutch (1986a). Figures 17 and 18 also show the model predictions which

use the same values of parameters of experimental conditions of Figures 17 and 18, respectively. The ionic-diffusion coefficients for this model are taken from Table VI in Chapter VI. The detailed explanation of the ionic-diffusion coefficients will be given in the following chapter. As shown in Figures 17 and 18, the model predicted the trends of breakthrough curves well for cation exchange, but a deviation is observed for anion exchange at the high concentration range, especially of the cation/anion resin ratio of 1.0g/3.0g. This is probably due to the lack of model prediction. Anion breakthrough curves in model prediction have a tendency to increase sharply. Another possibility is the larger selectivity coefficient, supplied by the manufacturer, than the actual value observed in experiments. However, this would not likely be the reason because Type I strong base anion-exchange resins have selectivity coefficients of 15 to 20 (Anderson, 1975).

Harries (1988) also pointed out that the influence of pH on the anion exchange is greater than that for the cation exchange. Thus, the slope change of anion breakthrough curve is greater than that of cation breakthrough curve when the resin ratio is changed. This is shown when the amount of cation resin is changed from 1.0 to 3.0 g in Figure 18, but not serious when the

cation resin is increased to 5.0 g. Sodium breakthrough curves in Figure 17 have similar slope changes when the anion resin is changed from 1.0 to 3.0 g and from 3.0 to 5.0 g.

Effect of Bed Homogeneity

The mixed-bed ion-exchange technique uses a single column of intimately mixed strong acid and strong base ion-exchange resins. This experiment uses the resins in hydrogen and hydroxide forms. The mixed-bed configuration is analogous to operating an infinite number of two stage ion exchangers in series to produce water. The complete mixing of the cation and anion-exchange resins in the mixed-bed column is important. Incomplete mixing will cause a partial separation of the mixed bed. This means that the lighter anion resin is rich in the upper portion of the column, and the cation resin is rich in the bottom of the bed. Thus, incomplete mixing will make anion exchange take place in a more acidic solution since upward flow was used in this experiment. Cation exchange will take place in a less alkaline solution. This results in a decreased cation exchange rate and an increased anion exchange rate.

This effect was investigated by comparing a totally segregated bed with a completely mixed bed. A totally mixed bed was prepared by the previous method. A totally

segregated bed was made by adding 3.0 g of anion resin through the top to the 3.0 g of cation resin on the bottom of the bed. The resultant breakthrough curves are shown in Figure 19. Although the anion exchange took place in a more acidic solution than a completely mixed bed, a similar shape of breakthrough curve was observed because the chloride-breakthrough curve is already steep. This is similar to Figure 18 when 3.0 g or 5.0 g of cation resin was used with 3.0 g of anion resin. Similar responses were observed in this Figure except when the anion resin was almost exhausted. However, the sodium breakthrough curve shows a broader shape than with a totally mixed bed. This is probably due to the low mass transfer rate because the solution is less alkaline than the totally mixed bed.

Unmixed Bed

Unmixed cation and anion-exchange resins were placed in two columns. Thus, this is not a mixed bed, but two homogeneous beds. This can be an extension to the effect of oppositely-charged resin on breakthrough curve, and this is an extreme condition. One column used 6.0 g of cation exchange resin, and the other column used 6.0 g of anion exchange resin. The experimental results are shown in Figure 20 for the sodium and chloride breakthrough curves simultaneously. Breakthrough curves are expected

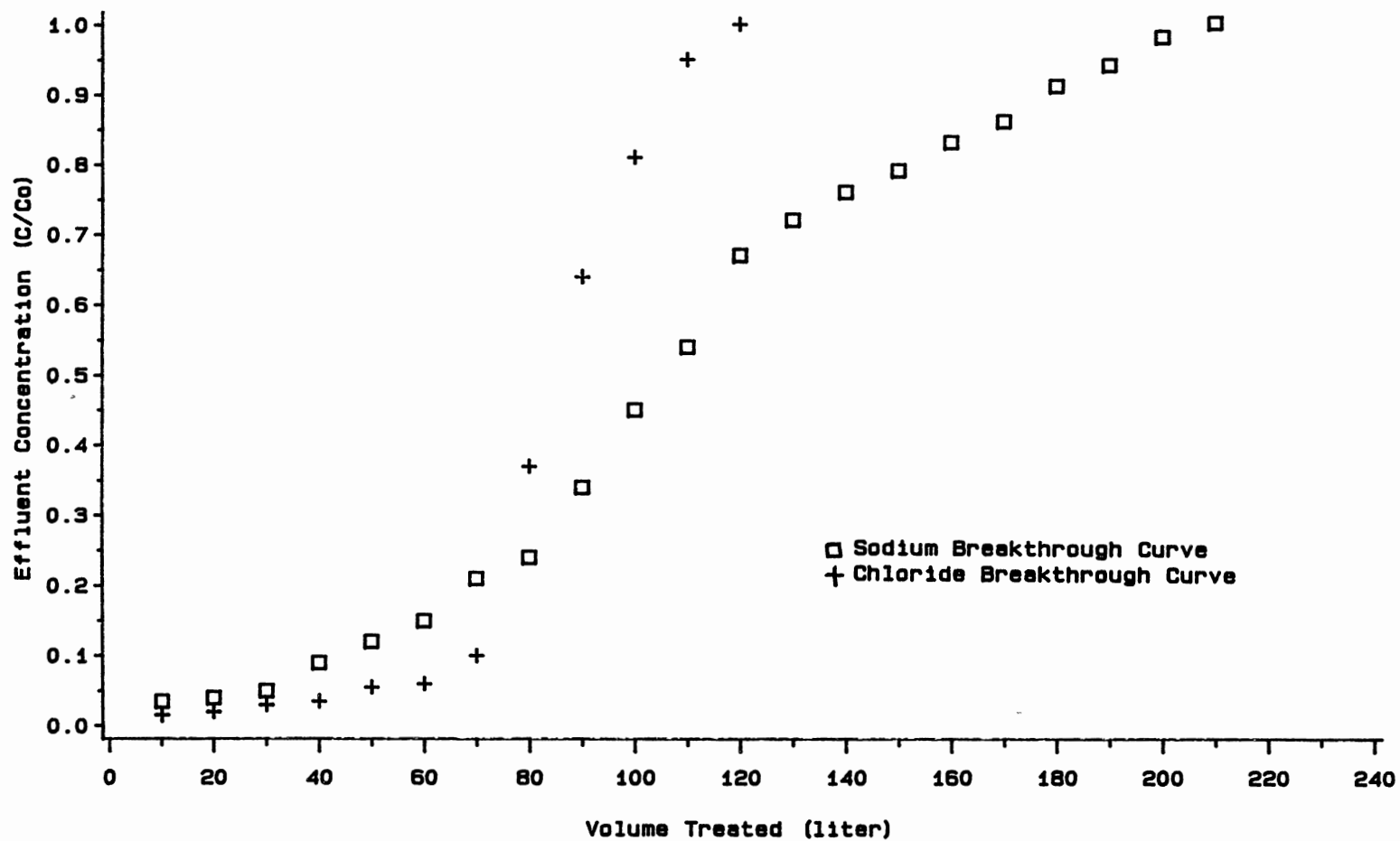


Figure 19. Effect of Bed Homogeneity
(Upper Anion Resin and Lower Cation Resin)

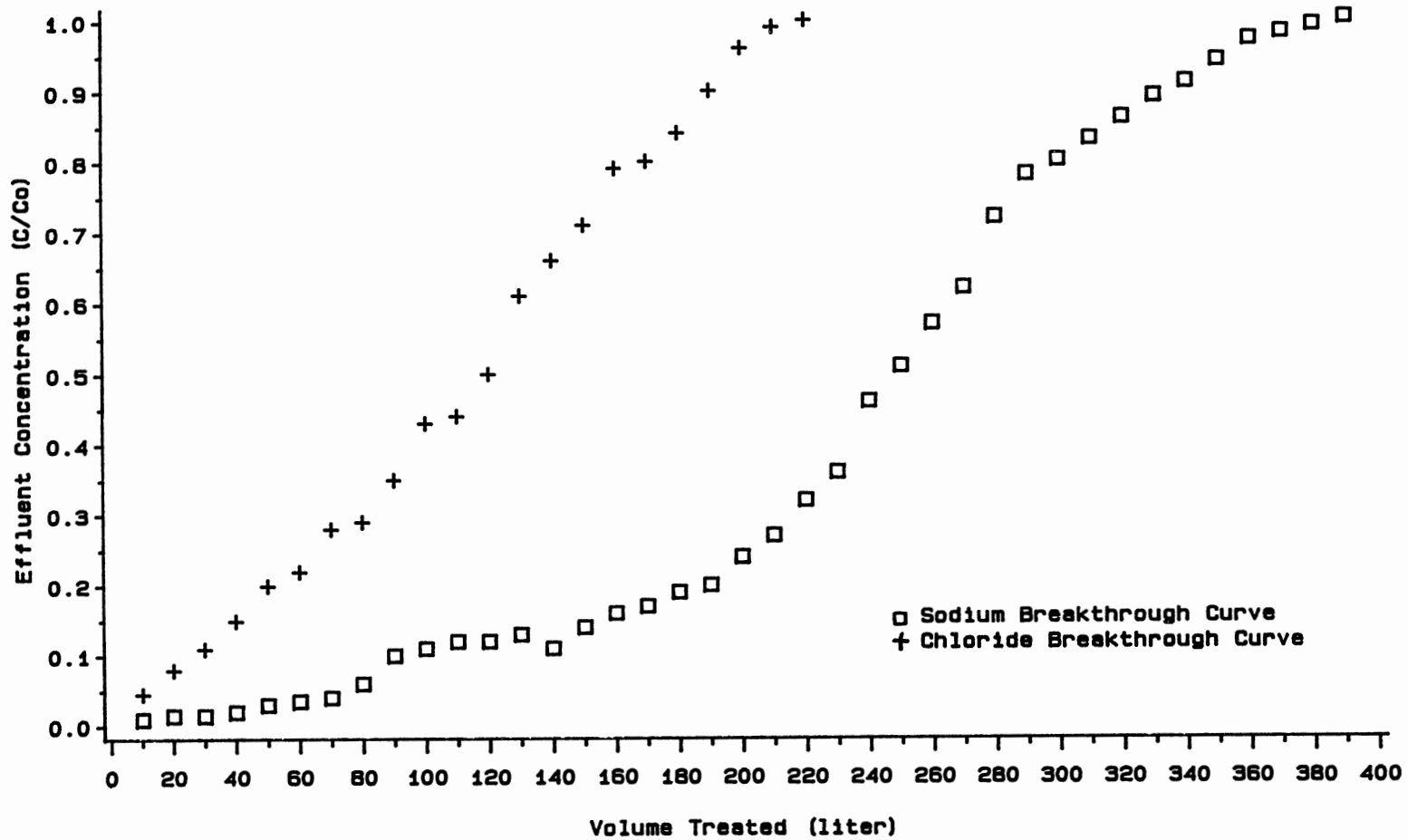


Figure 20. Sodium and Chloride Breakthrough Curves for an Unmixed Bed

to be very broad because of the low mass-transfer rates. In these extreme conditions, breakthrough curves are found to be almost linear in Figure 20.

CHAPTER VI

DISCUSSION

The experimental results of this study are compared with the mathematically developed model of Haub and Foutch (1986a). The deviations between the experimental and the theoretical results will be discussed in this Chapter. Using the different ionic-diffusion coefficients or the mass-transfer coefficients from the literature, experimental results will be discussed to describe the system. The correlations to the actual ionic-diffusion coefficients and mass-transfer coefficients for the mixed-bed ion-exchange model will be suggested.

Experimental Technique

The results from experimentally derived data from a laboratory scale test apparatus may predict the actual performance in industry. Many column configurations outlined in Chapters III and IV were tried, and glass columns with upward flow was chosen to obtain effluent concentrations as a function of time and column position. Although upward flow in the glass mixed-bed column with a

frit solved the pressure drop problem due to resin blockage, this mixed-bed ion-exchange system is not observed in the literature. Maximum flow rate to maintain a homogeneous bed with the mixed cation and anion resins was lower than that of an industrial process. Thus, the method should be improved to get higher flow rates with a homogeneous mixed bed.

Accuracy and Reproducibility

The purpose of this study is to show the adequacy of a mathematically derived model, so accuracy and reproducibility of the experimental results follow to test the mathematical model.

Errors are basically associated with the quantitative measurements. The possible sources of errors are; preparation of feed solution with salt crystals and pure water, preparation of standard solutions for ion chromatography, measurement of dry resin weight, measurement of solution flow rates, temperature variation, and the analysis of ion chromatography.

Measurement of sodium chloride crystals to 0.0029 g by the electronic balance appeared to cause the biggest error, and the bound of this error was analyzed. Sample calculations of this error are shown in Appendix A. Errors caused by weight measurement of air dry resins in

the laboratory were not significant compared to the sodium chloride crystals, and the calculated errors are shown in Appendix A. All of the other errors are also calculated and shown in Appendix A. Accuracy of a well-mixed feed solution and constant flow rate was discussed in Chapter V. The standard deviation from average volumetric flow rate of 0.42 liter/hour for the condition of cation/anion resin ratio of 3.0 g/3.0 g in Figure 6 was found to be 0.00649 in Appendix A.

Experiments were duplicated in order to check the experimental reproducibility. A sample measurement of the reproducibility of the experiments is shown in Figure 21, where the breakthrough curves of two runs were made at condition of cation/anion resin ratio of 3.0 g/3.0 g of six months apart. The agreement is entirely satisfactory, with the difference of less than 3.0 % (Appendix A). Additional duplicated runs were not made to check reproducibility.

Mathematical Model of Haub and Foutch

The model of Haub and Foutch (1986a) approached the limit of water purity obtainable with neutralization reaction from the mixed-bed ion-exchange units. They treated cation and anion-exchange resins in a mixed bed separately which enabled the study of variation of the cation-to-anion resin ratio. As usual, this model made

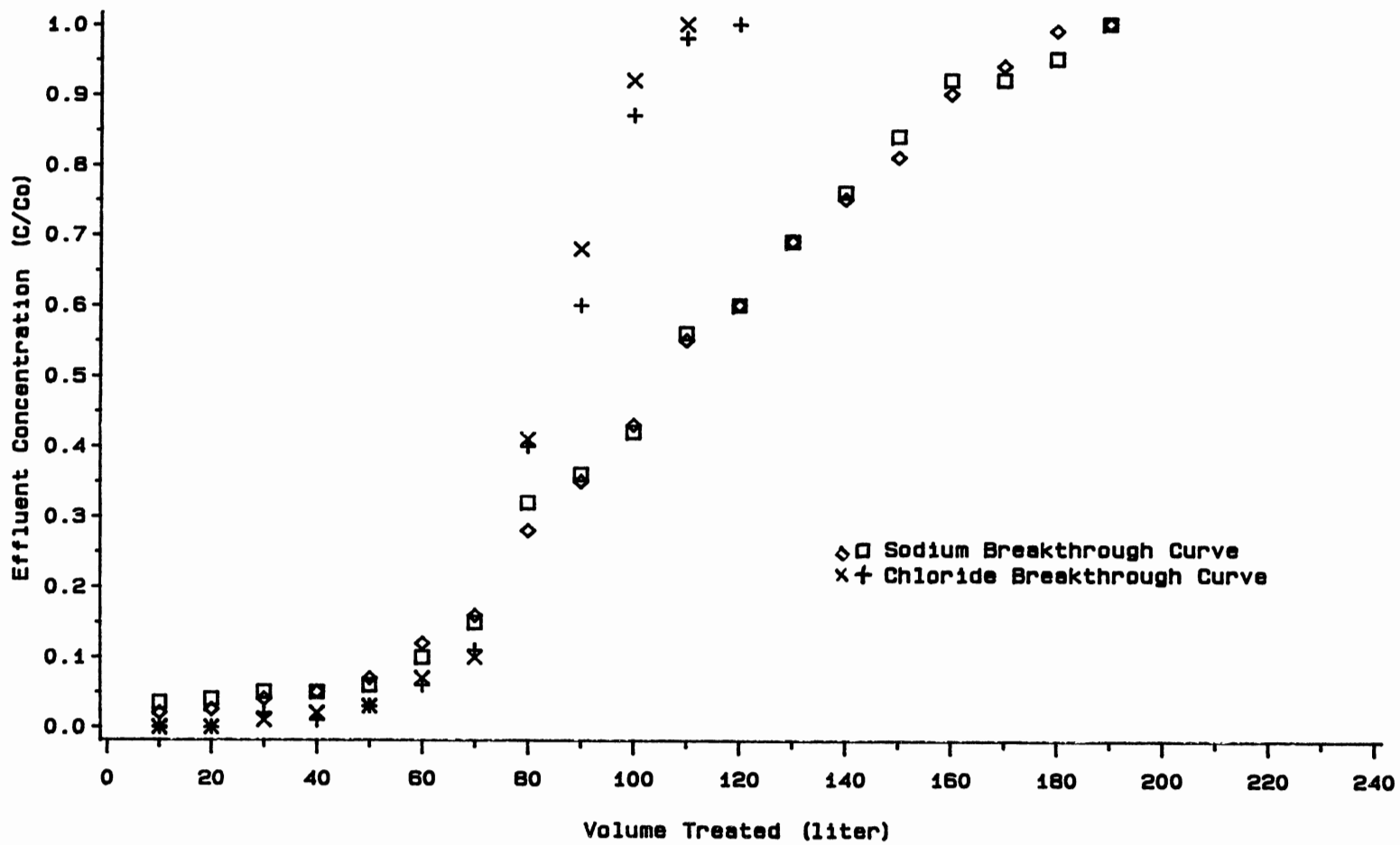


Figure 21. Reproducibility of Experiments for Cation/Anion Resin Ratio of 3.0 g/3.0 g

some simplifying assumptions; (1) uniform bulk liquid and surface compositions at the particle, (2) equilibrium at particle-film interface, (3) instantaneous neutralization reactions, (4) constant activity coefficient, i.e., unity in dilute solutions, (5) pseudo-steady state of mass transfer across the film layer, (6) isothermal conditions, and (7) neglected dispersion in the bed. The validity of these assumptions are well described in their paper (Haub and Foutch, 1986a).

Effluent ion concentrations on the order of one part per billion were obtained by taking into consideration reversible exchange, neutralization, and dissociation of water molecules in this model. Neutralization reactions occur at the resin-film interface, within the film, or in the bulk liquid due to the cation-to-anion resin ratio in the solution ionic composition.

The ionic flux equations were obtained by using the Nernst-Planck equation for the flux of each ion, and the static-film model for liquid-phase mass transfer in ion exchange. The nonionic mass-transfer coefficients for packed beds were obtained by using the correlations of Carberry (1960) and Kataoka, et al (1972). These coefficients account for the bed geometry and fluid flow effects in the ion-exchange rates. The correlations of Carberry and Kataoka, et al., are, respectively,

$$k_1 = 1.15 \frac{u}{e} (\text{Sc})^{-2/3} (\text{Re})^{-1/2} \quad (2)$$

and

$$k_1 = 1.85 \frac{u}{e} \left(\frac{e}{1-e}\right)^{1/3} (\text{Sc})^{-2/3} (\text{Re})^{-2/3} \quad (3)$$

For Reynolds numbers above 20, Carberry's equation was used. For Reynolds numbers below 20, the equation of Kataoka, et al., was used to get the mass-transfer coefficients.

The bulk-phase neutralization model considered two coions and the water dissociation equilibrium. The conditions of electroneutrality, no net current flow, and no net flux of coions were used to solve flux expressions. The general results were given in terms of an effective system diffusivity. The effective system diffusivity for cation exchange, D_e , depending on the ratio of existing to entering ion diffusivities, β_1 , selectivity coefficient, K_A^B , and equivalent fraction in resin phase, y_N , for neutralization in the bulk phase is expressed as

$$D_e = \frac{2\beta_1 D_{Na}}{(1 - \beta_1)(1 - X)} (\text{SX} + X - Y - 1) \quad (4)$$

where

$$X = \frac{C_{Na}^*}{C_{Na}^o} = \left[\frac{(\beta_1 Y + 1)(Y + 1)}{(\beta_1 S + 1)(S + 1)} \right]$$

$$S = K_H \frac{1 - Y_{Na}}{Y_{Na}}$$

$$Y = \frac{C_H^o}{C_{Na}^o}$$

$$\beta_1 = \frac{D_H}{D_{Na}}$$

The liquid-film neutralization model assumes a neutral bulk phase, and the ionic flux equations were obtained by combining flux expressions of two film sections for each cation or anion resin. This model adds system restraints, for example, $C_{OH} = C_H = 10^{-7}$ M at the reaction plane in addition to the conditions of the bulk-phase neutralization. The effective system diffusivity was derived with the relative position of the reaction plane to the total film thickness. The effective system diffusivity for anion exchanger of the liquid-film neutralization model is expressed as

$$D_e = \frac{(I)}{(1 - h)(C_{Cl}^o)(1 - C_{Cl}^*/C_{Cl}^o)} \quad (5)$$

where

$$I = \int_{C_{Cl}^o}^{C_{Cl}^r} \left[\frac{2D_{Cl}D_H(C_{Cl}C_H + 10^{-14})}{2D_H10^{-14} + D_H C_{Cl}C_H + D_{Cl}C_{Cl}C_H} \right] dC_{Cl}$$

$$h = \frac{2 D_{OH}D_{Cl}C_{Cl}^o (C_{OH}^o/C_{Cl}^o + C_{Cl}^r/C_{Cl}^o - Y)}{(-I) (D_{Cl} - D_{OH}) + 2D_{OH}D_{Cl}C_{Cl}^r (C_{OH}^r/C_{Cl}^r + C_{Cl}^o/C_{Cl}^r - Y)}$$

$$\frac{C_{Cl}^*}{C_{Cl}^o} = \frac{Y_{Cl}(A)^{1/2}}{[(\beta_2(1 - Y_{Cl})^{Cl}K_{OH} + Y_{Cl})((1 - Y_{Cl})^{Cl}K_{OH} + Y_{Cl})]^{1/2}}$$

$$Y = (A)^{1/2} \left[\frac{(1 - Y_{Cl})^{Cl}K_{OH} + Y_{Cl}}{\beta_2(1 - Y_{Cl})^{Cl}K_{OH} + Y_{Cl}} \right]^{1/2}$$

$$A = \left[\beta_2 \frac{C_{OH}^r}{C_{Cl}^o} + \frac{C_{Cl}^r}{C_{Cl}^o} \right] \left[\frac{C_{OH}^r}{C_{Cl}^o} + \frac{C_{Cl}^r}{C_{Cl}^o} \right]$$

$$\beta_2 = \frac{D_{OH}}{D_{Cl}}$$

The ionic-diffusion coefficients depend on the ionic concentration in solution, but the constant coefficients from the literature (Robinson and Stokes, 1959) were used in Equations (4) and (5) of the model of Haub and Foutch

(1986b). The ionic concentrations in the bed change with time and bed height. Thus, the exact ionic-diffusion coefficients for the system are needed to get a better model. This will be treated in the following sections.

System Parameters

As mentioned in Chapter V, many system parameters influence the performance of the mixed-bed ion-exchange column. Some of these parameters are interrelated. Since this thesis concentrates only on the effect of the cation-to-anion resin ratio for the packed bed, resin-selectivity coefficients, mass-transfer coefficients and ionic-diffusion coefficients strongly impact the shape of the breakthrough curves. Other system parameters are set to be constant.

Many resin properties, such as capacity, the degree of cross-linking, the physical and chemical nature of the polymer matrix, and the number of ions in the resin, influence resin selectivity. Thus, the selectivity coefficients for the sodium-hydrogen and chloride-hydroxide ion exchange are a function of the resin itself. Although experimental methods (Chu, et al., 1962) and numerical values and calculation examples of resin-selectivity coefficient (Anderson, 1975) are given in the literature to approximate the coefficients for the system, the constant values from the manufacturer

(McNulty, 1989) will give a better approximation. The coefficients from the manufacturer are used for the computer simulation.

The single ionic-diffusion coefficients in liquid phase are believed to be strongly dependent on other ions present and solution concentration in addition to a function of temperature. The single ionic-diffusion coefficients in water have been measured by many investigators (Robinson and Stokes, 1959; Harries and Ray, 1984; Petruzzelli, et al., 1987b). The coefficients of Petruzzelli, et al. (1987b), were calculated as limiting diffusivity at infinite dilution. The coefficients of Robinson and Stokes (1959) were derived from conductance data, and the coefficients of Harries and Ray were for 20°C from Robinson and Stokes. These coefficients were normally supported by a small amount of data, and experimental measurements should be made for a variety of systems. The single ionic-diffusion coefficients in water were used to describe the mixed-bed ion-exchange system (Harries and Ray, 1984, Haub and Foutch, 1986b).

Recently, Zecchini (1989) suggested an equation to calculate the single ionic-diffusion coefficients at dilute multi-ionic solutions. From the Nernst-Haskell equation for dilute solutions, the diffusion coefficient

based on molecular concentration can be calculated, for example in this study, as

$$D_{\text{NaCl}} = \frac{R T [(1/n_{\text{Na}}) + (1/n_{\text{Cl}})]}{F^2 [(1/q_{\text{Na}}) + (1/q_{\text{Cl}})]} \quad (6)$$

where the limiting ionic conductances q of Na, H, Cl, and OH at 25°C are 50.1, 349.8, 76.3, and 197.6 (A/cm²) (V/cm) (g-equiv/cm³), respectively (Reid, et al., 1987).

Involved ionic pairs for H are H-OH and H-Cl, for Na are Na-OH and Na-Cl, for OH are Na-OH and H-OH, and for Cl are Na-Cl and H-Cl. The diffusion coefficients for the ionic pairs are obtained using Equation (6). The ionic-diffusion coefficient for H is obtained as

$$D_{\text{H}} = \frac{1}{1/D_{\text{H-OH}} + 1/D_{\text{H-Cl}}} \quad (7)$$

The ionic-diffusion coefficients for Na, OH, and Cl can also be obtained in a similar manner using Equation (7). The ionic-diffusion coefficients of Na, Cl, H, and OH at a dilute solution in the literature and obtained by the suggestion of Zecchini (1989) are shown in Table V. The values from Robinson and Stokes (1959) were obtained from the following Equation (8) instead of Equation (7);

$$D_{\text{H}} = \left(\frac{R T}{F^2} \right) q_{\text{H}} \quad (8)$$

Equation (8) is obtained from Equation (6) by applying a single ion instead of a molecule.

TABLE V
 IONIC-DIFFUSION COEFFICIENTS IN DILUTE SOLUTIONS
 (VALUES IN 10^{-5} CM²/SEC)

Reference	D _{Na}	D _{Cl}	D _H	D _{OH}	Temperature (°C)
Robinson and Stokes (1959)	1.33	2.03	9.31	5.28	25
Harries and Ray (1984)	1.19	1.84	8.65	4.85	20
Petruzzelli, et al. (1987b)		0.976			25
Zecchini (1989)	0.916	1.085	2.23	1.615	25

The ionic-diffusion coefficients show a difference of more than four times for hydrogen ion. This is also true for the diffusivity coefficients within the ion-exchange resin. The variation of the single ionic-diffusion coefficient in the resin phase is of the order of two to three (Graham and Dranoff, 1982b).

With the diffusion coefficients of ions in water from the literature, the mixed-bed ion exchange was simulated using the model of Haub and Foutch (1986b).

Figure 22 compares the breakthrough curves of cation/anion resin ratio of 3.0 g/3.0 g from the experimental data in this study with theoretical results from the model of Haub and Foutch (1986b). The plot of effluent concentration (C/C_0) versus treated solution volume with the ionic-diffusion coefficients of Robinson and Stokes (1959) and Zecchini (1989) is shown in Figure 22. The results of Zecchini (1989) are closer to the experimental data than that of Robinson and Stokes (1959), but both breakthrough curves show much deviation from actual experimental data. Thus, these diffusion coefficients are inadequate to calculate the effective diffusion coefficients for the actual system. The following section suggests a new set of the single ionic-diffusion coefficients and correlation equations for use in the numerical model.

Diffusion Coefficients for the System

To get better results with the use of the Nernst-Planck equation in the mixed-bed ion-exchange model, better effective diffusivity should be chosen to fit the actual ion-exchange data. Helfferich (1965) found the most appropriate effective system diffusivity, and his derivations were thought to support the use of a constant effective system diffusivity for mixed bed. Tittle (1981) also used flux equations with a constant system

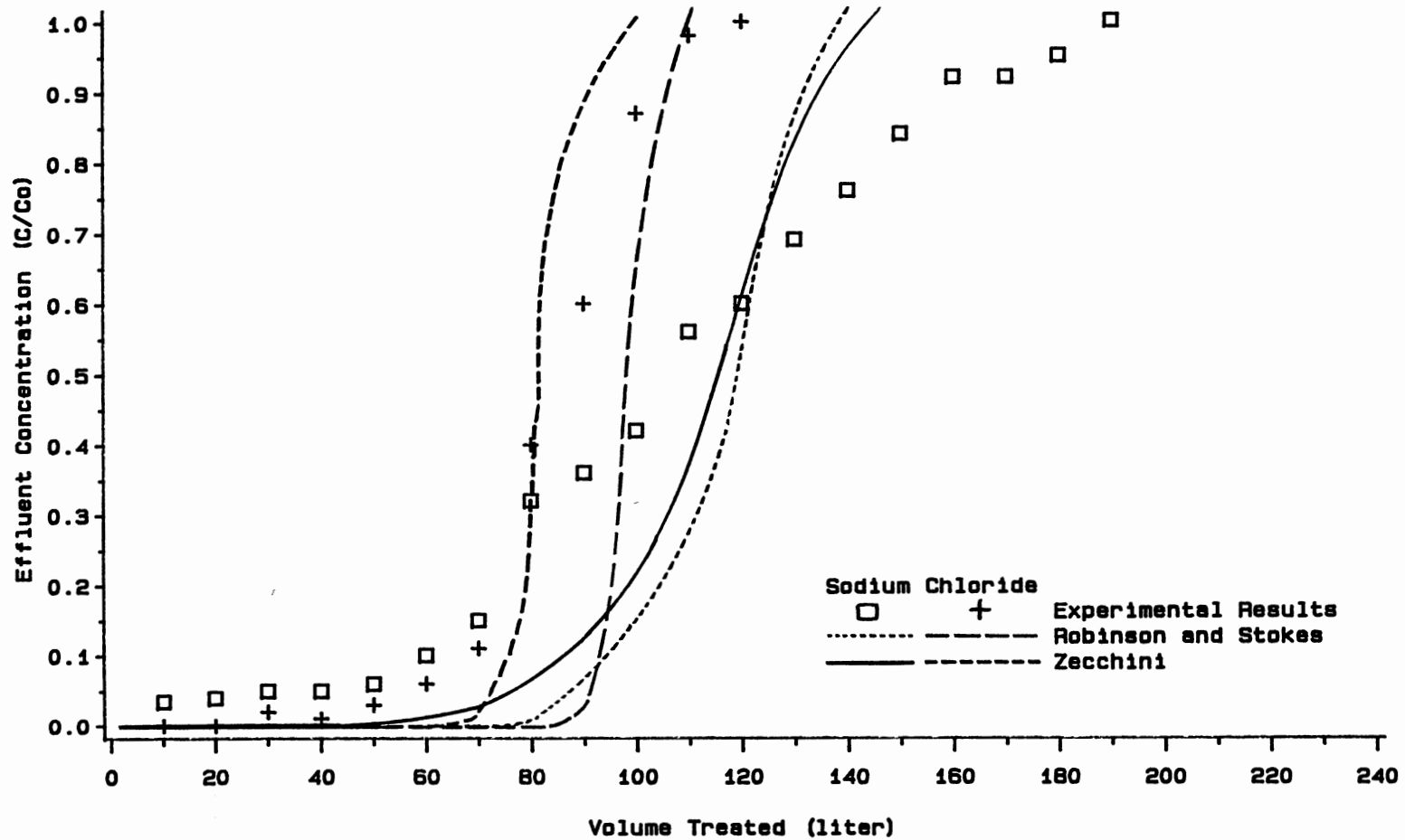


Figure 22. Breakthrough Curves of Experimental and Theoretical Results for Cation/Anion Resin Ratio of 3.0 g/3.0 g

diffusivity to model the mixed bed. From Equations (4) and (5), better diffusion coefficients of each ionic species are needed to get better effective system diffusivity which is not constant because the effective system diffusivity is a function of concentrations of ions. Figure 22 shows that the ionic-diffusion coefficient of each species from experiments appears to be much lower than the diffusion coefficients in the literature (Table V). Since uncertainty exists in the numerical value of effective diffusivity, the ionic-diffusion coefficients of single ions can be chosen to best fit the actual mixed-bed ion-exchange data to the model of Haub and Foutch (1986a).

To choose the ionic-diffusion coefficients, the order of magnitude of the values is changed from the values in the literature. When all of the coefficients are scaled down by a factor of ten, most plots of the theoretical results are close to the experimental data. By trial and error, the ionic-diffusion coefficients of sodium and chloride are determined as shown in Table VI. The coefficients in Table VI coincide with the results of Harries (1988) that the mass transfer coefficient varies with solution pH. The diffusion coefficients of hydrogen and hydroxide are constant.

TABLE VI
 IONIC-DIFFUSION COEFFICIENTS IN THE SYSTEM
 (VALUES IN 10^{-5} CM²/SEC)

Cation/Anion	D _{Na}	D _{Cl}	D _H	D _{OH}
1/2	0.167	0.143	0.934	0.525
1/1.5	0.165	0.145	0.934	0.525
1/1	0.162	0.152	0.934	0.525
1.5/1	0.160	0.155	0.934	0.525
2/1	0.158	0.157	0.934	0.525
3/5	0.166	0.144	0.934	0.525
3/1	0.156	0.160	0.934	0.525
1/3	0.170	0.140	0.934	0.525
5/3	0.159	0.156	0.934	0.525
6/0	0.100	0.200	0.934	0.525
0/6	0.450	0.030	0.934	0.525

The breakthrough curves from the model with new ionic-diffusion coefficients in Table VI are compared graphically with the curves for each run of the experiment. The example plot is shown for the case of cation/anion resin ratio of 3.0 g/3.0 g in Figure 23. The relatively good fit of the theoretical curve and the experimental data for the mixed-bed ion exchange provides a verification of the theoretical model. Although the

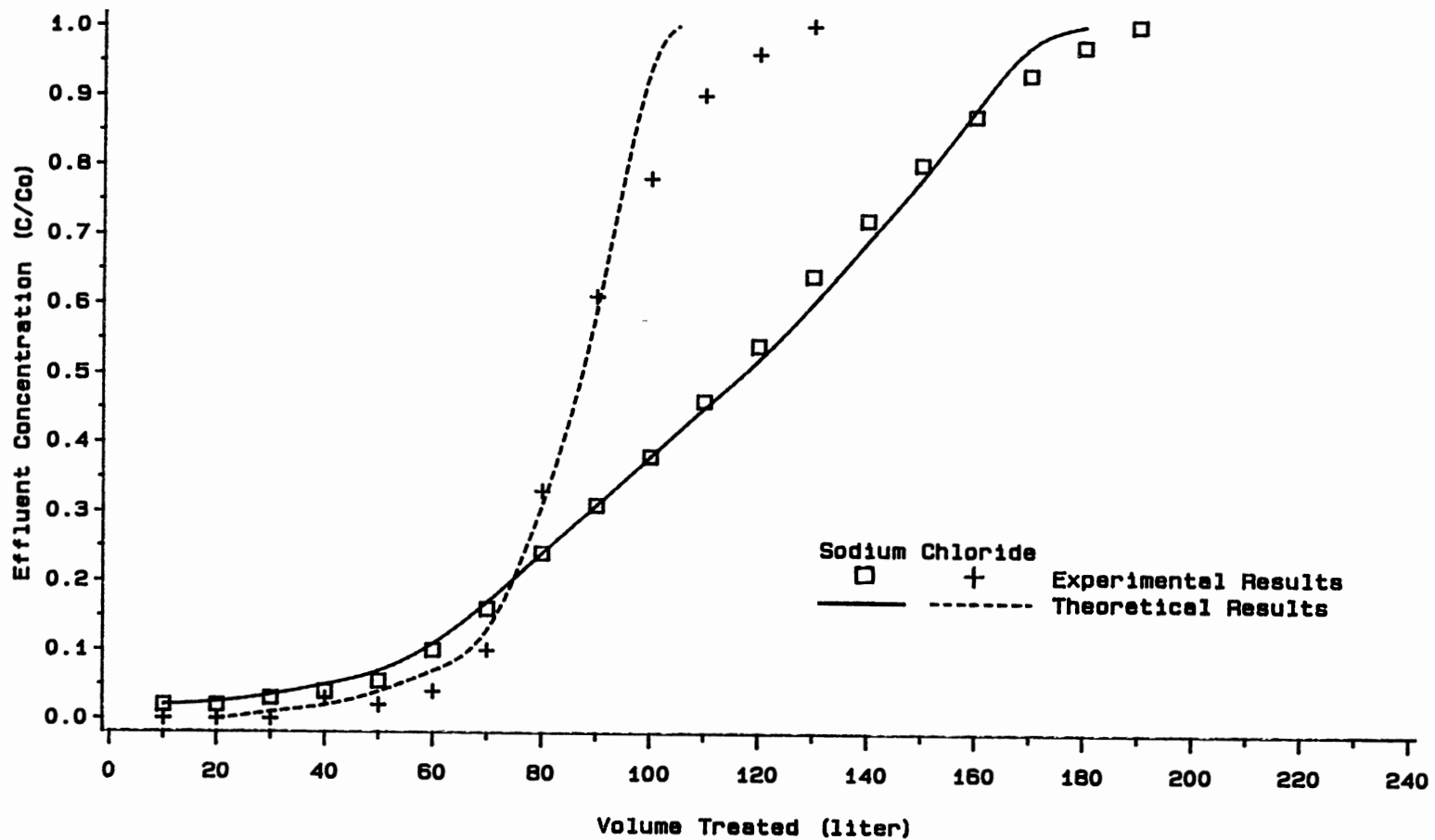


Figure 23. Deviations of Theoretical and Experimental Results for Cation/Anion Resin Ratio of 3.0 g/3.0 g (Using Constant Diffusivity)

fit for the chloride breakthrough curve is not very good, the theoretical curves represent the general shape of the data.

As the effective system diffusivity is not constant, the ionic-diffusion coefficients may not be constant, but a function of ion concentration in liquid phase. The ionic-diffusion coefficients are expressed as a function of ionic concentration for several trials. Linear, quadratic, or exponential equations were considered, but a linear equation is assumed to simplify the relationship between ionic-diffusion coefficient and ionic concentration as

$$D_{Na} = a_{Na} - b_{Na} (F_{Na} - C_{Na}),$$

and

$$D_{Cl} = a_{Cl} - b_{Cl} (F_{Cl} - C_{Cl}) \quad (9)$$

where a_i 's and b_i 's are constants with dimensions of cm^2/sec and $\text{cm}^5/\text{sec}/\text{meq.}$, respectively.

By trial and error, the constants of a_i and b_i in ultra-low solution concentration are obtained as shown in Table VII. The constants fit best all of the experimental data when the system is simulated using the model of Haub and Foutch (1986a). Thus, the correlation equations can be used for all of the cation-to-anion resin ratio in this system. The sample plot for the

cation/anion resin ratio of 3.0 g/3.0 g is shown in Figure 24.

TABLE VII
CONSTANTS FOR IONIC-DIFFUSION COEFFICIENTS
AS A FUNCTION OF IONIC CONCENTRATION

Ion\Constant	a (cm^2/sec)	b ($\text{cm}^5/\text{sec}/\text{meq.}$)
Na	0.45	2500
Cl	0.11	1500

A new set for resin ratios or correlation equations of ionic-diffusion coefficients gives relatively good fits for the mathematical model. However, the literature data (Robinson and Stokes, 1959) were obtained from experiments, and other experiments (Tyrell and Harris, 1984) support the data. The change of the order of magnitude of the data in order to fit the experimental results to the model without clear understanding as to why this may be true needs to be seriously considered. Thus, the mass-transfer coefficients for packed beds of Equations (2) and (3) are considered in the following section.

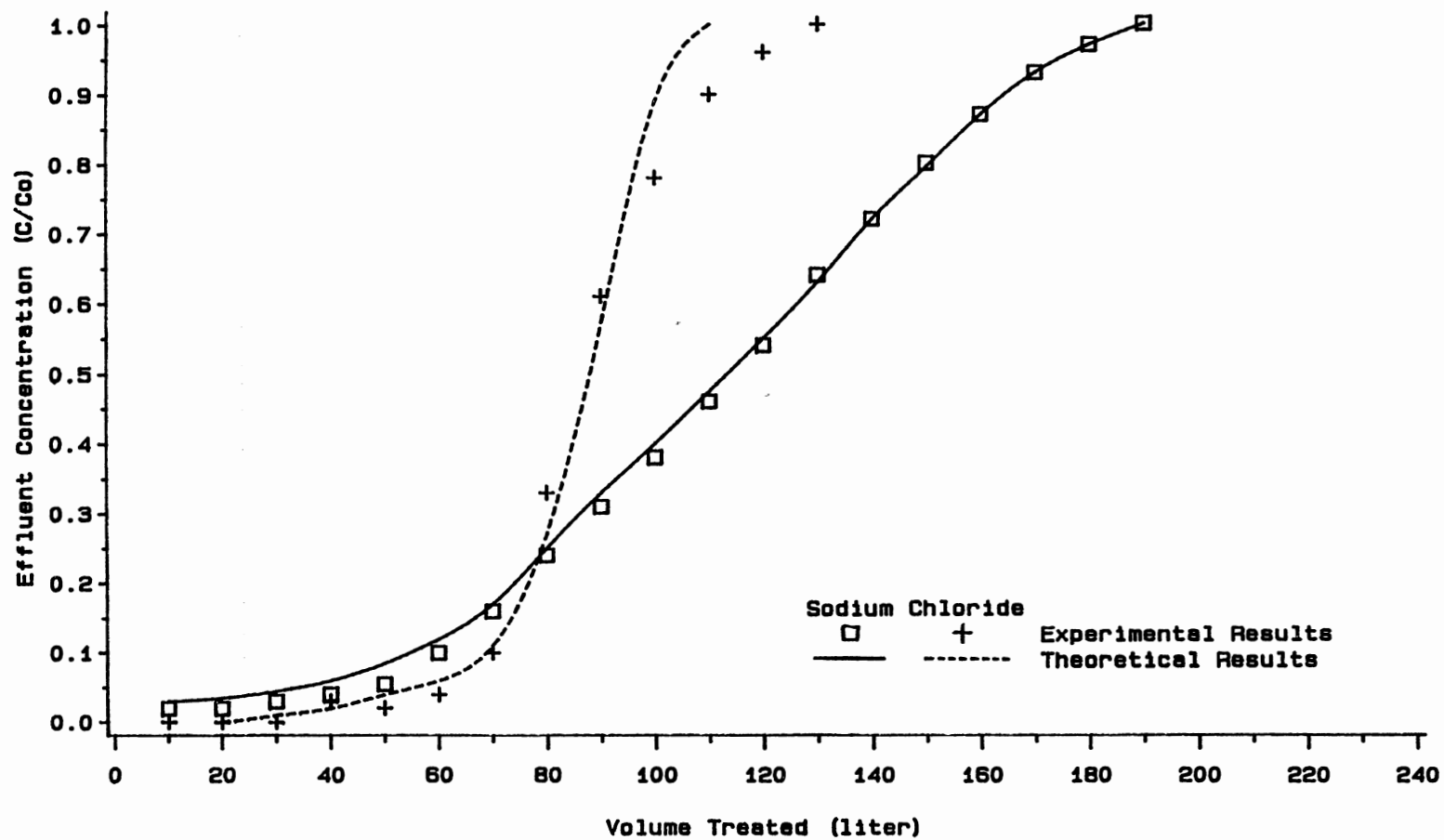


Figure 24. Deviations of Theoretical and Experimental Results for Cation/Anion Resin Ratio of 3.0 g/3.0 g (Using Variable Diffusivity)

Mass-Transfer Coefficients for the System

Van Brocklin and David (1972) described general empirical equations for nonelectrolyte packed-bed mass transfer as

$$k_1 = A \frac{u}{e} (Sc)^{-2/3} (Re)^n \quad (10)$$

The correlation equations (2) and (3) of Carberry (1960) and Kataoka, et al. (1972), respectively, which were used by Haub and Foutch (1986a), are those of the form of Equation (10). In a low Reynolds number region of less than 1.0 in these experiments, Equation (3) will give better correlation equations than Equation (4). The exponent $-2/3$ of Reynolds number in Equation (3) is also the same as the exponent of Pfeffer (1964) who obtained the mass-transfer coefficient correlation for fixed and fluidized beds at low Reynolds numbers.

The mass-transfer coefficient is related to the ionic-diffusion coefficient and film thickness in liquid phase. As the hydrodynamic factor, i.e., film thickness, increases, the exchanging ions diffuse through a thicker layer, and the observed mass-transfer coefficient decreases. Harries and Ray (1984) showed that the mass-transfer coefficient of chloride exchange is a function of influent concentration. For new anion resins in mixed bed, the mass-transfer coefficient slightly increased

with influent concentration. For used anion resins in mixed bed, the linear relationship between mass-transfer coefficient and the logarithm of influent concentration was observed (Harries, 1988). The mass-transfer coefficient is lower for the lower influent concentration because the film thickness increases as the influent concentration decreases.

The correlation equations of Kataoka, et al. (1973a), were obtained from higher influent concentration of 0.01 N than that of 0.0001 N of these experiments. Thus, the mass-transfer coefficients need to be reduced for the system. To keep the general form of the equation, the constant A in Equation (3) is corrected to fit the experimental results. The new constant A for sodium and chloride exchange is determined by trial and error with the constant ionic-diffusion coefficients of Robinson and Stokes (1959). The results are shown in Table VIII.

Table VIII shows the variation of constant A, and Figures 25 through 43 show the comparison between model predictions and experimental results. The values of A in Table VIII coincide with the results of Harries (1988) that the mass-transfer coefficient varies with solution pH. The mass-transfer coefficient of chloride exchange is high at low pH and low at high pH, and the mass-transfer coefficient of sodium exchange is high at high pH and low at low pH.

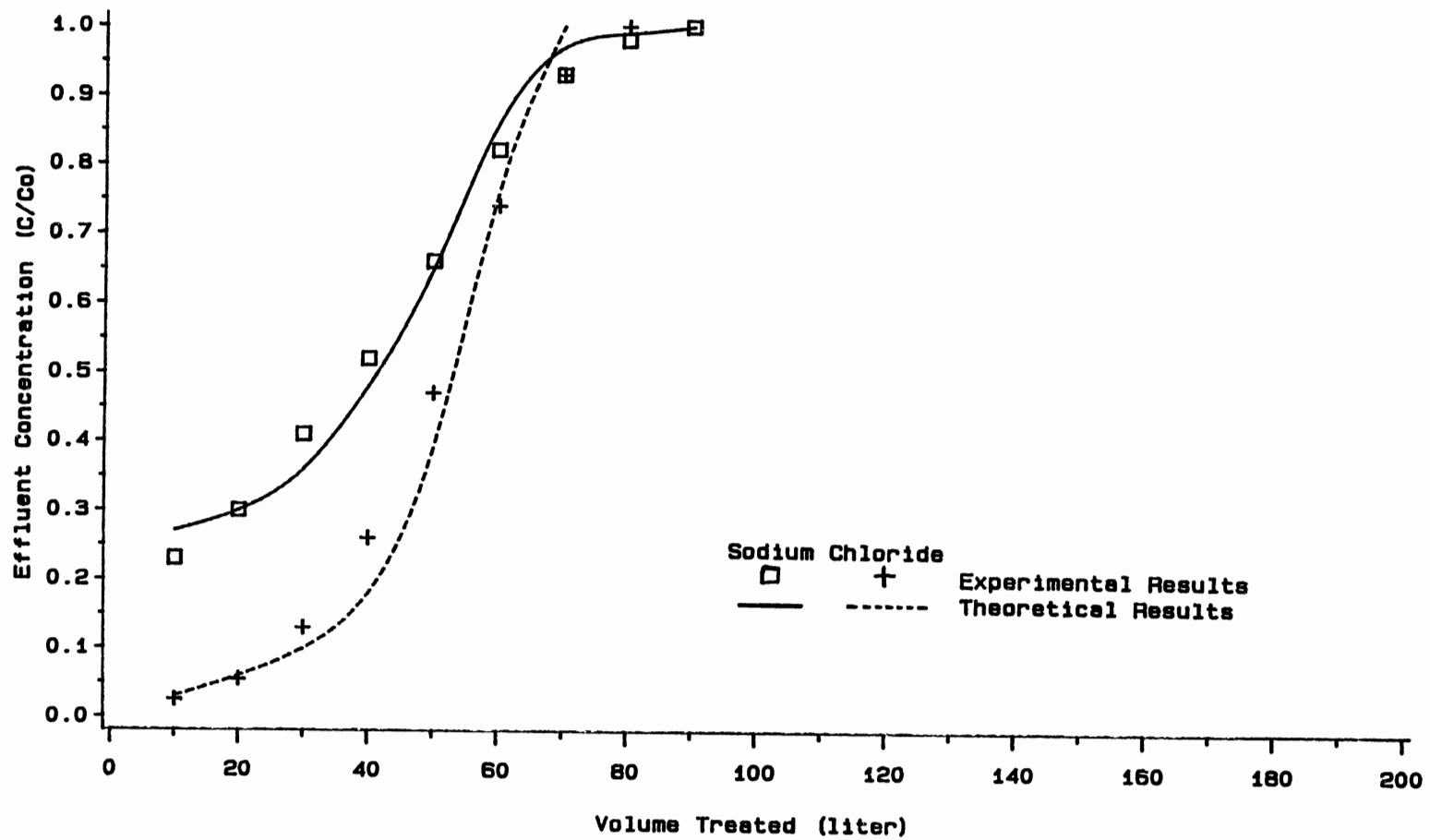


Figure 25. Deviations of Theoretical and Experimental Results for Cation/Anion Resin of 1.0 g/2.0 g with new constants in Table VIII

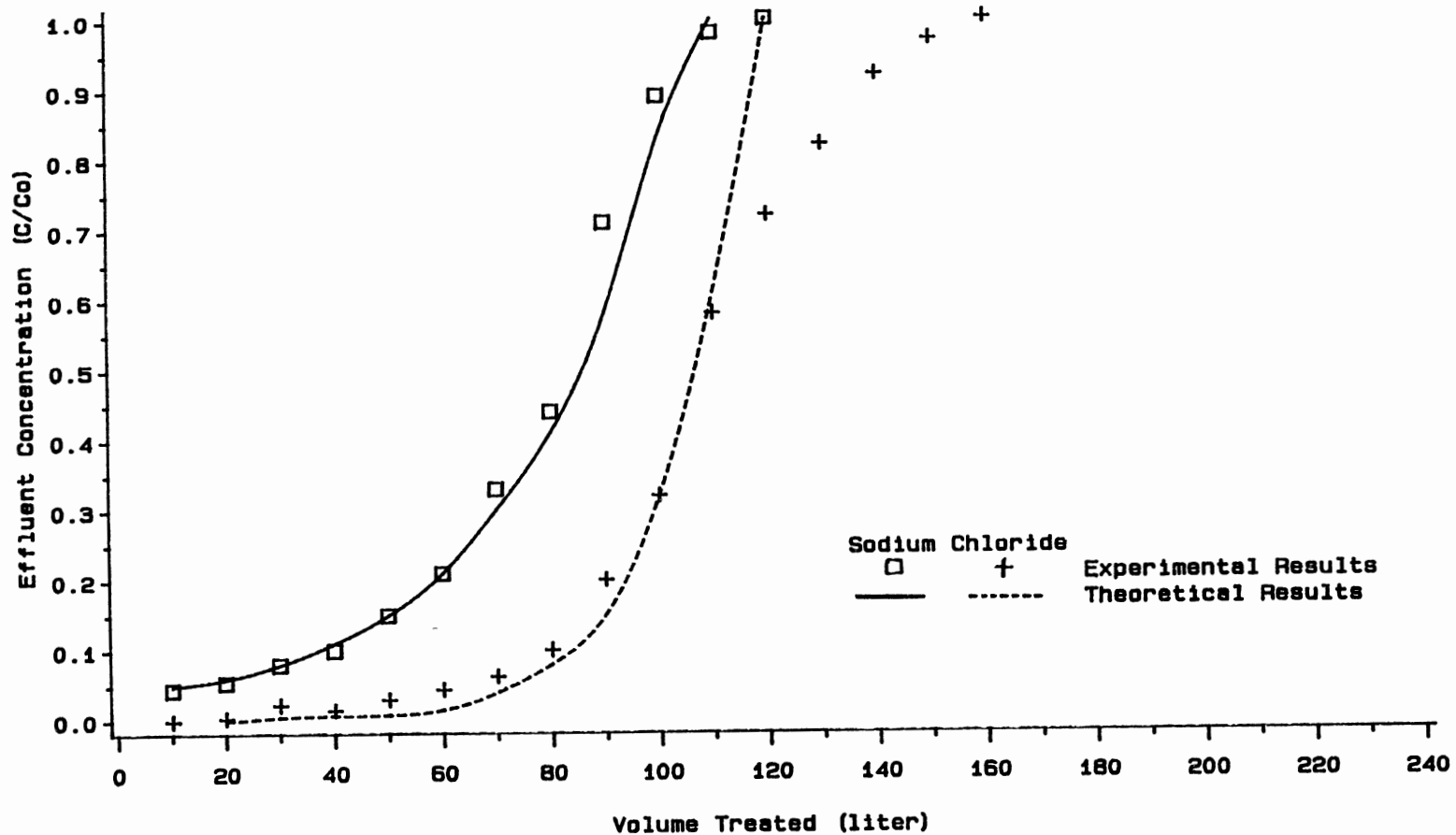


Figure 26. Deviations of Theoretical and Experimental Results for Cation/Anion Resin of 2.0 g/4.0 g with new constants in Table VIII

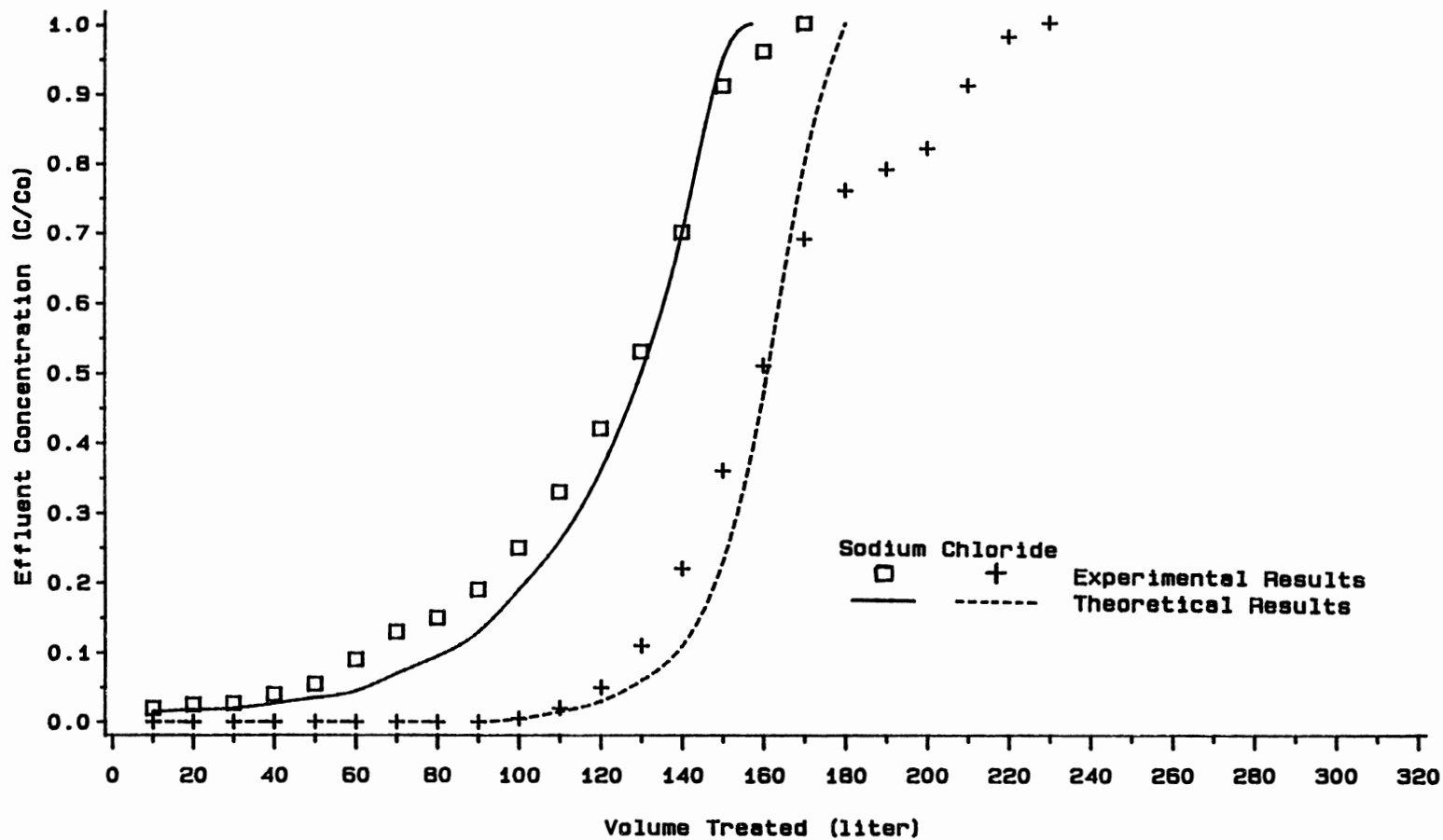


Figure 27. Deviations of Theoretical and Experimental Results for Cation/Anion Resin of 3.0 g/6.0 g with new constants in Table VIII

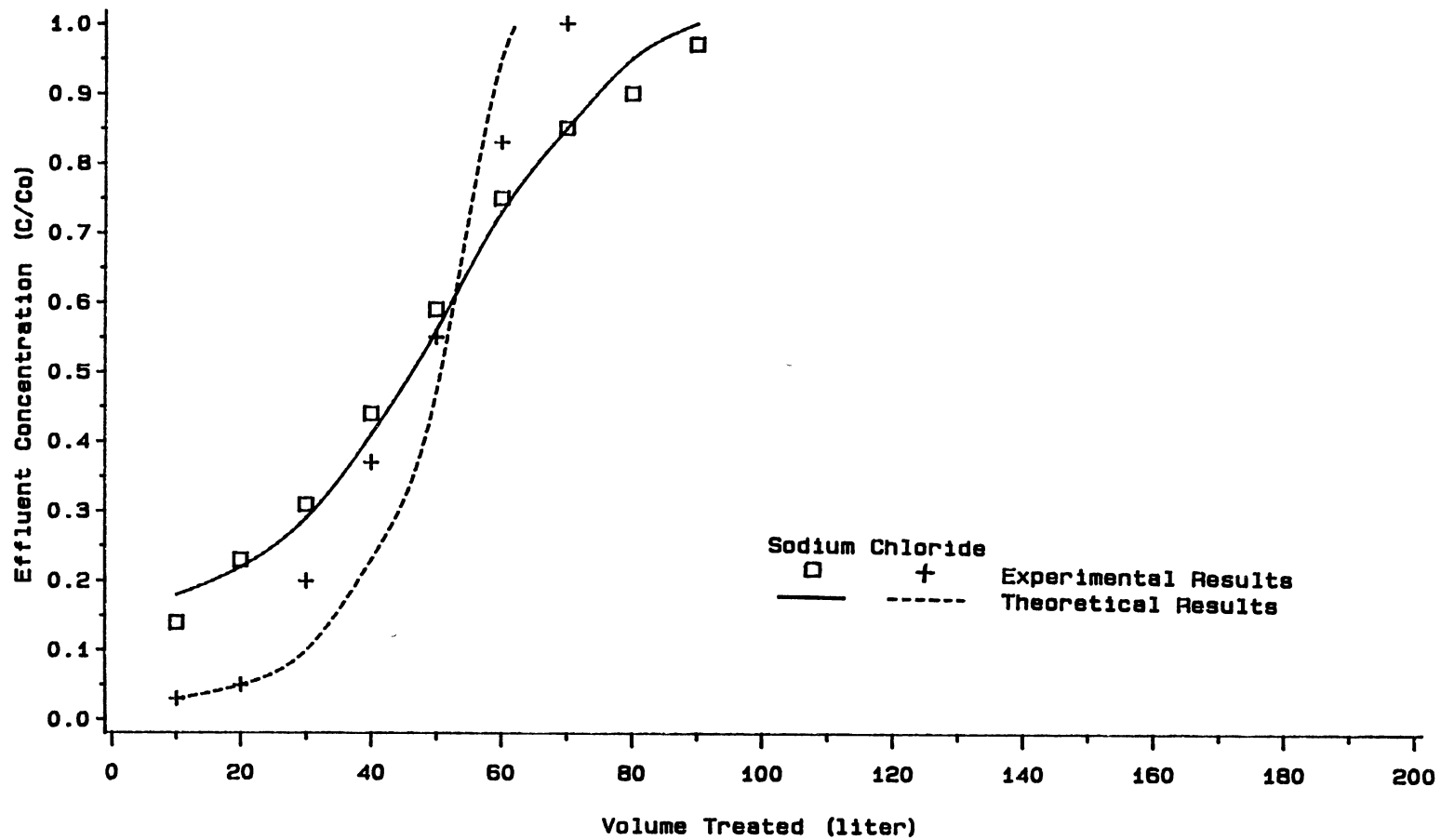


Figure 28. Deviations of Theoretical and Experimental Results for Cation/Anion Resin of 1.2 g/1.8 g with new constants in Table VIII

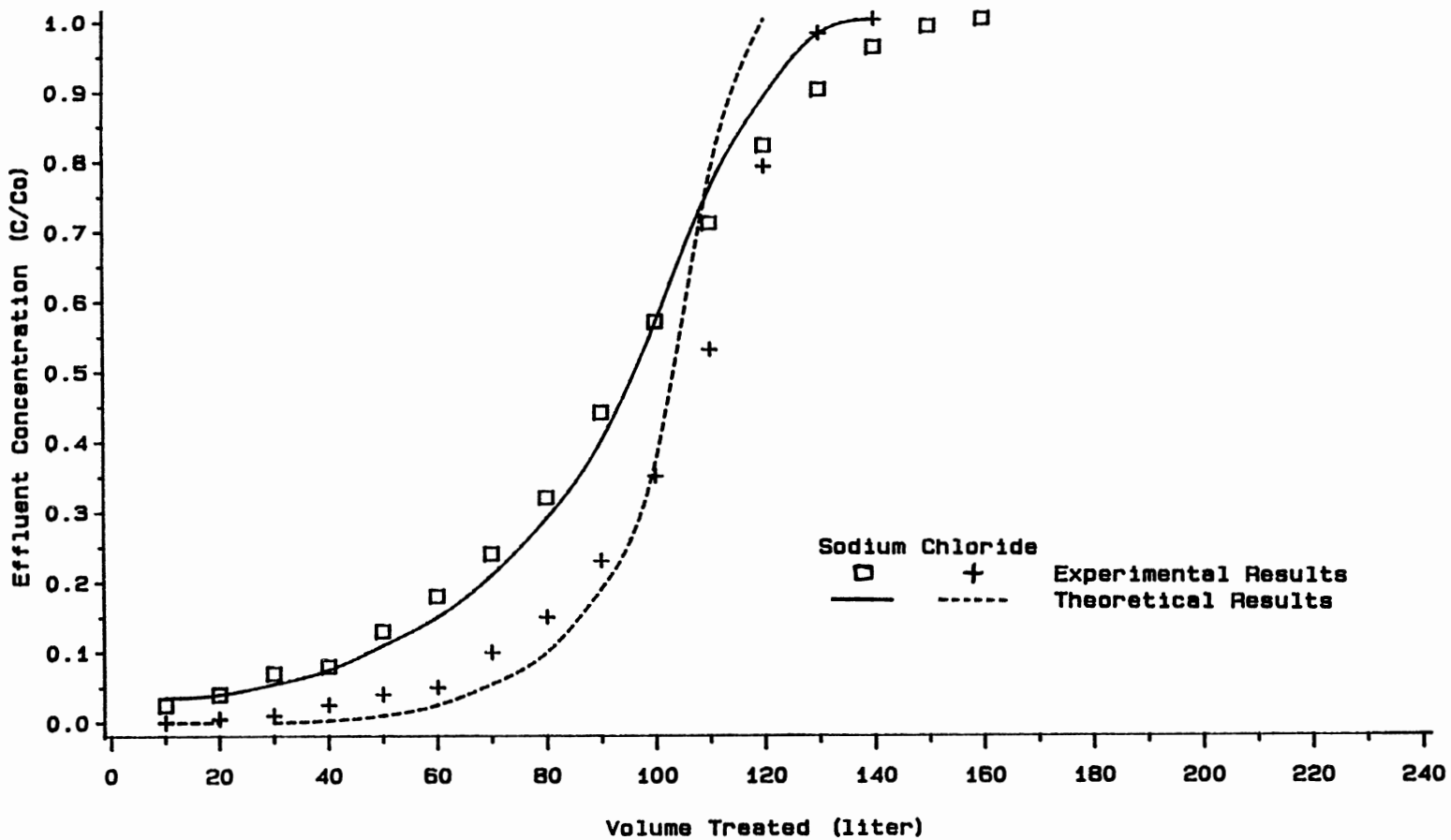


Figure 29. Deviations of Theoretical and Experimental Results for Cation/Anion Resin of 2.4 g/3.6 g with new constants in Table VIII

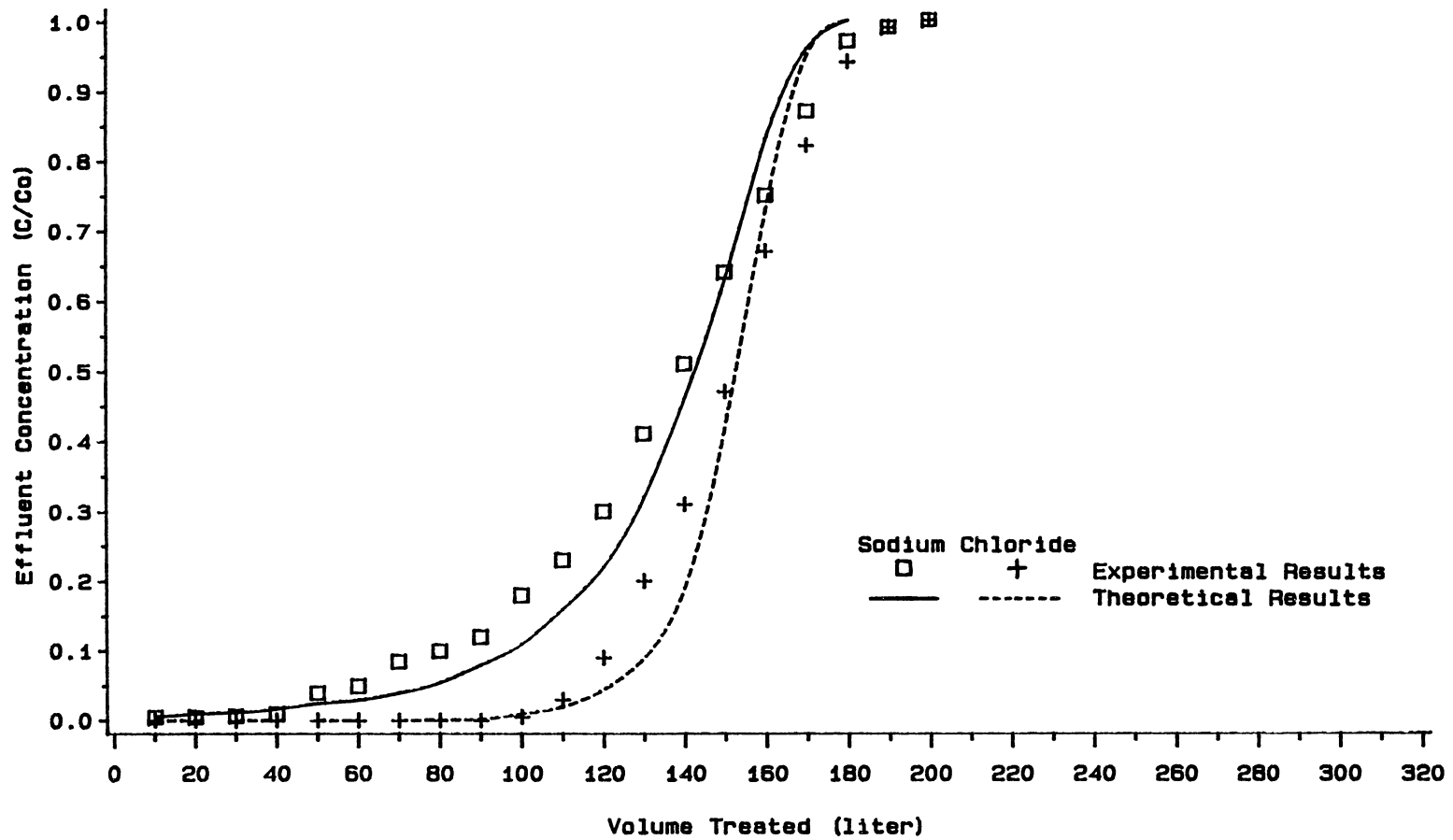


Figure 30. Deviations of Theoretical and Experimental Results for Cation/Anion Resin of 3.6 g/5.4 g with new constants in Table VIII

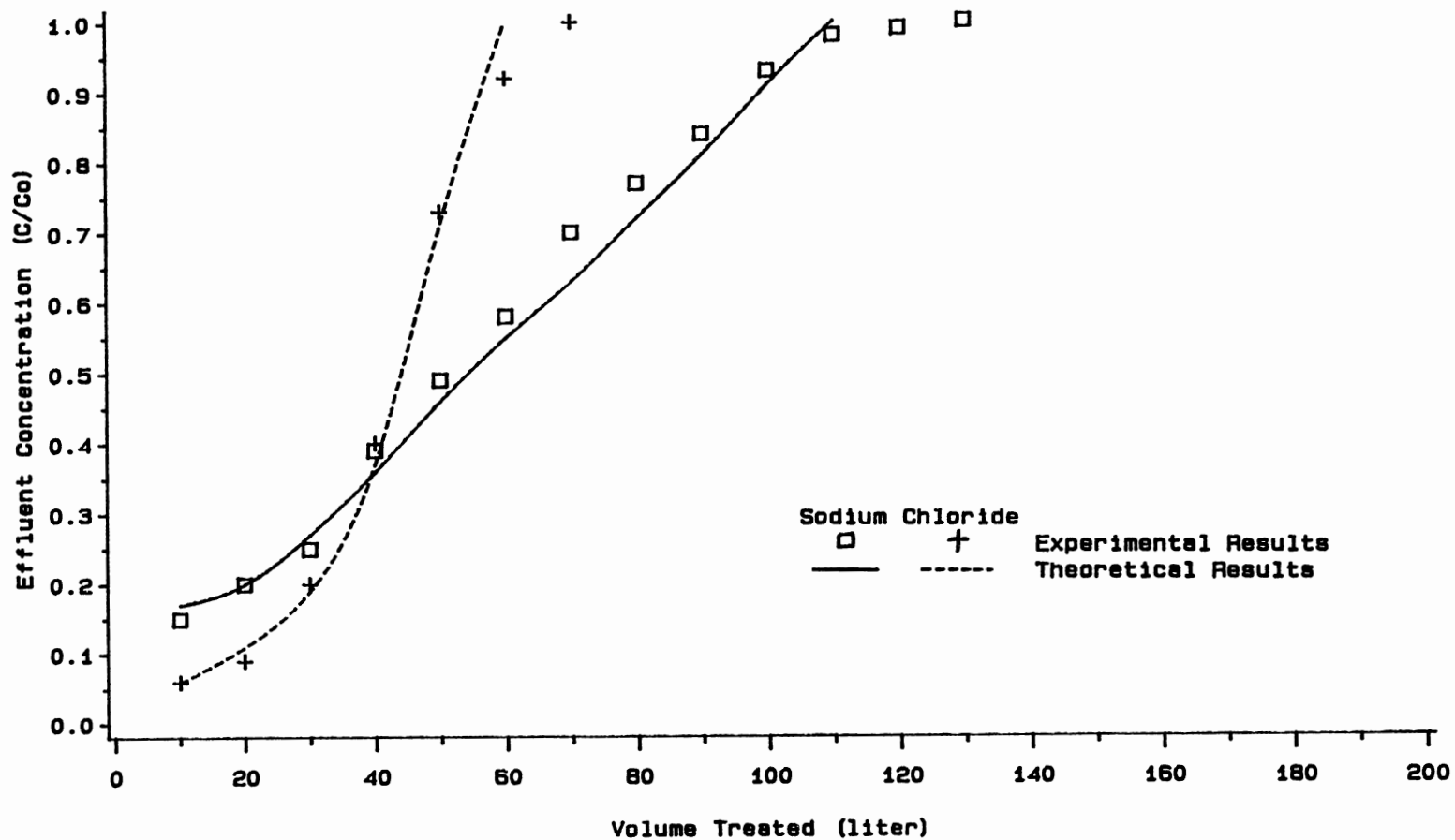


Figure 31. Deviations of Theoretical and Experimental Results for Cation/Anion Resin of 1.5 g/1.5 g with new constants in Table VIII

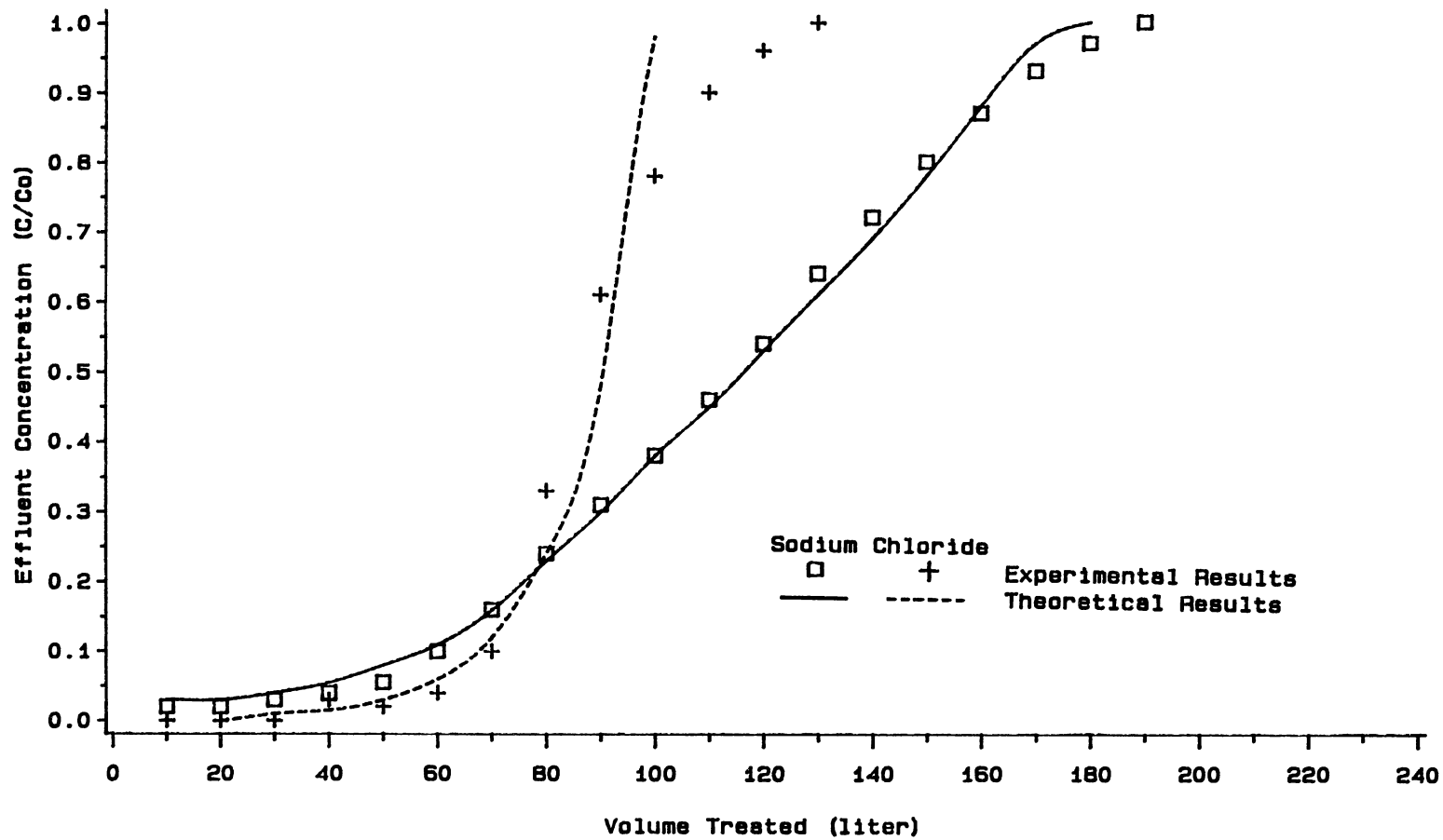


Figure 32. Deviations of Theoretical and Experimental Results for Cation/Anion Resin of 3.0 g/3.0 g with new constants in Table VIII

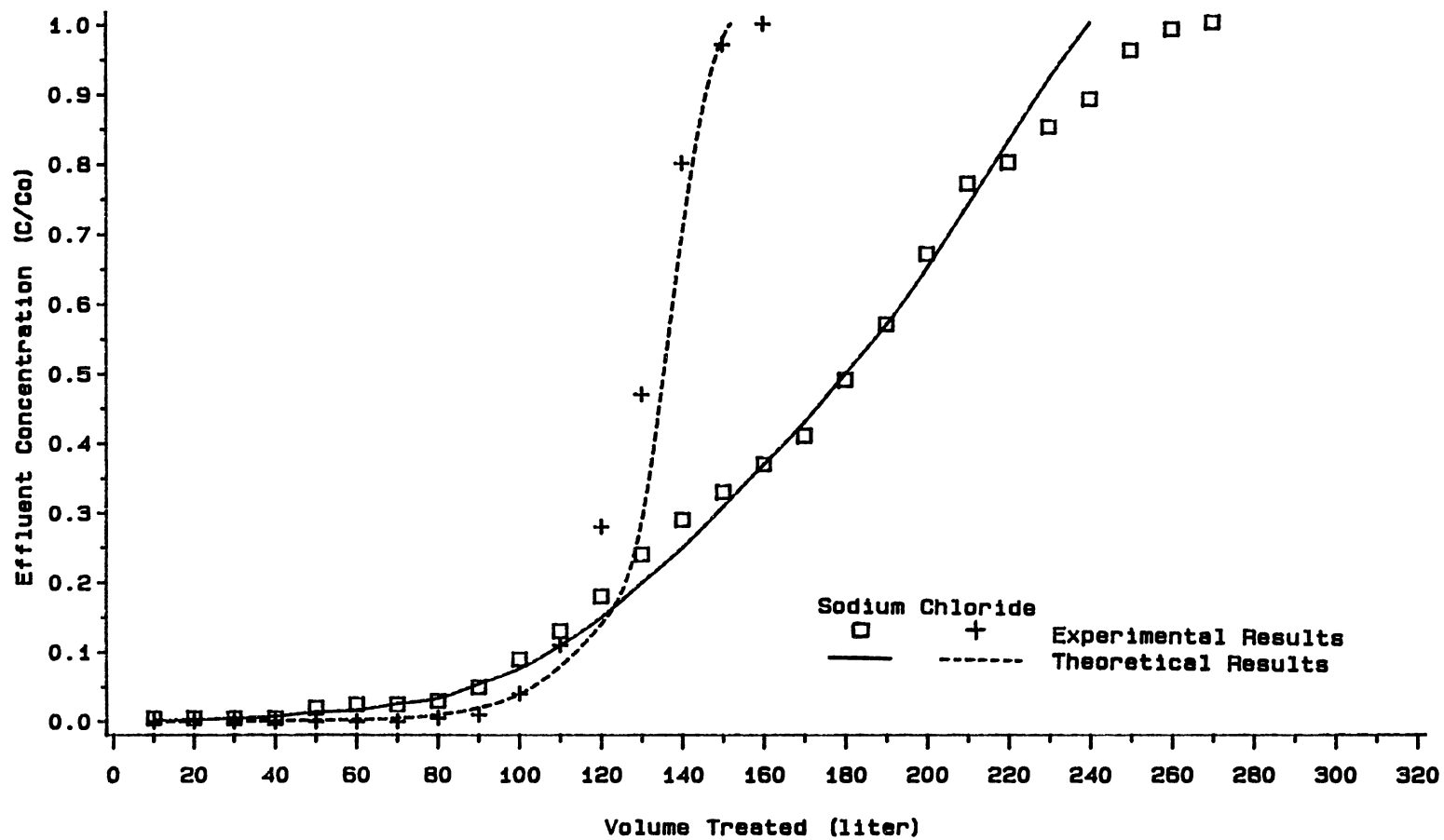


Figure 33. Deviations of Theoretical and Experimental Results for Cation/Anion Resin of 4.5 g/4.5 g with new constants in Table VIII

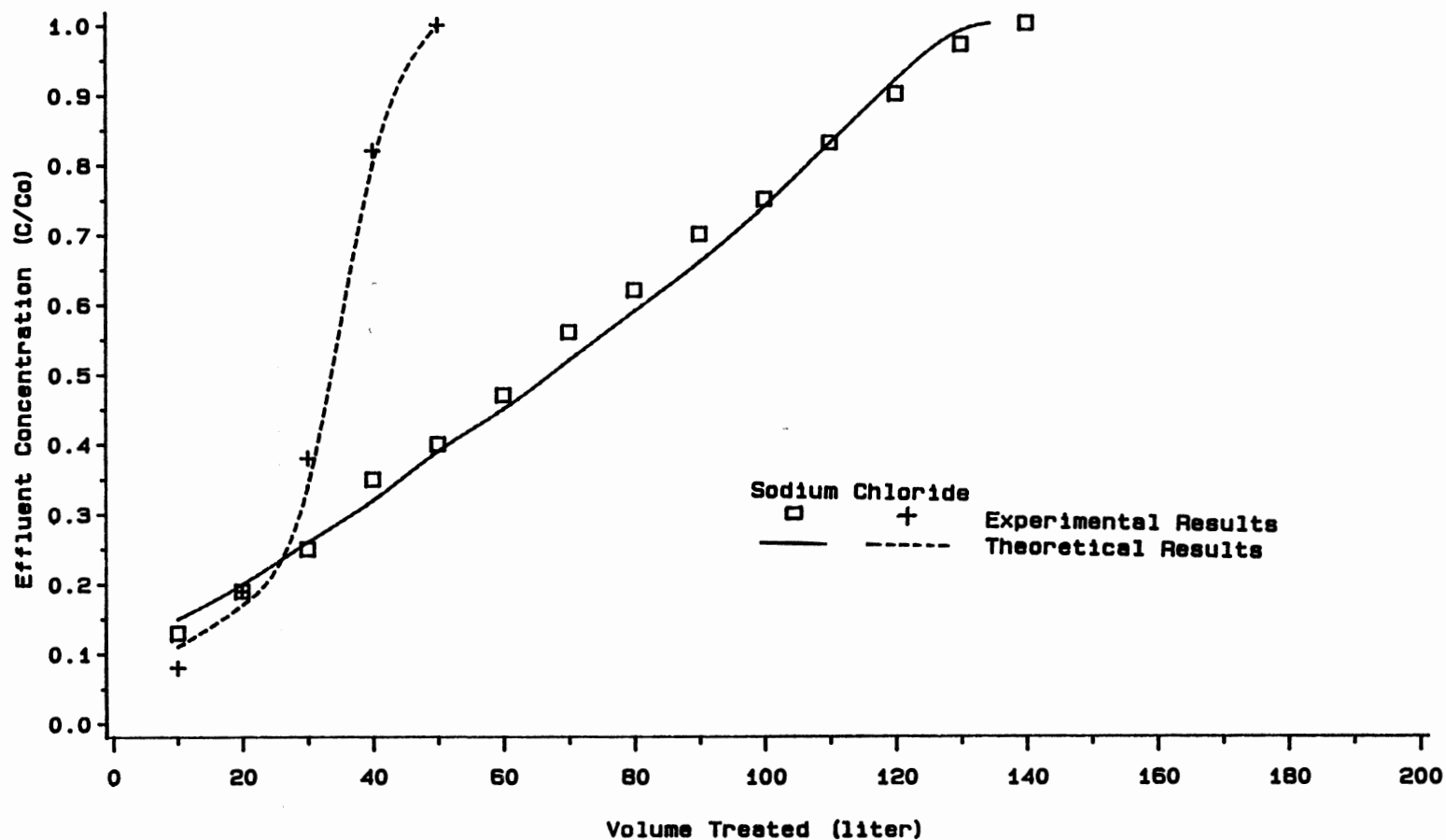


Figure 34. Deviations of Theoretical and Experimental Results for Cation/Anion Resin of 1.8 g/1.2 g with new constants in Table VIII

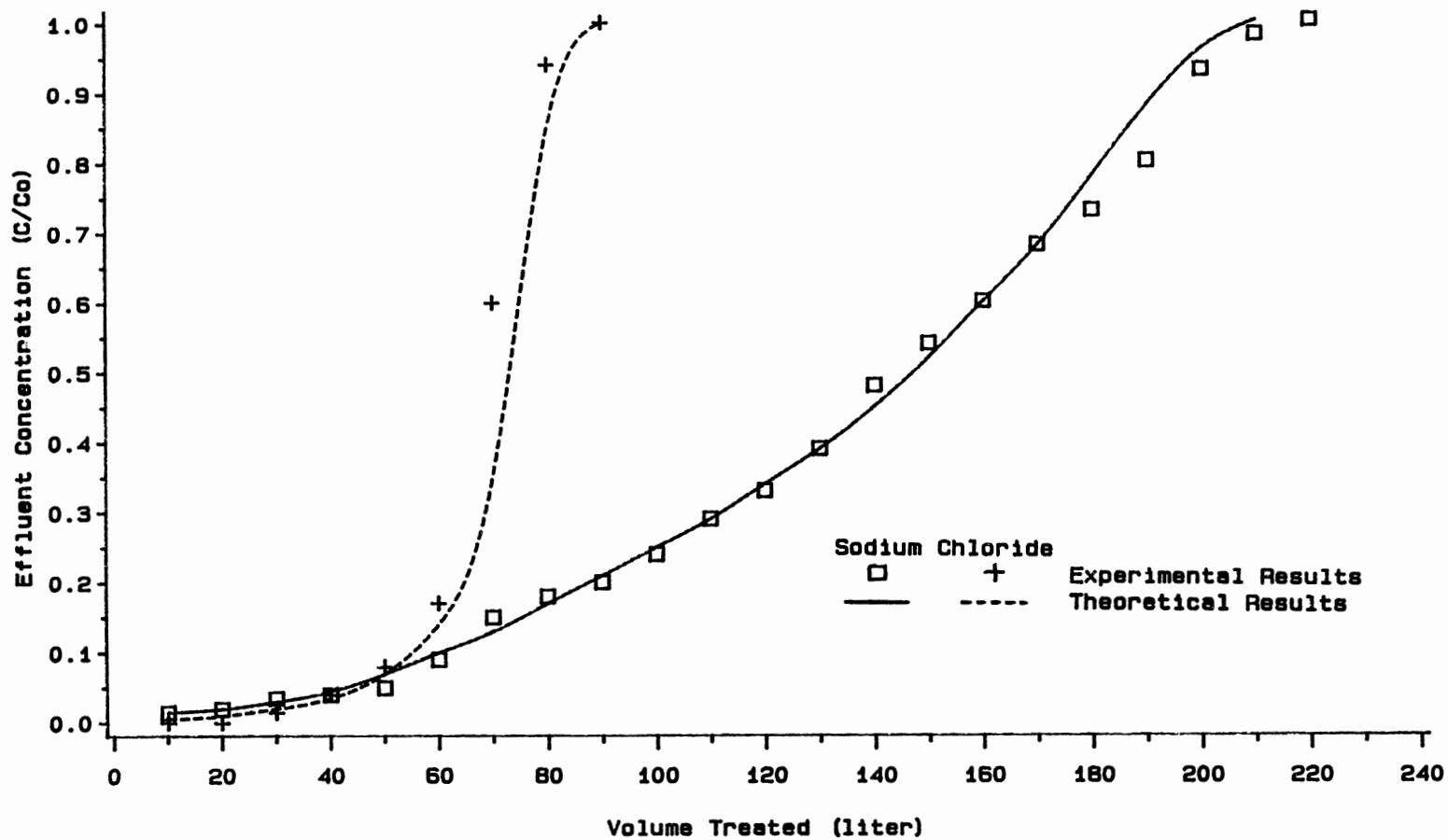


Figure 35. Deviations of Theoretical and Experimental Results for Cation/Anion Resin of 3.6 g/2.4 g with new constants in Table VIII

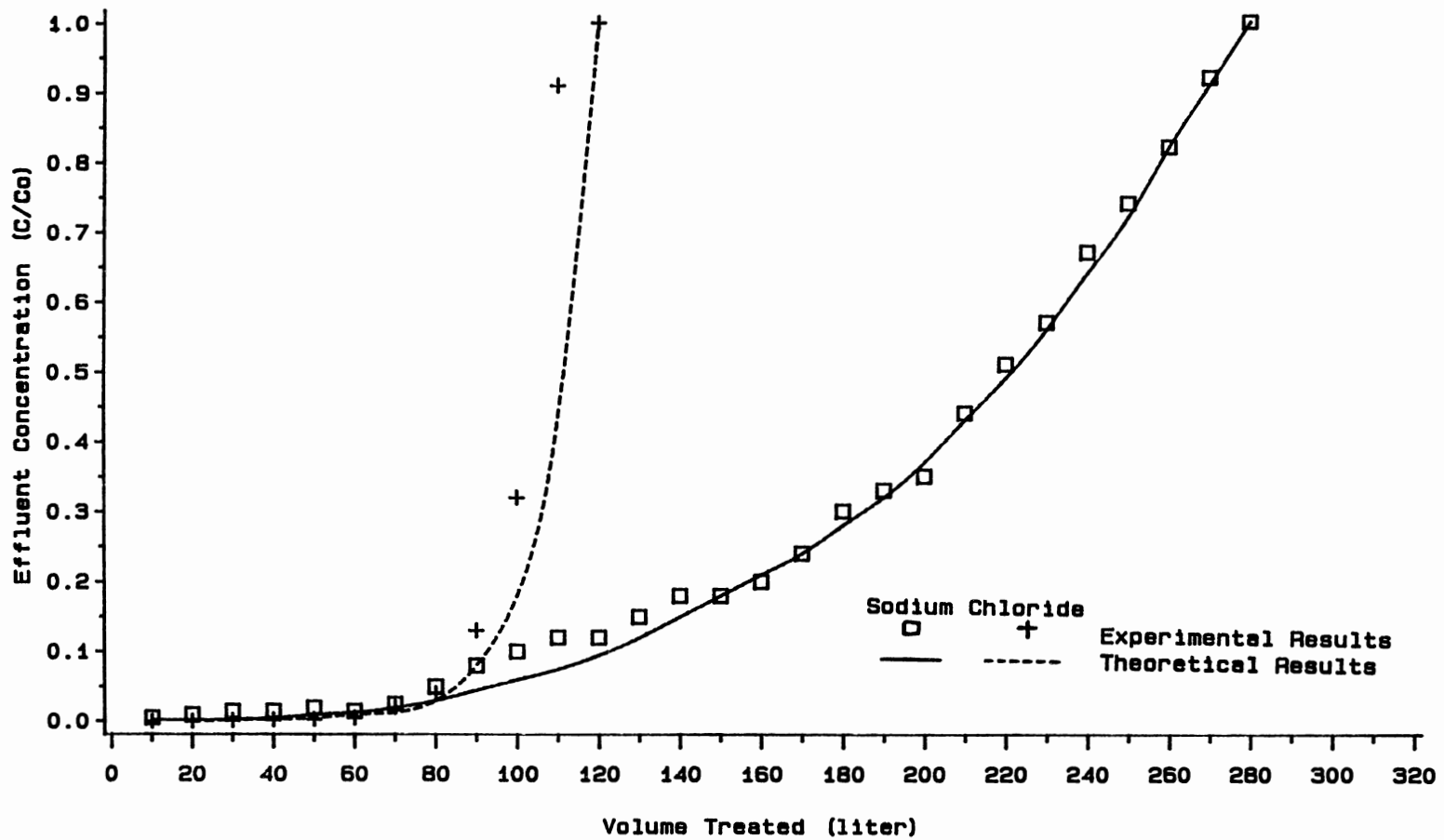


Figure 36. Deviations of Theoretical and Experimental Results for Cation/Anion Resin of 5.4 g/3.6 g with new constants in Table VIII

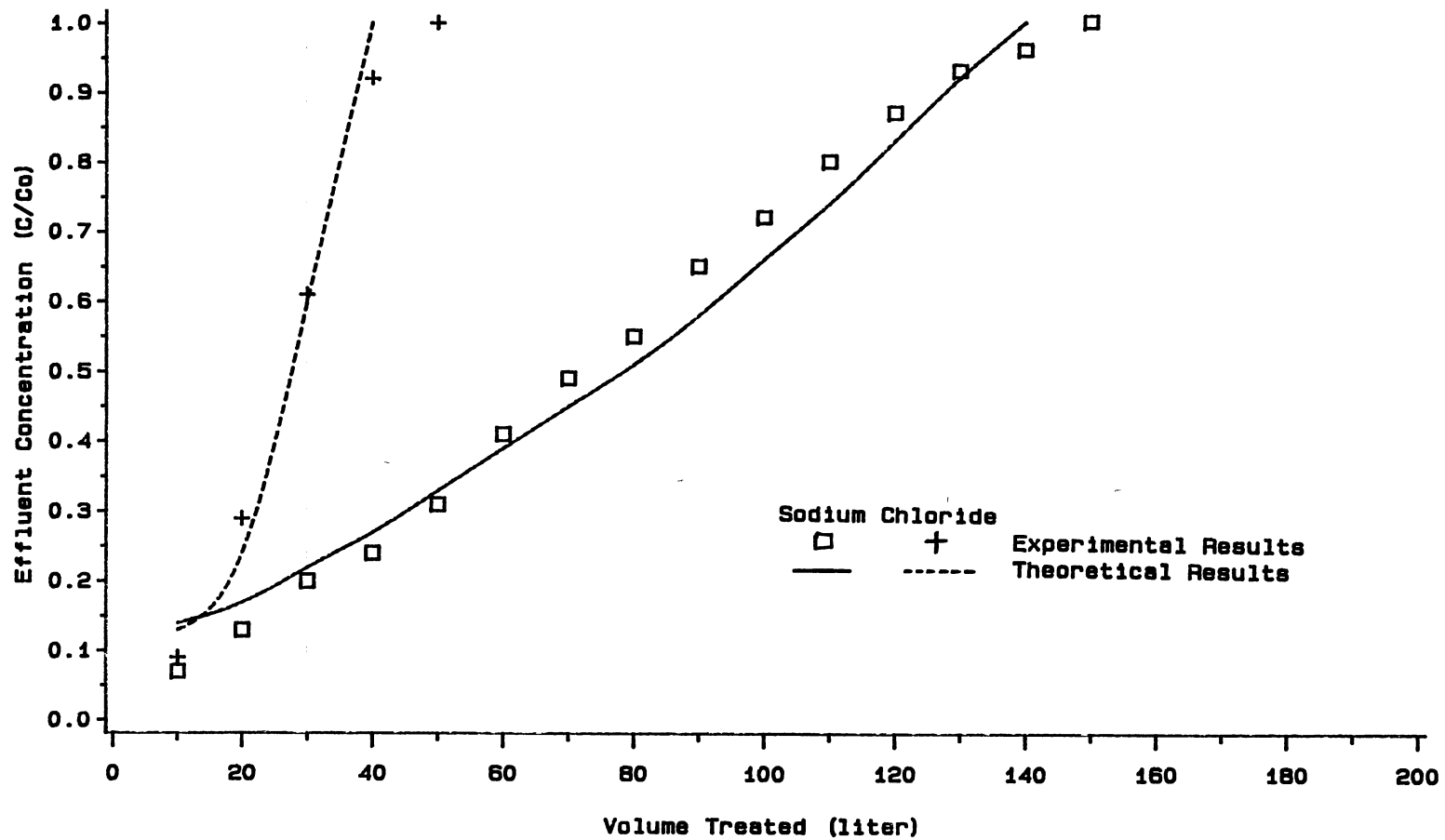


Figure 37. Deviations of Theoretical and Experimental Results for Cation/Anion Resin of 2.0 g/1.0 g with new constants in Table VIII

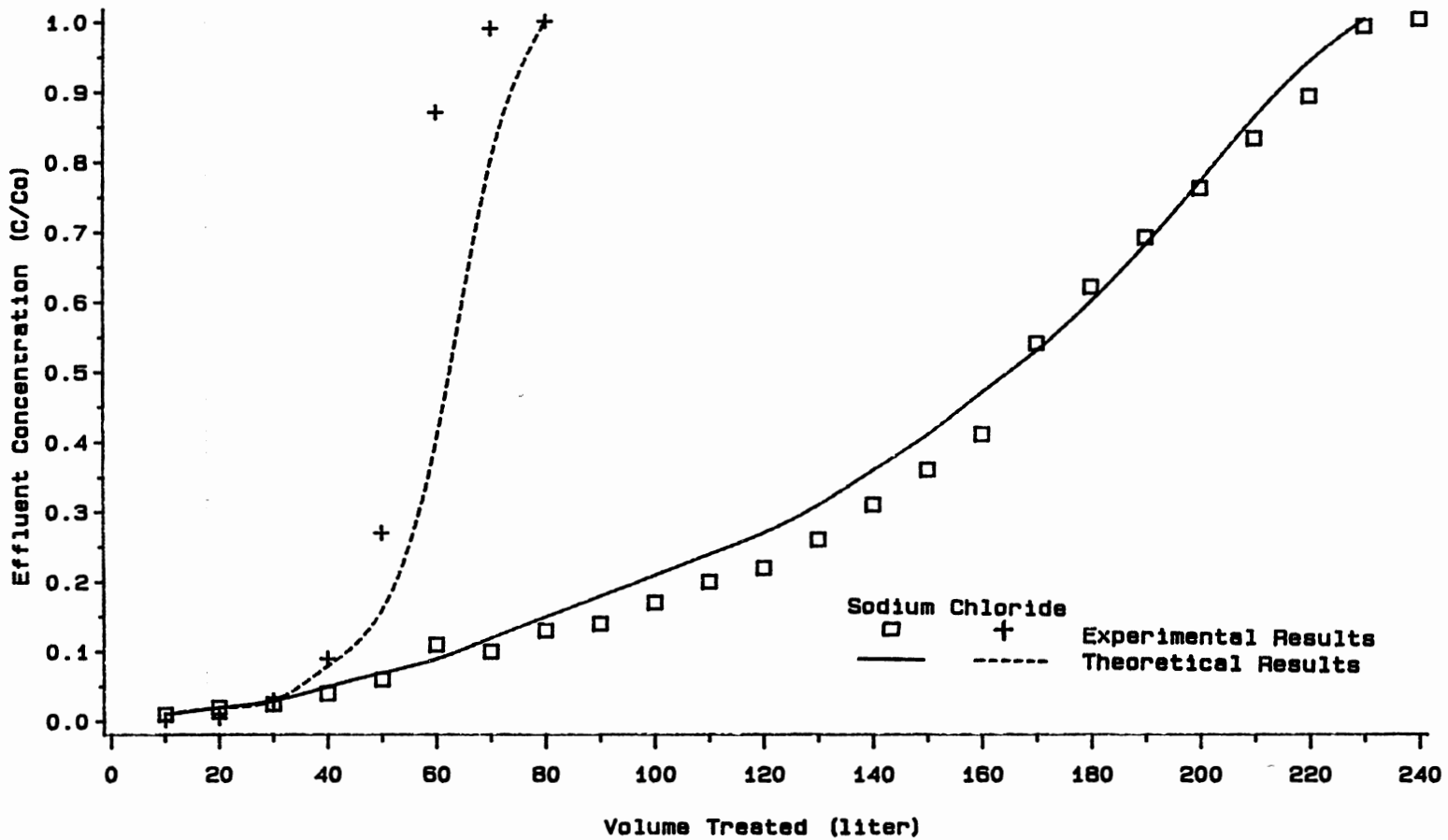


Figure 38. Deviations of Theoretical and Experimental Results for Cation/Anion Resin of 4.0 g/2.0 g with new constants in Table VIII

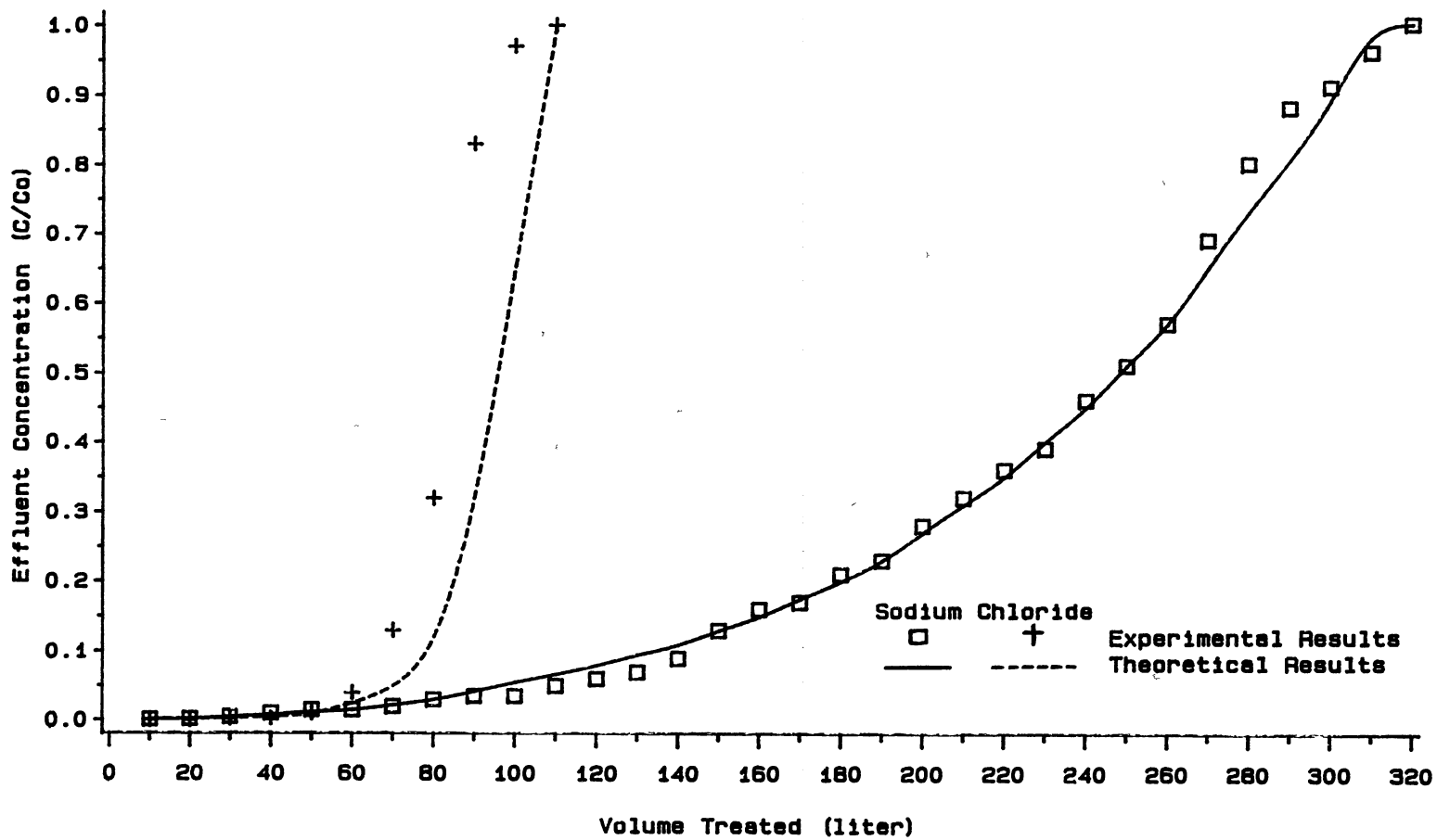


Figure 39. Deviations of Theoretical and Experimental Results for Cation/Anion Resin of 6.0 g/3.0 g with new constants in Table VIII

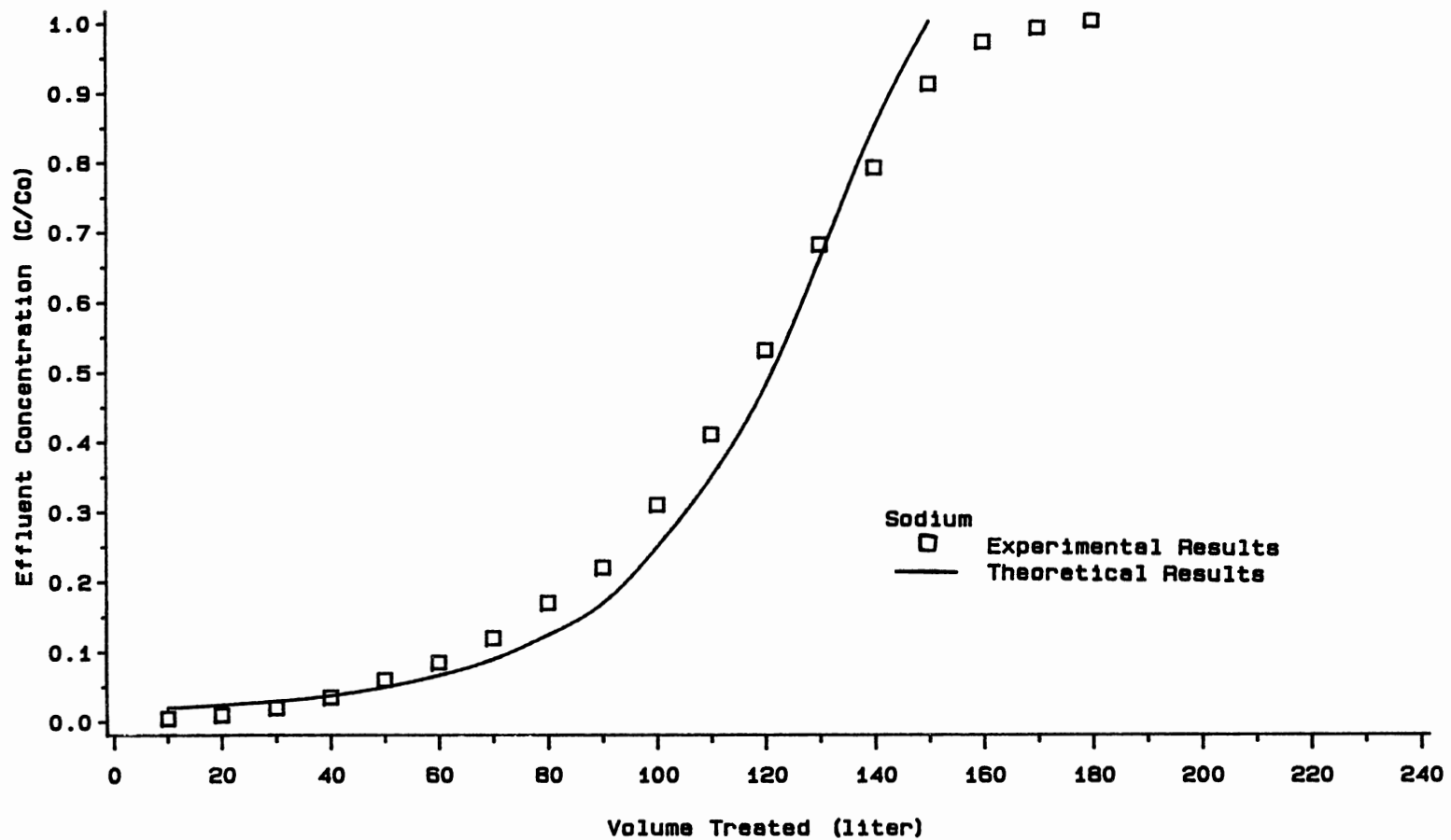


Figure 40. Deviations of Theoretical and Experimental Results for Cation/Anion Resin of 3.0 g/5.0 g with new constants in Table VIII

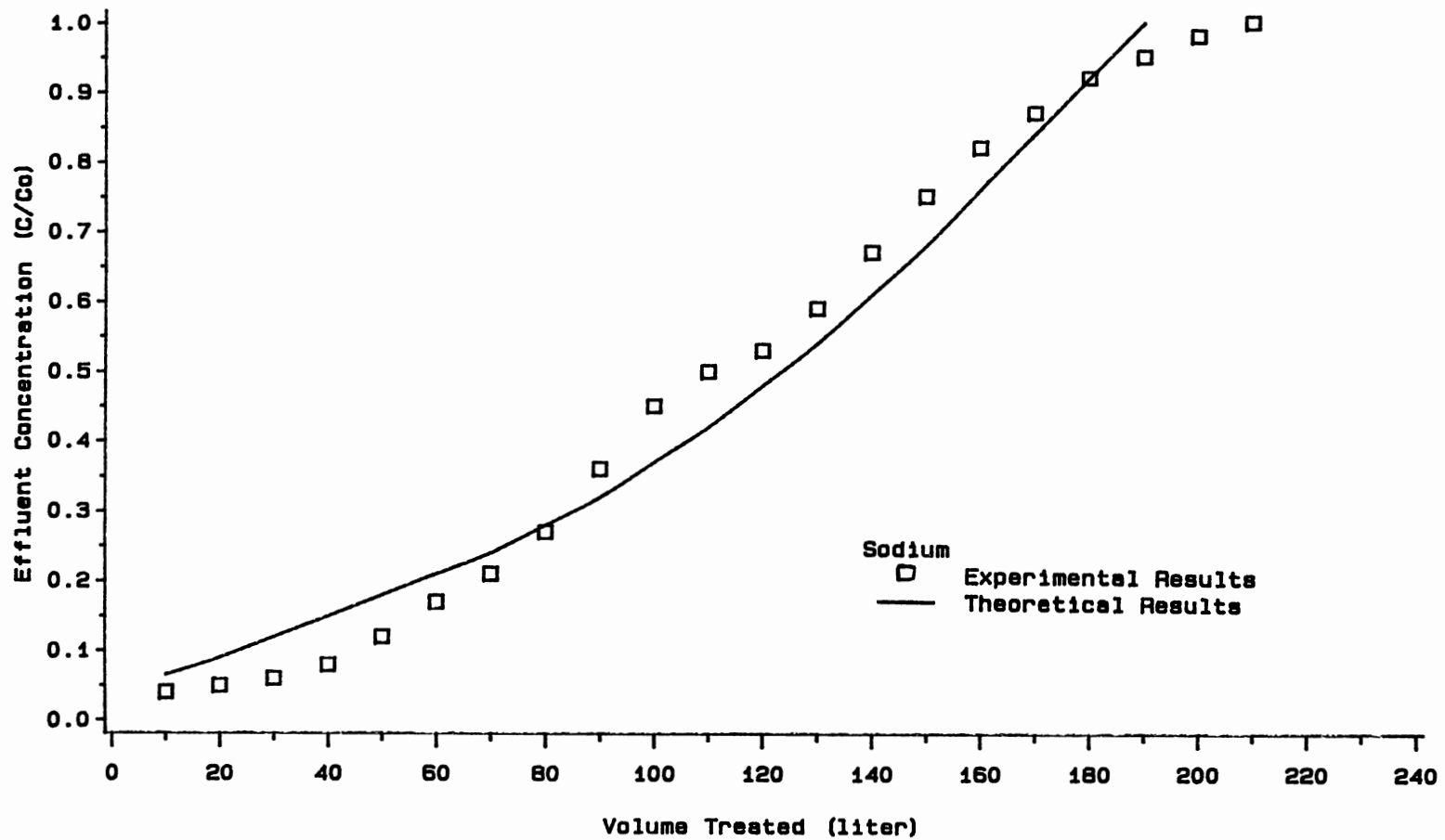


Figure 41. Deviations of Theoretical and Experimental Results for Cation/Anion Resin of 3.0 g/1.0 g with new constants in Table VIII

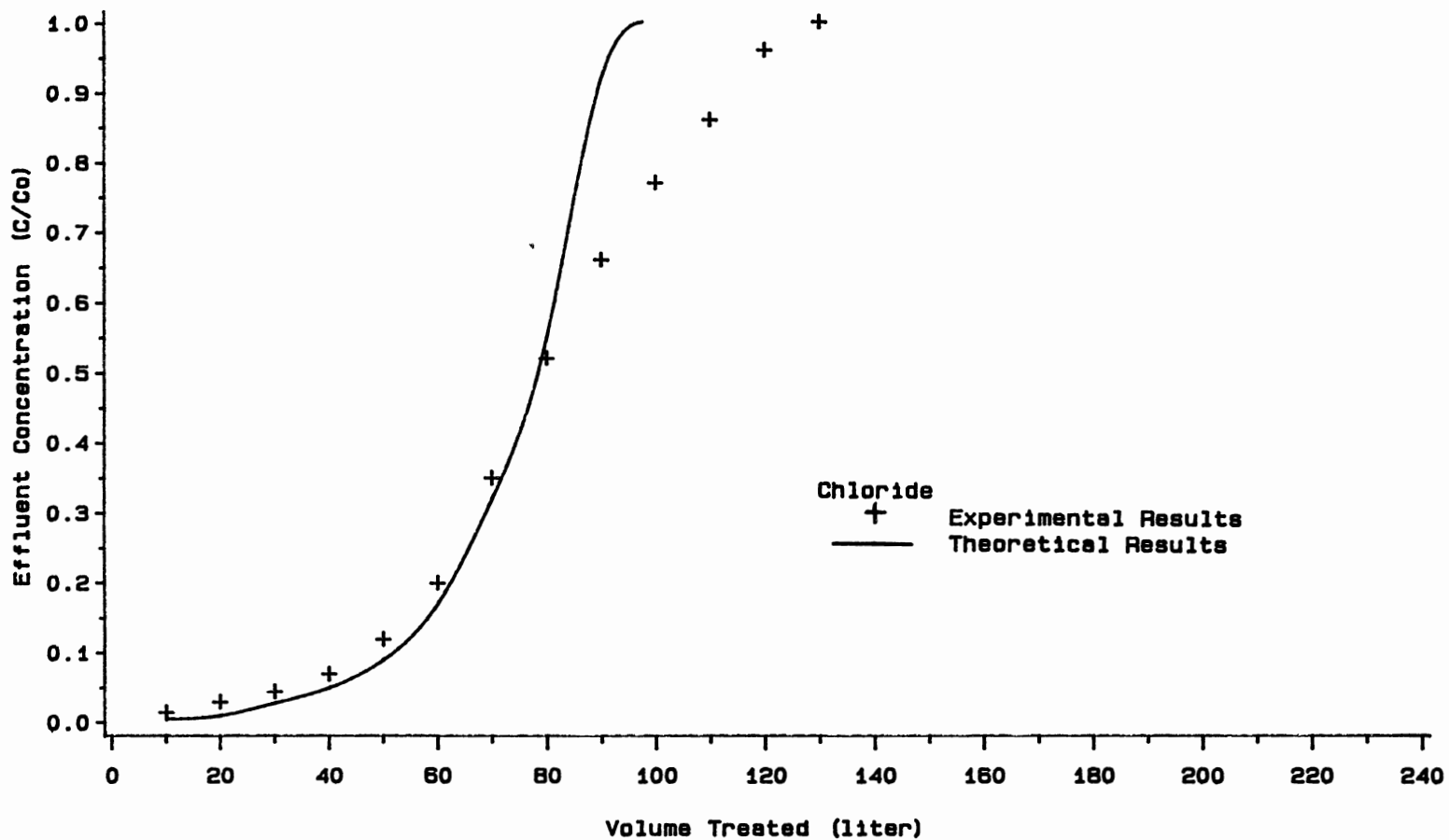


Figure 42. Deviations of Theoretical and Experimental Results for Cation/Anion Resin of 1.0 g/3.0 g with new constants in Table VIII

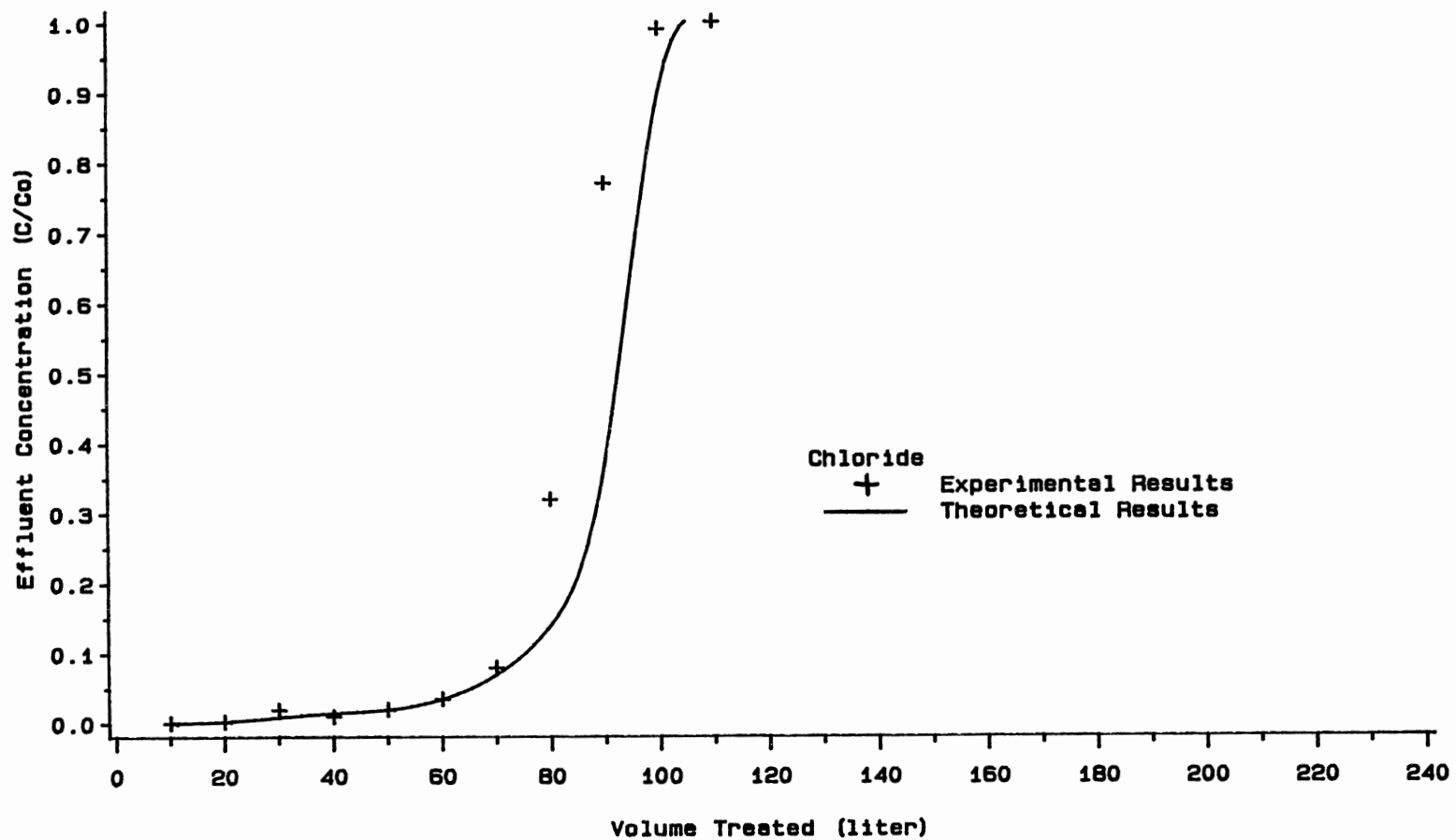


Figure 43. Deviations of Theoretical and Experimental Results for Cation/Anion Resin of 5.0 g/3.0 g with new constants in Table VIII

TABLE VIII
 CONSTANTS FOR MASS-TRANSFER COEFFICIENTS
 IN THE SYSTEM

Cation/Anion	Sodium Exchange	Chloride Exchange
1/3	0.55	0.37
1/2	0.50	0.38
3/5	0.49	0.38
1/1.5	0.47	0.39
1/1	0.45	0.39
1.5/1	0.43	0.41
5/3	0.42	0.41
2/1	0.40	0.42
3/1	0.38	0.45

From Table VIII, it is shown that the constant A for sodium exchange decreases and that for chloride exchange increases as the cation-to-anion resin ratio increases. Thus the constant A may be expressed as a function of cation-to-anion resin ratio by curve fitting. Since the constant for chloride exchange increases almost linearly as a function of cation-to-anion resin ratio, a linear equation is adapted (Figure 44). The constant for sodium exchange does not decrease linearly, so polynomial, exponential, and logarithmic equations were tried. The

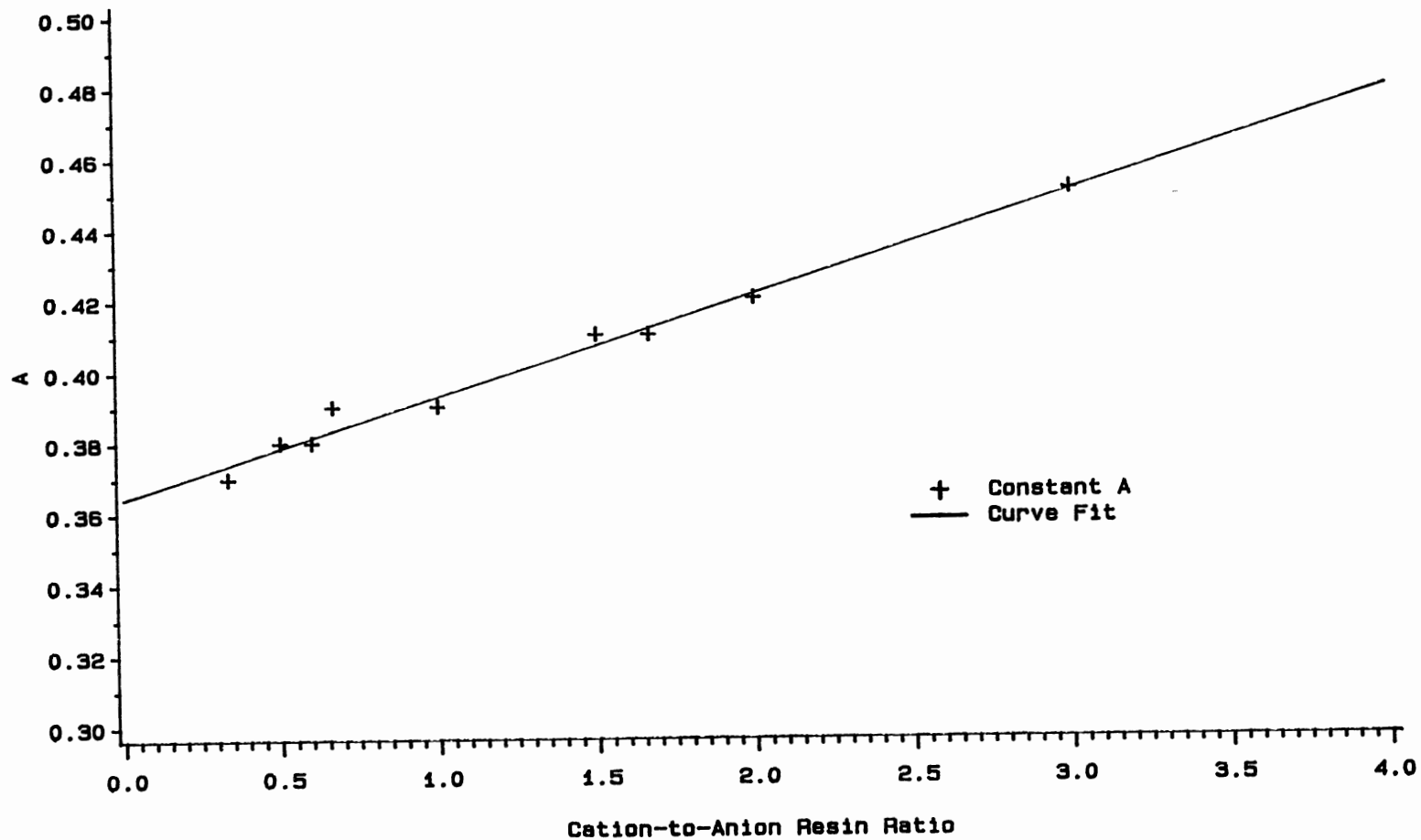


Figure 44. Curve Fit of Constant A and Cation-to-Anion Resin Ratio for Chloride Exchange

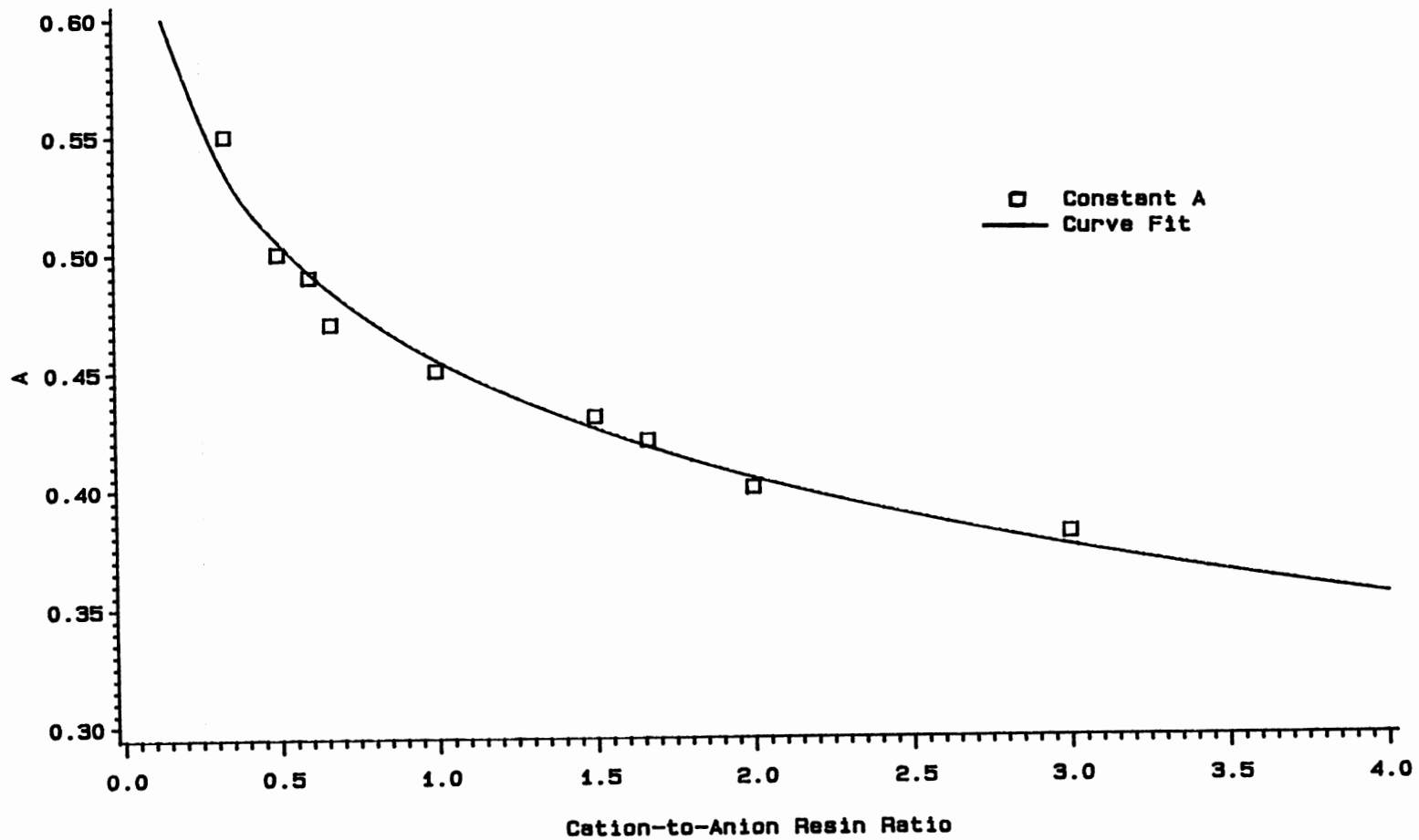


Figure 45. Curve Fit of Constant A and Cation-to-Anion Resin Ratio for Sodium Exchange

logarithmic equation is found to best fit the data (Figure 45). The relationships between the constant A and cation-to-anion resin ratio for sodium exchange and chloride exchange, respectively, are expressed as

$$A = 0.45445 - 0.16786 * \log (R_{C/A}),$$

and

$$A = 0.36443 + 0.028411 * R_{C/A} \quad (11)$$

where $R_{C/A}$ is the cation-to-anion resin ratio.

Some high effluent concentrations are exhibited at the very beginning of the cases with smaller amount of either cation or anion resin. This is probably partly due to the low ionic-diffusion coefficients or mass-transfer coefficients instead of the insufficient contact between the resin and solution because of the shallow-bed technique. This is shown in Figure 46 for the case of cation/anion resin ratio of 1.5 g/1.5 g. Although insufficient contact is expected, both sodium and chloride concentrations from theoretical results are slightly higher at the beginning portion of the breakthrough curves than the experimental results.

The crossover point is described as a function of the cation-to-anion resin ratio. The lower the cation-to-anion resin ratio, the higher the C/Co value of the crossover point, as shown in Table III. These

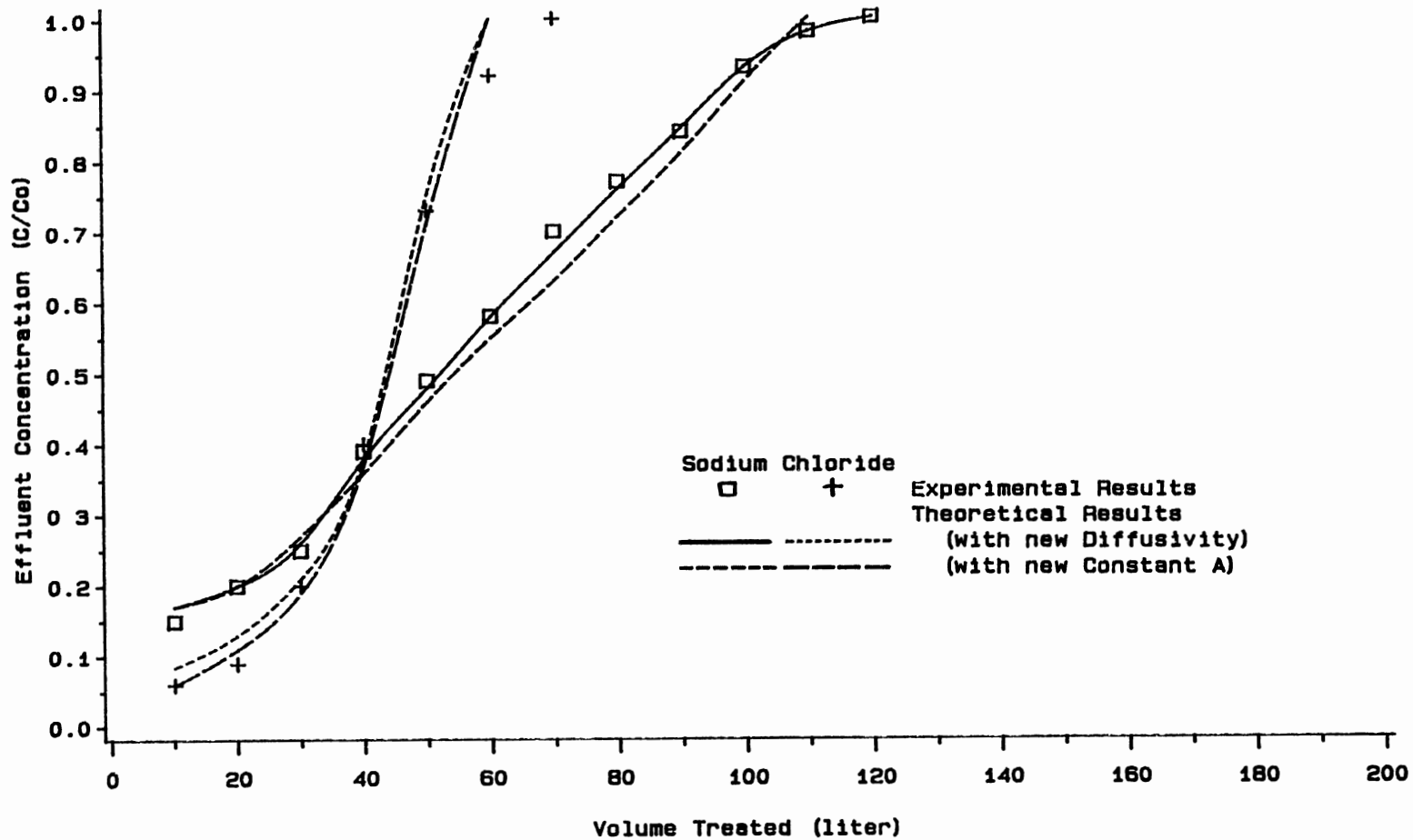


Figure 46. The Effect of Insufficient Contact Between Resin and Solution

experimental results agree favorably with the model prediction of Haub and Foutch (1986a). Sample comparisons between experimental results and model predictions for the case of cation/anion resin ratio of 3.0 g/3.0 g can be obtained from Figures 23 and 24. The crossover points of sodium and chloride breakthrough curves in these Figures are at 76 and 82 liters, and $C/Co = 0.22$ and 0.26 , respectively. In Figure 32, the crossover point is at 80 liter and $C/Co = 0.23$. These values are a little larger than the values in Table III, but the trends look reasonable.

Finally, two possible reasons for the relative lack of agreement between experimental and theoretical results can be considered. One is error in experimental data for the mixed-bed ion exchange, and the other is inadequacies of the theoretical model. The first possibility seems unlikely in this study, especially in view of the reproducibility of the data. The second possibility seems more likely, although the model generally describe the phenomena, and the new ionic-diffusion coefficients and the mass-transfer coefficients are suggested to better fit the actual data. A more complete mechanism with less assumptions, possibly involving particle diffusion as well as film diffusion, will be required to improve the model.

CHAPTER VII

CONCLUSIONS AND RECOMMENDATIONS

The results and discussion of this study are summarized, and some experimental and theoretical efforts are suggested for future studies.

Conclusions

In light of the experimental results for the upward flow mixed-bed ion-exchange column to obtain effluent concentrations as a function of time and column position, the following conclusions can be drawn in this study:

1. Breakthrough curves are obtained as a function of bed depth using the same cation-to-anion resin ratio and different total resin weight. The bed depth affects the pattern of the sodium breakthrough curve but not the chloride breakthrough curve in beds because of the selectivity difference.

2. Resin selectivity determines the shape of breakthrough curves. Some sodium and chloride breakthrough curves cross at a point as a function of resin ratio. The lower cation-to-anion resin ratio shows the higher effluent concentration of the crossover point.

3. The anion resin affects the sodium breakthrough curve, and the cation resin affects the chloride breakthrough curve. The large amount of oppositely-charged resin gives a sharper breakthrough while the small amount gives a wide breakthrough curve. This is due to the difference of mass transfer coefficient of ions in alkaline and acidic solution.

4. A totally segregated bed shows the effect of bed homogeneity. The resultant lower or higher mass transfer coefficient of ions in solution affects the shape of the sodium and chloride breakthrough curves. This trend is also observed in a homogeneous bed of either cation or anion resin.

5. Since the ionic-diffusion coefficients in the literature are much larger than the values from the experimental results, a set of an order of magnitude lower coefficients gives reasonable fit for this mixed-bed ion exchange as a function of cation-to-anion resin ratio.

6. A correlation equation of the ionic-diffusion coefficients of an order of magnitude lower gives reasonable fit as a function of ionic concentration. This linear equation can be used for all of the cation-to-anion resin ratio in this system.

7. The nonionic mass-transfer coefficients for packed beds are suggested for this system. The constant

from the correlation of Kataoka, et al., (1972) was corrected for the low influent concentration of these experiments.

Recommendations

The above results describe only the effect of the variation of the cation-to-anion resin ratio. To understand the mixed-bed ion exchange process well, the following recommendations are suggested for comprehensive study:

1. This study has determined the effect of cation-to-anion resin ratio. The mathematical model can predict the variation of the cation and anion resin diameters and size distributions. Experimental data are needed to test the model.

2. To get the full capacity of the resin, incomplete resin regeneration, or incomplete resin separation before regeneration should be avoided. Thus, the so-called "Triobed" system, which utilizes an intermediate layer of inert polymer having an intermediate density between the top anion resin and the bottom cation resin, is used to separate the mixed bed perfectly by an upflow expansion when exhausted. This system reduces the effect of regenerant on the opposite resin when the mixed bed is not completely separated. Thus, the effect of inert polymer can be investigated by

studying the incomplete resin separation and regeneration.

3. In a condensate polishing process with low influent impurities, maximum effluent purity and high flow rates, cation resins create no problem, but anion resins exhibit serious kinetic deterioration after a short service life, sometimes as little as six months. Replacement of resin is required every four or five years. Thus, the kinetic deterioration of anion resin should be studied.

4. Using an old base resin, Harries (1988) showed that the organic fouling, cross contamination during regeneration, and age of anion exchange resin affect the mass-transfer coefficient. Organic foulants at the bead surface disturb ionic species diffusing from and to the bulk solution, so affect the rate-controlling step. Thus, the effect of used and new resins can be studied to show bead surface chemistry. The bead surface properties of the used anion resins are more deteriorated than that of the new resins while the bulk resin properties of two resins are similar.

5. Harries and Tittle (1986) showed that the mass-transfer coefficients are dependent on the type of the resin. Thus, the kinetics as a function of resin type need to be investigated.

6. Harries (1988) showed the effect of pH on cation and anion-exchange rates in solution phase. The cation exchange is faster in an alkaline solution, while the anion exchange is rapid in an acidic medium. This coincides with the experimental results of this study. The new constants for the correlation equation of Kataoka, et al. (1972), were suggested in this study as a function of cation-to-anion resin ratio. The resin ratio influences solution pH, and then the mass-transfer coefficients. Thus, the model, which includes the variation of pH and feed concentration, will more accurately predict the behavior of the breakthrough curve.

7. Liquid phase exchange model is important in the mixed-bed ion-exchange process since this process usually deals with low ionic concentrations. However, a correct resin phase transfer model is also needed to predict bed performance accurately.

REFERENCES

Acrivos, A., "Method of Characteristics Technique - Application to Heat and Mass Transfer Problems," Industrial and Engineering Chemistry, Engineering, Design, and Process Development, Vol.48, No.4, pp.703-709 (1956).

Adamson, A. W. and Grossman, J. J., "A Kinetic Mechanism for Ion-Exchange," The Journal of Chemical Physics, Vol.17, No.10, pp.1002-1003 (1949).

Allen, R. M., Addison, P. A., and Dechapunya, A. H., "The Characterization of Binary and Ternary Ion Exchange Equilibria," The Chemical Engineering Journal, Vol.40, pp.151-158 (1989).

Anderson, R. E., "Estimation of Ion EXchange Process Limits by Selectivity Calculations," AIChE Symposium Series, No.152, Vol.71, pp.236-242 (1975).

Bajpai, R. K., Gupta, A. K., and Rao, M. G., "Single Particle Studies of Binary and Ternary Cation Exchange Kinetics," AIChE Journal, Vol.20, No.5, pp.989-995 (1974).

Beyer, W. A. and James, D. B., "Independence of the Performance of an Ion-Exchange Column on its Shape," Industrial, and Engineering Chemistry, Fundamentals, Vol.5, No.3, pp.433-434 (1966).

Bieber, H., Steidler, F. E., and Selke, W. A., "Ion Exchange Rate Mechanism," Chemical Engineering Progress Symposium Series, No.14, Vol.50, pp.17-21 (1954).

Blickenstaff, R. A., Wagner, J. D., and Dranoff, J. S., "The Kinetics of Ion Exchange Accompanied by Irreversible Reaction. I. Film Diffusion Controlled Neutralization of a Strong Acid Exchanger by Strong Bases," The Journal of Physical Chemistry, Vol.71, No.6, pp.1665-1669 (1967a).

Blickenstaff, R. A., Wagner, J. D., and Dranoff, J. S., "The Kinetics of Ion Exchange Accompanied by Irreversible Reaction. II. Intraparticle Diffusion Controlled Neutralization of a Strong Acid Exchanger by Strong Bases," The Journal of Physical Chemistry, Vol.71, No.6, pp.1670-1674 (1967b).

Boyd, G. E., Adamson, A. W., and Myers, L. S. Jr., "The Exchange Adsorption of Ions from Aqueous Solutions by Organic Zeolites. II. Kinetics," Journal of the American Chemical Society, Vol.69, pp.2836-2848 (1947).

Buck, R. P., "Kinetics of Bulk and Interfacial Ionic Motion: The Microscopic Basis and Limits for the Nernst-Planck-Poisson System," in "Fundamentals and Applications of Ion Exchange," NATO ASI Series, Martinus Nijhoff Publishers, pp.370-451, 1985.

Caddell, J. R. and Moison, R. L., "Mixed-Bed Deionization at High Flow Rates," Chemical Engineering Progress Symposium Series, No.14, Vol.50, pp.1-5 (1954).

Carberry, J. J., "A Boundary-Layer Model of Fluid-Particle Mass Transfer in Fixed Beds," AIChE Journal, Vol.6, No.3, pp.460-463 (1960).

Chemical Engineering Progress, "New Ion-Exchange Resins by Resinous Products & Chem. Co.," Vol.44, No.8, p.18 (1948).

Chu, B., Whitney, D. C. and Diamond, R. M., "On Anion-Exchange Resin Selectivities," Journal of Inorganic and Nuclear Chemistry, Vol.24, pp.1405-1415 (1962).

Cooney, D. O., "Column Configuration and Performance in Fixed-Bed Ion Exchange Systems," Industrial and Engineering Chemistry Fundamentals, Vol.6, No.1, pp.159-160 (1967).

Cooper, R. S., "Slow Particle Diffusion in Ion Exchange Columns," Industrial and Engineering Chemistry Fundamentals, Vol.4, No.3, pp.308-313 (1965).

Coppola, A. P. and Levan, M. D., "Adsorption with Axial Diffusion in Shallow Beds," Chemical Engineering Science, Vol.38, No.7, pp.991-997 (1983).

Costa, C., Rodrigues, A., and Loureiro, J., "Numerical Methods," in "Ion Exchange: Science and Technology," Edited by A. E. Rodrigues, NATO ASI Series, Martinus Nijhoff Publishers, pp.227-254 (1986).

Darji, J. D. and McGilbra, A. F., "Ion Exchange Equilibrium- A Key to Condensate Polisher Performance," Proceedings of the American Power Conference, Vol.42, pp.1101-1108 (1980).

Dionex, "Basic Ion Chromatography," Dionex Corporation, 1983.

Dranoff, J. and Lapidus, L., "Equilibrium in Ternary Ion Exchange Systems," Industrial and Engineering Chemistry, Vol.49, No.8, pp.1297-1302 (1957).

Dranoff, J. and Lapidus, L., "Multicomponent Ion Exchange Column Calculations," Industrial and Engineering Chemistry, Vol.50, No.11, pp.1648-1653 (1958).

Dranoff, J. and Lapidus, L., "Ion Exchange in Ternary Systems," Industrial and Engineering Chemistry, Vol.53, No.1, pp.71-76 (1961).

Evangelista, F. and Berardino, F. C. D, "Modelling of Multicomponent Fixed Bed Ion Exchange Operations," in "Ion Exchange: Science and Technology," Edited by A. E. Rodrigues, NATO ASI Series, Martinus Nijhoff Publishers, 1986.

Frisch, N. W. and Kunin, R., "Kinetics of Mixed-Bed Deionization:I," AIChE Journal, Vol.6, No.4, pp.640-647 (1960).

Gilliland, E. R. and Baddour, R. F., "The Rate of Ion Exchange," Industrial and Engineering Chemistry, Vol.45, No.2, pp.330-337 (1953).

Gilliland, E. R., Baddour, R. F., and Goldstein, D. J., "Counter Diffusion of Ions in Water," Canadian Journal of Chemical Engineering, Vol.35, No.1, pp.10-17 (1957).

Glaski, F. A. and Dranoff, J. S., "Ion Exchange Kinetics: A Comparison of Models," AIChE Journal, Vol.9, No.3, pp.426-431 (1963).

Glueckauf, E. and Coates, J. I., Journal of the American Chemical Society, p.1315 (1947).

Gomez-Vaillard, R., Kershenbaum, L. S., and Streat, M., "The Performance of Continuous, Cyclic Ion-Exchange Reactors-I," Chemical Engineering Science, Vol.36, pp.307-317 (1981a).

Gomez-Vaillard, R., and Kershenbaum, L. S., "The Performance of Continuous Cyclic Ion-Exchange Reactors-II, Reaction with Intraparticle Diffusion Controlled Kinetics" Chemical Engineering Science, Vol.36, pp.319-326 (1981b).

Goto, S., Goto, M., and Teshima, H., "Simplified Evaluations of Mass Transfer Resistances from Batch-Wise Adsorption and Ion-Exchange Data. 1. Linear Isotherms," Industrial and Engineering Chemistry Fundamentals, Vol.20, No.4, pp.368-371 (1981a).

Goto, M., Goto, S., and Teshima, H., "Simplified Evaluations of Mass Transfer Resistances from Batch-Wise Adsorption and Ion-Exchange Data. 2. Nonlinear Isotherms," Industrial and Engineering Chemistry Fundamentals, Vol.20, No.4, pp.371-375 (1981b).

Graham, E. E., "Application of the Stefan-Maxwell Equations to Multicomponent Ion Exchange," in "Fundamentals and Applications of Ion Exchange," NATO ASI Series, Martinus Nijhoff Publishers, pp.458-467 (1985)

Graham, E. E. and Dranoff, J. S., "Kinetics of Anion Exchange Accompanied by Fast Irreversible Reaction," AIChE Journal, Vol.18, No.3, pp.608-613 (1972).

Graham, E. E. and Dranoff, J. S., "Application of the Stefan-Maxwell Equations to Diffusion in Ion Exchangers. 1. Theory," Industrial and Engineering Chemistry Fundamentals, Vol.21, pp.360-365 (1982a).

Graham, E. E. and Dranoff, J. S., "Application of the Stefan-Maxwell Equations to Diffusion in Ion Exchangers. 2. Experimental Results," Industrial and Engineering Chemistry Fundamentals, Vol.21, pp.365-369 (1982b).

Grammont, P., Rothschild, W., Sauer, C., and Katsahian, J., "Ion Exchange in Industry," in "Ion Exchange: Science and Technology," Edited by Rodrigues, A. E., NATO Advanced Science Institutes Series, Martinus Nijhoff Publishers, 1986.

Grimshaw, R. W. and Harland, C. E., "Ion Exchange: Introduction to Theory and Practice," The Chemical Society, London, England, 1975.

Harries, R. R., "Ultrapure Water-Ion Exchange Kinetics in Condensate Purification," Chemistry and Industry, No.4, pp.104-109 (1987).

Harries, R. R., "The Role of pH in Ion Exchange Kinetics," in "Ion Exchange for Industry," Edited by Streat, M., Ellis Horwood Limited, Chichester, England, 1988.

Harries, R. R. and Ray, N. J., "Anion Exchange in High Flow Rate Mixed Beds," Effluent and Water Treatment Journal, Vol.24, No.4, pp.131-139 (1984).

Haub, C. E., "Model Development for Liquid Resistance-Controlled Reactive Ion Exchange at Low Solution Concentrations with Application to Mixed Bed Ion Exchange," M.S. Thesis, Oklahoma State University, Stillwater, Oklahoma, 1984.

Haub, C. E. and Foutch, G. L., "Mixed-Bed Ion Exchange at Concentrations Approaching the Dissociation of Water. 1. Model Development," Industrial and Engineering Chemistry Fundamentals, Vol.25, No.3, pp.373-381 (1986a).

Haub, C. E. and Foutch, G. L., "Mixed-Bed Ion Exchange at Concentrations Approaching the Dissociation of Water. 2. Column Model Applications," Industrial and Engineering Chemistry Fundamentals, Vol.25, No.3, pp.381-385 (1986b).

Helfferich, F., "Ion Exchange," McGraw-Hill Book Company, New York, 1962.

Helfferich, F., "Ion-Exchange Kinetics. IV. Demonstration of the Dependence of the Interdiffusion Coefficient on Ionic Composition," Journal of Physical Chemistry, Vol.67, pp.1157-1159 (1963).

Helfferich, F., "Ion-Exchange Kinetics. V. Ion Exchange Accompanied by Reactions," The Journal of Physical Chemistry, Vol.69, No.4, pp.1178-1187 (1965).

Helfferich, F., "Chapter 2. Ion Exchange Kinetics," in "Ion Exchange," Volume I, Edited by J. A. Marinsky, Marcel Dekker, Inc., New York, 1966.

Helfferich, F. G., "Multicomponent Ion Exchange in Fixed Beds, Generalized Equilibrium Theory for Systems with Constant Separation Factors," Industrial and Engineering Chemistry Fundamentals, Vol.6, No.3, pp.362-364 (1967).

Helfferich, F. G., "Conceptual View of Column Behavior in Multicomponent Adsorption or Ion-Exchange Systems," AICHE Symposium Series, Vol.80, No.233, pp.1-13 (1984).

Helfferich, F. and Plesset, M. S., "Ion Exchange Kinetics. A Nonlinear Diffusion Problem," The Journal of Chemical Physics, Vol.28, No.3, pp.418-424 (1958).

Hering, B. and Bliss, H., "Diffusion in Ion Exchange Resins," AICHE Journal, Vol.9, No.4, pp.495-503 (1963).

Hiester, N. K., Radding, S. B., Nelson, Jr., R. L., and Vermeulen, T., "Interpretation and Correlation of Ion Exchange Column Performance Under Nonlinear Equilibria," AICHE Journal, Vol.2, p.404-411 (1956).

Hiester, N. K. and Vermeulen, T., "Saturation Performance of Ion-Exchange and Adsorption Columns," Chemical Engineering Progress, Vol.48, No.10, pp.505-516 (1952).

Hill, R. and Lorch, W., "Ion Exchange," in Chapter 7 "Handbook of Water Purification," Second Edition, Edited by W. Lorch, John Wiley and Sons, 1988.

Huang, T. C. and Li, K. Y., "Ion-Exchange Kinetics for Calcium Radiotracer in a Batch System," Industrial and Engineering Chemistry Fundamentals, Vol.12, No.1, pp.50-55 (1973).

Huang, T. C. and Tsai, F. N., "Kinetic Parameters of Isotopic Exchange Reaction in Finite Bath," Canadian Journal of Chemical Engineering, Vol.55, p.301-306 (1977).

Hwang, Y. L. and Helfferich, F. G., "Generalized Model for Multispecies Ion-Exchange Kinetics Including Fast Reversible Reactions," Reactive Polymers, Vol.5, pp.237-253 (1987).

Hwang, Y. L., Helfferich, F. G., and Leu, R. J., "Multicomponent Equilibrium Theory for Ion-Exchange Columns Involving Reactions," AICHE Journal, Vol.34, No.10, pp.1615-1626 (1988).

Kataoka, T., Sato, N. and Ueyama, K., "Effective Liquid Phase Diffusivity in Ion Exchange," Journal of Chemical Engineering of Japan, Vol.1, No.1, pp.38-42 (1968).

Kataoka, T., Yoshida, H. and Ueyama, K., "Mass Transfer in Laminar Region Between Liquid and Packing Material Surface in the Packed Bed," Journal of Chemical Engineering of Japan, Vol.5, No.2, pp.132-136 (1972).

Kataoka, T., Yoshida, H. and Yamada, T., "Liquid Phase Mass Transfer in Ion Exchange Based on the Hydraulic Radius Model," Journal of Chemical Engineering of Japan, Vol.6, No.2, pp.172-177 (1973a).

Kataoka, T., Nishiki, T. and Ueyama, K., "Mass Transfer in Ion Exchange By Liquid Anion Exchanger," Journal of Chemical Engineering of Japan, Vol.6, No.4, pp.320-324 (1973b).

Kataoka, T., Yoshida, H. and Sanada, H., "Estimation of the Resin Phase Diffusivity in Isotopic Ion Exchange," Journal of Chemical Engineering of Japan, Vol.7, No.2, pp.105-109 (1974).

Kataoka, T. and Yoshida, H., "Resin Phase Mass Transfer in Ion Exchange Between Different Ions Accompanied by Resin Volume Change," Journal of Chemical Engineering of Japan, Vol.8, No.6, pp.451-456 (1975).

Kataoka, T. and Yoshida, H., "Estimating Equation of Resin Phase Self-Diffusivity," Journal of Chemical Engineering of Japan, Vol.9, No.1, pp.74-75 (1976a).

Kataoka, T., Yoshida, H. and Shibahara, Y., "Liquid Phase Mass Transfer in Ion Exchange Accompanied by Chemical Reaction," Journal of Chemical Engineering of Japan, Vol.9, No.2, pp.130-135 (1976b).

Kataoka, T. and Yoshida, H., "Breakthrough Curve For Liquid Phase Diffusion Controlling in Irreversible Ion Exchange," Journal of Chemical Engineering of Japan, Vol.9, No.4, pp.326-328 (1976c).

Kataoka, T. and Yoshida, H., "Breakthrough Curve in Ion Exchange Between Divalent Ion and Monovalent Ion-Liquid Phase Diffusion Control," Journal of Chemical Engineering of Japan, Vol.10, No.3, pp.245-247 (1977a).

Kataoka, T. and Yoshida, H., "Breakthrough Curve in Ion Exchange Column-Particle Diffusion Control," Journal of Chemical Engineering of Japan, Vol.10, No.5, pp.385-390 (1977b).

Kataoka, T., Yoshida, H. and Ozasa, Y., "Intraparticle Ion Exchange Mass Transfer Accompanied by Instantaneous Irreversible Reaction," Chemical Engineering Science, Vol.32, pp.1237-1240 (1977c).

Kataoka, T. and Yoshida, H., "Effect of Electric Field and Equilibrium Relation on Breakthrough Curve in Ion Exchange Column - Resin Phase Diffusion Control," Journal of Chemical Engineering of Japan, Vol.11, No.5, pp.408-410 (1978).

Kataoka, T. and Yoshida, H., "Ion Exchange Equilibria in Ternary Systems," Journal of Chemical Engineering of Japan, Vol.13, No.4, pp.328-330 (1980).

Kataoka, T., Yoshida, H., and Uemura, T., "Liquid-Side Ion Exchange Mass Transfer in a Ternary System," AIChE Journal, Vol.33, No.2, pp.202-210 (1987).

Kataoka, T. and Yoshida, H., "Kinetics of Ion Exchange Accompanied by Neutralization Reaction," AIChE Journal, Vol.34, No.6, pp.1020-1026 (1988).

Klein, G., "Fixed-Bed Ion Exchange with Formation or Dissolution of Precipitate," in "Ion Exchange: Science and Technology," Edited by A. E. Rodrigues, NATO ASI Series, Martinus Nijhoff Publishers, pp.199-226 (1986).

Klein, G., Tondeur, D., and Vermeulen, T., Industrial and Engineering Chemistry Fundamentals, Vol.6, p.339 (1967).

Kunin, R., "Elements of Ion Exchange," Reinhold, New York, 1960.

Kunin, R. and McGarvey, F. X., "Monobed Deionization with on Exchange Resins," Industrial and Engineering Chemistry, Engineering and Process Development, Vol.43, no.3, pp.734-740 (1951).

Kuo, J. C. W. and David, M. M., "Single Particle Studies of Cation-Exchange Rates in Packed Beds: Barium Ion-Sodium Ion System," AIChE Journal, Vol.9, No.3, pp.365-370 (1963).

Lapidus, L. and Rosen, J. B., "Experimental Investigations of Ion Exchange Mechanisms in Fixed Beds by Means of an Asymptotic Solution," Chemical Engineering Progress Symposium Series, No.14, Vol.50, pp.97-102 (1954).

Liapis, A. I. and Rippin, D. W., "The Simulation of Binary Adsorption in Continuous Countercurrent Operation and a Comparison with Other Operating Modes," AIChE Journal, Vol.25, p.455-460 (1979).

Loureiro, J., Costa, C., Dias, M., Lopes, J., and Rodrigues, A., "Design Methods for Ion-Exchange Equipment," in "Fundamentals and Applications of Ion exchange," Edited by L. Liberti and J. R. Millar, NATO ASI Series, Martinus Nijhoff Publishers, pp.245-260 (1985).

Martin, O., "Water Demineralisation by Mixed Bed Ion Exchange," The Industrial Chemist, pp.448-450, October (1952).

McNulty, J. T., Personal Communication, Rohm and Haas Company, Spring House, Pennsylvania, 1989.

Michaels, A. S., "Simplified Method of Interpreting Kinetic Data in Fixed-Bed Ion Exchange," Industrial and Engineering Chemistry, Engineering and Process Development, Vol.44, No.8, pp.1922-1930 (1952).

Moison, R. L. and O'Hern, Jr., H. A., "Ion Exchange Kinetics," Chemical Engineering Progress Symposium Series, Vol.55, No.24, pp.71-85 (1959).

Morig, C. R. and Rao, M. G., "Diffusion in Ion Exchange Resins: Sodium Ion-Strontium Ion System," Chemical Engineering Science, Vol.20, pp.889-893 (1965).

Myers, A. L. and Byington, S., "Thermodynamics of Ion Exchange: Prediction of Multicomponent Equilibria from Binary Data," in "Ion Exchange: Science and Technology," Edited by A. E. Rodrigues, NATO ASI Series, Martinus Nijhoff Publishers, pp.119-145 (1986).

Nachod, F. C. and Wood, W., "The Reaction Velocity of Ion Exchange," Journal of the American Chemical Society, Vol.66, pp.1380-1384 (1944).

Omatete, O. O., Clazie, R. N., and Vermeulen, T., "Column Dynamics of Ternary Ion Exchange, Part I: Diffusional and Mass Transfer Relations," Chemical Engineering Journal, Vol.19, p.229-240 (1980).

Petruzzelli, D., Helfferich, F. G., Liberti, L., Millar, J. R., and Passino, R., "Kinetics of Ion Exchange with Intraparticle Rate Control: Models Accounting for Interactions in the Solid Phase," Reactive Polymers, Vol.7, pp.1-13 (1987a).

Petruzzelli, D., Liberti, L., Passino, R., Helfferich, F. G., and Hwang, Y. L., "Chloride/Sulfate Exchange Kinetics: Solution for Combined Film and Particle Diffusion Control," Reactive Polymers, Vol.5, pp.219-226 (1987b).

Petruzzelli, D., Liberti, L., Boghetich, G., Helfferich, F. G., and Passino, R., "Ion Exchange Kinetics on Anion Resins. Concentration Profiles and Transient Phenomena in the Solid Phase," Reactive Polymers, Vol.7, pp.151-157 (1988).

Pfeffer, R., "Heat and Mass Transport in Multiparticle Systems," Industrial and Engineering Chemistry, Fundamentals, Vol.3, No.4, pp.380-383 (1964).

Pieronni, L. J. and Dranoff, J. S., "Ion Exchange Equilibria in a Ternary System," AIChE Journal, Vol.9, No.1, pp.42-45 (1963).

Pinto, N. G. and Graham, E. E., "Characterization of Ionic Diffusivities in Ion-Exchange Resins," Industrial and Engineering Chemistry, Research, Vol.26, No.11, pp.2331-2336 (1987).

Plesset, M. S., Helfferich, F., and Franklin, J. N., "Ion Exchange Kinetics. A Nonlinear Diffusion Problem. II. Particle Diffusion Controlled Exchange of Univalent and Bivalent Ions," The Journal of Chemical Physics, Vol.29, No.5, No.1064-1069 (1958).

Rao, M. G. and David, M. M., "Single-Particle Studies of Ion Exchange in Packed Beds: Cupric Ion-Sodium Ion System," AIChE Journal, Vol.10, No.2, pp.213-219 (1964).

Rao, M. G. and Gupta, A. K., "Kinetics of Ion-Exchange in Weak-Base Anion Exchange Resins," AIChE Symposium Series, No.219, Vol.78, pp.96-102 (1982a).

Rao, M. G. and Gupta, A. K., "Ion Exchange Processes Accompanied by Ionic Reactions," The Chemical Engineering Journal, Vol.24, pp.181-190 (1982b).

Reichenberg, D., "Properties of Ion-Exchange Resins in Relation to their Structure. III. Kinetics of Exchange," Journal of the American Chemical Society, Vol.75, pp.589-597 (1953).

Reid, R. C., Prausnitz, J. M., and Poling, B. E., "The Properties of Gases and Liquids," McGraw-Hill Book Company, New York, 1987.

Robinson, R. A. and Stokes, R. H., "Electrolyte Solutions," Butterworths Scientific Publications, London, 1959.

Rodrigues, A. E. and Costa, C. A., "Fixed Bed Processes: A Strategy for Modelling," in "Ion Exchange: Science and Technology," Edited by A. E. Rodrigues, NATO ASI Series, Martinus Nijhoff Publishers, pp.271-287 (1986).

Saunders, L., "Water Physics and Chemistry," in Chapter 2 "Handbook of Water Purification," Second Edition, Edited by W. Lorch, John Wiley and Sons, 1988.

Schloegl, R. and Helfferich, F., "Comment on the Significance of Diffusion Potentials in Ion Exchange Kinetics," The Journal of Chemical Physics, Vol.26, No.1, pp.5-7 (1957).

Shallcross, D. C., Herrmann, C. C., and McCoy, B. J., "An Improved Model for the Prediction of Multicomponent Ion Exchange Equilibria," Chemical Engineering Science, Vol.43, No.2, pp.279-288 (1988).

Small, H., Stevens, T. S., and Bauman, W. C., "Novel Ion Exchange Chromatographic Method Using Conductimetric Detection," Analytical Chemistry, Vol.47, No.11, pp.1801-1809 (1975).

Smith, D. M., "Moment Analysis of Ion Exchange Kinetics: Particle Diffusion Control," Chemical Engineering Science, Vol.40, No.12, pp.2369-2373 (1985).

Smith, T. G. and Dranoff, J. S., "Film Diffusion-Controlled Kinetics in Binary Ion Exchange," Industrial and Engineering Chemistry Fundamentals, Vol.3, No.3, pp.195-200 (1964).

Streat, M., "Kinetics of Slow Diffusing Species in Ion Exchangers," Reactive Polymers, Vol.2, pp.79-91 (1984).

Streat, M., "Continuous Ion Exchange Technology," in "Ion Exchange: Science and Technology," Edited by A. E. Rodrigues, NATO ASI Series, Martinus Nijhoff Publishers, pp.319-335 (1986).

Thomas, H. C., "Solid Diffusion in Chromatography," Journal of Chemical Physics, Vol.19, p.1213 (1951).

Tittle, K., "Mixed-Bed Performance in a Condensate Polishing Plant," Proceedings of the American Power Conference, Vol.43, pp.1126-1130 (1981).

Tittle, K., Tyldelsey, J. D., Tasker, P. W., and Butcher, C. J., "Mixed Bed Performance in a Condensate Polishing Plant," Water Chemistry, BNSF, Paper 23, pp.119-124 (1980).

Tondeur, D. and Bailly, M., "Design Methods for Ion-Exchange Processes Based on the Equilibrium Theory," in "Ion Exchange: Science and Technology," Edited by A. E. Rodrigues, NATO ASI Series, Martinus Nijhoff Publishers, pp.147-197 (1986).

Tsai, F. N., "Film Diffusion-Controlled Kinetics of Isotopic Exchange in a Finite Bath," AIChE Journal, Vol.28, No.4, pp.698-700 (1982a).

Tsai, F. N., "Kinetics of Ion Exchange with Combined Film and Particle Diffusion in a Finite Bath," Journal of Physical Chemistry, Vol.86, No.13, pp.2339-2344 (1982b).

Tsai, F. N. and Huang, T. C., "Effects of Film and Particle Diffusion on the Kinetics of Isotopic Exchange," The Chemical Engineering Journal, Vol.30, pp.39-44 (1985).

Turner, J. C. R., "Nernst-Planck or No?" in "Fundamentals and Applications of Ion Exchange," NATO ASI Series, Martinus Nijhoff Publishers, pp.452-457 (1985)

Turner, J. C. R. and Snowdon, C. B., "Liquid-Side Mass Transfer Coefficients in Ion Exchange: An Examination of the Nernst-Planck Model," Chemical Engineering Science, Vol.23, p.221 (1968).

Tyrell, H. J. V. and Harris, K. R., "Diffusion in Liquids," Chapter 8, Butterworths Monographs in Chemistry, London, 1984.

Van Brocklin, L. P. and David, M. M., "Coupled Ionic Migration and Diffusion During Liquid-Phase Controlled Ion Exchange," Industrial and Engineering Chemistry Fundamentals, Vol.11, No.1, pp.91-99 (1972).

Van Brocklin, L. P. and David, M. M., "Ionic Migration Effects During Liquid Phase Controlled Ion Exchange," AIChE Symposium Series, No.152, Vol.71, pp.191-201 (1975).

Vermeulen, T., "Theory for Irreversible and Constant-Pattern Solid Diffusion," Industrial and Engineering Chemistry, Vol.45, No.8, pp.1664-1670 (1953).

Vermeulen, T. and Hiester, N. K., "Kinetic Relationships for Ion Exchange Processes," Chemical Engineering Progress Symposium Series, Vol.55, No.24, pp.61-69 (1959).

Vermeulen, T., Le Van, M. D., Hiester, N. K., and Klein, G., "Section 16, Adsorption and Ion Exchange," in "Perry's Chemical Engineers' Handbook," Edited by P. H. Perry and D. Green, McGraw-Hill Book Company, New York, 1984.

Wesselingh, J. A. and Van der Meer, A. P., "Counter-Current Ion Exchange," in "Ion Exchange: Science and Technology," Edited by A. E. Rodrigues, NATO ASI Series, Martinus Nijhoff Publishers, pp.289-318 (1986).

Wildhagen, G. R. S., Qassim, R. Y., Haque, W. and Rahman, K., "Ion Exchange Mass Transfer in Fluidized Bed Contactors: Film Diffusion Controlled Kinetics," Chemical Engineering Science, Vol.40, No.8, pp.1591-1594 (1985).

Wilke and Hougen, Trans. Am. Inst. Chem. Eng., 41, p.445 (1945)

Wilson, D. J., "Modeling of Ion-Exchange Column Operation. II. Mass Transport Kinetics," Separation Science and Technology, Vol.21, No.10, pp.991-1008 (1986).

Yoshida, H. and Kataoka, T., "Intraparticle Ion-Exchange Mass Transfer in Ternary System," Industrial and Engineering Chemistry, Research, Vol.26, No.6, pp.1179-1184 (1987).

Zecchini, E J., Personal Communication, Oklahoma State University, Stillwater, Oklahoma, 1989.

APPENDIXES

APPENDIX A

ERROR ANALYSIS FOR THE SYSTEM

Any experimental measuring device has certain uncertainties associated with it. Most uncertainties for the equipment have been determined through the repeated experimental analysis. The errors caused by the system are analyzed in this section. The errors of ion chromatography and mixed-bed ion-exchange column make the whole system error.

Accuracy of Ion Chromatography Analysis

The accuracy of the ion chromatographic analysis was checked regularly through the experiments. This was done by injecting the same samples three times successively. The selected chromatograms were compared with each other in terms of the peak heights and the ionic concentrations calculated. Table IX shows an example calculation of the analysis. The effluent sodium and chloride concentrations in this Table are for the case of cation/anion resin ratio of 3.0 g/3.0 g. This is when the 90.0 liter of solution was treated. The maximum

deviation from average and the standard deviation are shown to be 2.61 % and 0.0065, respectively.

TABLE IX
ACCURACY OF ION CHROMATOGRAPHY ANALYSIS

Breakthrough Curve	C/Co	Deviation from Average (%)	Standard Deviation
Sodium	0.354	-2.61	0.0065
	0.342	0.87	
	0.339	1.74	
Chloride	0.600	-1.35	0.0059
	0.590	0.34	
	0.586	1.01	

Experimental Error for the System

The reproducibility of the experimental data was evaluated by the cation/anion resin ratio of 3.0 g/3.0 g, which is shown in Figure 23. By taking the maximum concentration difference of the breakthrough curves, the difference was found to be less than 3.0 %.

The accuracy of reading the weights of the sodium chloride crystals by the electronic balance was estimated to be ± 0.0003 g. The reading of 0.0584 g NaCl to make feed solution of 10^{-4} M gives an error of 0.51 %.

Preparation of standard solution for the ion chromatography caused the biggest error because 0.0029 g of NaCl needed to be measured for the calibration of $C/Co = 0.05$. However, concentration plots in Figures 4 and 5 show the linear relationship between peak height and ion concentration. For attenuation 10 in Figure 4, which has the biggest deviation between line and data, the slope is found to be 163.8 with standard deviation of 1.59. Thus, the error for the calibration of peak height is less than 0.97 %.

The measurement accuracy of pure water to a 10 liter carboy is estimated to be ± 50 ml, so the error for water measurement is 0.5 %. The maximum deviation of the solution flow rate in Figure 6 for the case of cation/anion resin ratio of 3.0 g/3.0 g was 3.9 %, and the standard deviation was found to be 0.00649.

The dry resin was very accurately measured with the maximum error of 0.03 % for 1.0 g of either cation or anion resin. As pointed out in Chapter III, air dry cation and anion resins have moisture contents of 4.9 % and 5.9 %, respectively, and the measurement can vary day to day. However, dry resins which were equilibrated with atmosphere in the laboratory showed an almost consistent weight measurement with a difference of less than 0.5 % when they were measured one month apart.

The temperature variation will affect the resin selectivity coefficients, ionization constant for water, bulk phase viscosity, and ionic diffusion-coefficients in the system. The variation of $\pm 2^{\circ}\text{C}$ at 23°C shows the maximum deviation of 2.05 %, 0.48 %, 4.8 %, and 3.5 %, respectively. The average error of 3.1 % is estimated to the temperature variation.

From the above considerations, the cumulative error of preparation of feed solution, preparation of standard solution, measurement of dry resin weight, measurement of solution flow, temperature variation, and the analysis of ion chromatography is found to be ± 5.78 %.

APPENDIX B

EXPERIMENTAL RESULTS

The data of the sodium and chloride breakthrough curves are presented in the following Table as a function of solution volume treated.

TABLE X
EXPERIMENTAL RESULTS

Volume Treated (Liter)	Ionic Concentrations (C/Co)	
	Sodium	Chloride
(Cation/Anion = 1.0 g/2.0 g)		
10.7	0.23	0.025
20.0	0.30	0.057
30.1	0.41	0.13
37.4	0.49	0.21
47.5	0.61	0.46
55.6	0.74	0.61
65.9	0.89	0.88
75.4	0.96	0.98
82.2	0.99	1.0
90.0	1.0	
(Cation/Anion = 1.2 g/1.8 g)		
8.7	0.13	0.028
14.0	0.16	0.041
20.9	0.23	0.059
30.0	0.31	0.22
33.9	0.37	0.28

TABLE X (Continued)

Volume Treated (Liter)	Ionic Concentrations (C/Co)	
	Sodium	Chloride
41.8	0.47	0.43
50.4	0.59	0.55
55.4	0.69	0.72
63.7	0.81	0.92
71.4	0.86	1.0
79.4	0.89	
87.7	0.96	
93.6	0.98	
101.6	1.0	

(Cation/Anion = 1.5 g/1.5 g)

8.6	0.14	0.035
13.8	0.15	0.04
20.6	0.20	0.082
29.6	0.25	0.24
33.4	0.29	0.31
41.3	0.41	0.58
49.9	0.51	0.65
54.8	0.52	0.81
63.3	0.62	0.92
71.4	0.72	1.0
80.3	0.79	
90.0	0.82	
96.9	0.84	
106.6	0.91	
114.3	0.97	
124.1	1.0	

(Cation/Anion = 1.8 g/1.2 g)

9.1	0.12	0.068
14.7	0.17	0.13
22.0	0.21	0.21
31.7	0.26	0.49
35.8	0.31	0.71
44.2	0.39	0.91
53.4	0.41	1.0
58.6	0.46	
67.9	0.53	
76.6	0.59	
86.2	0.67	

TABLE X (Continued)

Volume Treated (Liter)	Ionic Concentrations (C/Co)	
	Sodium	Chloride
96.6	0.72	
103.9	0.79	
114.4	0.86	
122.5	0.91	
133.1	0.98	
142.8	1.0	

(Cation/Anion = 2.0 g/1.0 g)

8.5	0.065	0.072
13.7	0.095	0.17
20.4	0.14	0.28
29.5	0.19	0.59
33.2	0.21	0.78
41.0	0.26	0.97
49.5	0.30	1.0
54.4	0.37	
62.8	0.44	
70.9	0.51	
79.8	0.55	
89.5	0.64	
96.4	0.71	
106.1	0.78	
113.7	0.82	
123.4	0.89	
132.4	0.93	
138.8	0.96	
146.2	0.98	
154.4	1.0	

(Cation/Anion = 2.0 g/4.0 g)

3.2	0.047	0.001
9.2	0.048	0.003
12.8	0.048	0.005
18.4	0.052	0.008
22.0	0.057	0.01
31.5	0.085	0.025
36.6	0.092	0.016
40.3	0.10	0.02
45.4	0.12	0.023
50.9	0.15	0.032

TABLE X (Continued)

Volume Treated (Liter)	Ionic Concentrations (C/Co)	
	Sodium	Chloride
57.3	0.19	0.041
61.5	0.22	0.045
67.0	0.29	0.057
71.6	0.35	0.065
79.1	0.42	0.088
85.0	0.61	0.14
88.6	0.69	0.18
94.3	0.76	0.25
98.8	0.88	0.31
104.9	0.96	0.51
113.5	1.0	0.65
117.4		0.69
122.2		0.75
127.4		0.81
134.9		0.88
141.5		0.93
146.7		0.96
155.5		0.99
163.4		1.0

(Cation/Anion = 2.4 g/3.6 g)

3.1	0.01	0.000
9.2	0.025	0.000
12.8	0.023	0.000
18.4	0.033	0.002
22.0	0.043	0.002
31.4	0.052	0.015
36.5	0.060	0.03
40.1	0.057	0.30
45.2	0.074	0.031
50.6	0.093	0.036
56.9	0.11	0.046
61.1	0.15	0.056
66.6	0.20	0.08
71.2	0.21	0.13
78.6	0.31	0.14
84.5	0.37	0.19
88.1	0.45	0.23
93.7	0.52	0.28
98.1	0.54	0.31
104.1	0.62	0.44
112.5	0.68	0.63

TABLE X (Continued)

Volume Treated (Liter)	Ionic Concentrations (C/Co)	
	Sodium	Chloride
116.5	0.70	0.68
121.2	0.75	0.81
126.4	0.79	0.84
133.9	0.81	0.90
140.5	0.86	0.93
145.6	0.86	0.94
154.3	0.90	0.97
162.2	0.94	0.97
168.9	0.94	1.0
178.1	0.98	
188.7	1.0	

(Cation/Anion = 3.0 g/3.0 g)

3.3	0.02	0.000
9.7	0.02	0.000
13.5	0.02	0.000
19.5	0.02	0.000
23.3	0.03	0.000
33.3	0.04	0.022
38.8	0.04	0.044
42.6	0.04	0.028
48.0	0.05	0.025
53.9	0.07	0.025
60.6	0.10	0.041
65.1	0.12	0.056
71.0	0.18	0.11
75.9	0.25	0.18
83.7	0.31	0.5
90.0	0.32	0.61
93.8	0.31	0.7
99.8	0.37	0.75
104.5	0.41	0.85
110.9	0.50	0.92
119.9	0.51	0.95
124.1	0.54	0.97
129.1	0.66	0.98
134.6	0.71	0.99
142.6	0.73	1.0
149.6	0.81	
155.2	0.88	
164.5	0.91	
173.0	0.92	

TABLE X (Continued)

Volume Treated (Liter)	Ionic Concentrations (C/Co)	
	Sodium	Chloride
180.1	0.96	
190.1	1.0	
(Cation/Anion = 3.6 g/2.4 g)		
3.3	0.01	0.004
9.7	0.014	0.002
13.5	0.017	0.001
19.4	0.018	0.003
23.3	0.018	0.01
33.3	0.039	0.027
38.7	0.035	0.038
42.5	0.040	0.045
48.0	0.051	0.08
53.8	0.048	0.098
60.5	0.095	0.17
65.0	0.12	0.32
70.9	0.15	0.71
75.7	0.17	0.82
83.6	0.20	0.98
89.9	0.20	0.99
93.7	0.24	1.0
99.7	0.24	
104.4	0.25	
110.8	0.28	
119.8	0.33	
123.9	0.36	
128.9	0.38	
134.4	0.42	
142.4	0.48	
149.4	0.52	
154.9	0.57	
164.2	0.62	
172.5	0.69	
179.5	0.73	
189.2	0.81	
199.3	0.92	
209.4	0.98	
216.4	1.0	

TABLE X (Continued)

Volume Treated (Liter)	Ionic Concentrations (C/Co)	
	Sodium	Chloride
(Cation/Anion = 4.0 g/2.0 g)		
3.3	0.007	0.001
9.6	0.011	0.001
13.4	0.013	0.002
19.2	0.018	0.004
23.0	0.016	0.009
32.8	0.024	0.035
38.2	0.032	0.043
41.9	0.038	0.14
47.3	0.045	0.23
53.1	0.075	0.43
59.6	0.11	0.85
64.1	0.10	0.94
69.9	0.11	0.99
74.6	0.12	1.0
82.4	0.14	
88.6	0.13	
92.3	0.15	
98.2	0.16	
102.7	0.17	
109.0	0.19	
117.8	0.22	
121.9	0.21	
126.8	0.24	
132.2	0.28	
140.1	0.31	
147.0	0.34	
152.5	0.38	
161.6	0.45	
169.9	0.54	
176.8	0.60	
186.4	0.68	
197.5	0.73	
209.7	0.84	
218.0	0.88	
230.0	1.0	
(Cation/Anion = 3.0 g/6.0 g)		
5.5	0.015	0.000
13.7	0.02	0.000
22.7	0.024	0.000

TABLE X (Continued)

Volume Treated (Liter)	Ionic Concentrations (C/Co)	
	Sodium	Chloride
29.6	0.028	0.000
38.8	0.035	0.000
48.4	0.052	0.000
53.0	0.061	0.000
61.1	0.11	0.001
71.0	0.13	0.001
78.2	0.14	0.002
88.8	0.19	0.004
99.6	0.25	0.005
105.2	0.29	0.012
112.1	0.35	0.025
120.8	0.44	0.055
129.6	0.54	0.098
136.4	0.63	0.18
143.8	0.83	0.29
153.0	0.92	0.43
159.8	0.97	0.51
164.5	0.99	0.62
171.5	1.0	0.71
179.9		0.75
188.2		0.77
193.0		0.81
203.0		0.84
211.0		0.91
217.8		0.97
222.0		1.0

(Cation/Anion = 3.6 g/5.4 g)

5.5	0.002	0.000
13.7	0.003	0.000
22.7	0.002	0.000
29.7	0.005	0.000
38.8	0.01	0.000
48.4	0.028	0.000
53.0	0.041	0.000
61.0	0.048	0.001
70.7	0.092	0.002
77.9	0.098	0.004
88.4	0.11	0.002
99.1	0.17	0.004
104.6	0.21	0.015
111.4	0.24	0.045

TABLE X (Continued)

Volume Treated (Liter)	Ionic Concentrations (C/Co)	
	Sodium	Chloride
120.0	0.29	0.09
128.6	0.37	0.16
135.4	0.44	0.26
142.5	0.56	0.32
151.5	0.66	0.48
158.2	0.71	0.67
162.8	0.81	0.72
169.7	0.89	0.82
177.9	0.96	0.92
186.1	0.99	0.98
190.8	1.0	0.99
200.6		1.0

(Cation/Anion = 4.5 g/4.5 g)

5.9	0.001	0.000
14.9	0.001	0.000
24.6	0.003	0.000
32.0	0.003	0.000
41.8	0.005	0.000
52.2	0.015	0.000
57.2	0.018	0.001
65.8	0.025	0.003
76.5	0.03	0.003
84.3	0.035	0.005
95.7	0.075	0.025
107.2	0.11	0.082
113.3	0.14	0.16
120.7	0.19	0.29
130.0	0.24	0.52
139.4	0.29	0.78
146.8	0.29	0.93
154.6	0.36	0.99
164.5	0.38	1.0
171.9	0.43	
176.9	0.48	
184.5	0.54	
193.5	0.58	
202.6	0.71	
207.7	0.77	
218.5	0.79	
227.2	0.83	
235.6	0.87	

TABLE X (Continued)

Volume Treated (Liter)	Ionic Concentrations (C/Co)	
	Sodium	Chloride
245.6	0.94	
259.2	0.99	
268.8	1.0	
(Cation/Anion = 5.4 g/3.6 g)		
5.7	0.002	0.000
14.1	0.005	0.000
23.4	0.01	0.000
30.5	0.015	0.000
40.0	0.015	0.001
49.9	0.018	0.003
54.4	0.015	0.003
62.0	0.018	0.005
68.7	0.022	0.015
76.3	0.038	0.028
87.3	0.068	0.11
98.5	0.11	0.29
104.3	0.11	0.82
111.6	0.12	0.96
120.6	0.12	1.0
129.7	0.15	
136.8	0.17	
144.3	0.18	
153.8	0.19	
160.9	0.21	
165.8	0.22	
173.1	0.25	
181.8	0.32	
190.5	0.33	
195.5	0.33	
205.8	0.42	
214.2	0.47	
222.2	0.51	
231.8	0.59	
244.9	0.69	
254.1	0.77	
264.5	0.87	
274.2	0.96	
283.7	1.0	

TABLE X (Continued)

Volume Treated (Liter)	Ionic Concentrations (C/Co)	
	Sodium	Chloride
(Cation/Anion = 6.0 g/3.0 g)		
5.7	0.001	0.000
14.4	0.001	0.000
23.9	0.003	0.001
31.1	0.004	0.003
40.7	0.006	0.003
50.7	0.012	0.005
55.6	0.015	0.018
64.1	0.018	0.05
74.3	0.02	0.19
82.0	0.025	0.34
93.1	0.035	0.89
104.4	0.038	1.0
110.3	0.05	
117.5	0.06	
126.5	0.062	
135.7	0.10	
143.0	0.09	
150.5	0.13	
160.1	0.16	
167.2	0.15	
172.1	0.18	
179.5	0.19	
188.3	0.22	
197.0	0.27	
202.0	0.28	
212.4	0.34	
220.9	0.36	
229.0	0.39	
238.7	0.44	
251.8	0.51	
261.1	0.57	
271.5	0.70	
280.9	0.81	
290.1	0.88	
295.8	0.89	
308.9	0.96	
320.7	1.0	

TABLE X (Continued)

Volume Treated (Liter)	Ionic Concentrations (C/Co) Sodium Chloride
(Cation/Anion = 3.0 g/5.0 g)	
10.8	0.003
22.3	0.009
33.6	0.02
44.0	0.045
54.2	0.072
65.7	0.10
76.1	0.16
87.3	0.22
97.5	0.28
108.2	0.38
118.9	0.51
130.0	0.69
140.4	0.80
150.3	0.91
162.5	0.98
174.0	0.99
184.2	1.0
(Cation/Anion = 3.0 g/1.0 g)	
10.1	0.045
20.8	0.055
31.4	0.064
41.1	0.087
50.5	0.13
61.2	0.18
70.8	0.21
81.2	0.28
90.7	0.36
100.6	0.45
110.5	0.49
120.6	0.53
130.2	0.60
139.3	0.68
150.6	0.77
161.2	0.83
170.6	0.88
181.2	0.92
191.2	0.95
201.3	0.99
210.1	1.0

TABLE X (Continued)

Volume Treated (Liter)	Ionic Concentrations (C/Co)	
	Sodium	Chloride
(Cation/Anion = 5.0 g/3.0 g)		
9.8		0.000
20.0		0.001
30.5		0.002
40.4		0.006
49.9		0.015
61.6		0.045
72.5		0.09
82.2		0.49
93.2		0.93
103.6		1.0
(Cation/Anion = 1.0 g/3.0 g)		
10.0		0.016
20.6		0.027
31.4		0.047
41.6		0.08
51.3		0.12
63.3		0.25
74.6		0.45
84.5		0.62
95.8		0.74
106.4		0.83
117.2		0.94
126.7		0.99
136.1		1.0
(Cation/Anion = 3.0 g (bottom)/3.0 g (top))		
10.0	0.037	0.016
20.4	0.042	0.022
31.1	0.055	0.03
41.0	0.095	0.033
50.0	0.12	0.045
60.2	0.15	0.058
68.8	0.21	0.085
75.6	0.23	0.19
82.2	0.25	0.49
88.0	0.32	0.61
94.2	0.38	0.71

TABLE X (Continued)

Volume Treated (Liter)	Ionic Concentrations (C/Co)	
	Sodium	Chloride
99.3	0.45	0.84
104.2	0.50	0.91
110.3	0.57	0.96
112.8	0.58	0.97
119.9	0.66	1.0
127.4	0.71	
133.8	0.74	
140.3	0.76	
149.3	0.79	
156.2	0.82	
164.2	0.85	
169.9	0.87	
176.3	0.90	
182.4	0.92	
190.7	0.95	
199.2	0.98	
206.3	0.99	
212.4	1.0	

(Cation/Anion = 0.0 g/6.0 g)

3.2	0.009
9.5	0.042
13.2	0.045
19.0	0.078
22.7	0.082
32.5	0.11
37.9	0.13
41.6	0.16
46.9	0.18
52.6	0.21
59.1	0.22
63.5	0.22
69.2	0.28
74.0	0.29
81.6	0.29
87.7	0.28
91.4	0.40
97.2	0.44
101.8	0.43
116.7	0.48
120.8	0.52
125.7	0.58

TABLE X (Continued)

Volume Treated (Liter)	Ionic Concentrations (C/Co) Sodium	Chloride
131.1		0.62
138.8		0.66
145.5		0.69
150.9		0.71
159.8		0.79
167.9		0.80
174.6		0.83
183.9		0.87
194.5		0.93
206.1		0.98
214.0		1.0

(Cation/Anion = 6.0 g/0.0 g)

5.9	0.008
14.8	0.015
24.5	0.018
31.9	0.015
41.8	0.032
52.1	0.038
57.1	0.035
64.7	0.038
71.5	0.035
79.4	0.055
90.8	0.10
102.5	0.11
108.5	0.12
115.9	0.12
125.3	0.13
134.7	0.13
142.1	0.12
149.9	0.14
159.9	0.15
167.3	0.16
172.3	0.16
179.9	0.18
189.0	0.20
198.0	0.23
203.2	0.24
214.0	0.30
222.7	0.32
231.1	0.35
241.0	0.46

TABLE X (Continued)

Volume Treated (Liter)	Ionic Concentrations (C/Co) Sodium Chloride
254.6	0.53
264.1	0.59
274.9	0.67
284.8	0.75
294.7	0.79
300.6	0.80
313.9	0.84
326.8	0.88
335.5	0.89
351.0	0.94
365.4	0.97
385.8	1.0

2

VITA

Taekyung Yoon

Candidate for the Degree of
Doctor of Philosophy

Thesis: THE EFFECT OF THE CATION TO ANION RESIN RATIO
ON MIXED-BED ION EXCHANGE PERFORMANCE
AT ULTRA-LOW CONCENTRATIONS

Major Field: Chemical Engineering

Biographical:

Education: Born and Educated from the Elementary School to the University at Busan in Korea; Received the Bachelor of Engineering Degree in Chemical Engineering and the Master of Engineering Degree in Chemical Engineering from the Busan National University in February, 1979 and 1981, respectively; Another Degree of the Master of Science in Chemical Engineering was received from University of Nebraska-Lincoln in May, 1986; Completed requirements for the Doctor of Philosophy Degree at Oklahoma State University in May, 1990.

Professional Experience: Full-Time Instructor and Assistant Professor at the Department of Chemical Engineering, Sungji Institute of Technology, Busan, Korea, 1981-1983 and 1983-1984, respectively; Research Internship at the Nebraska State Department of Transportation, Lincoln, Nebraska, 1985-1986; Research Assistant at the School of Chemical Engineering, Oklahoma State University, June, 1986, to December, 1989.

Professional Societies: The Korean Scientists and Engineers Association in America.